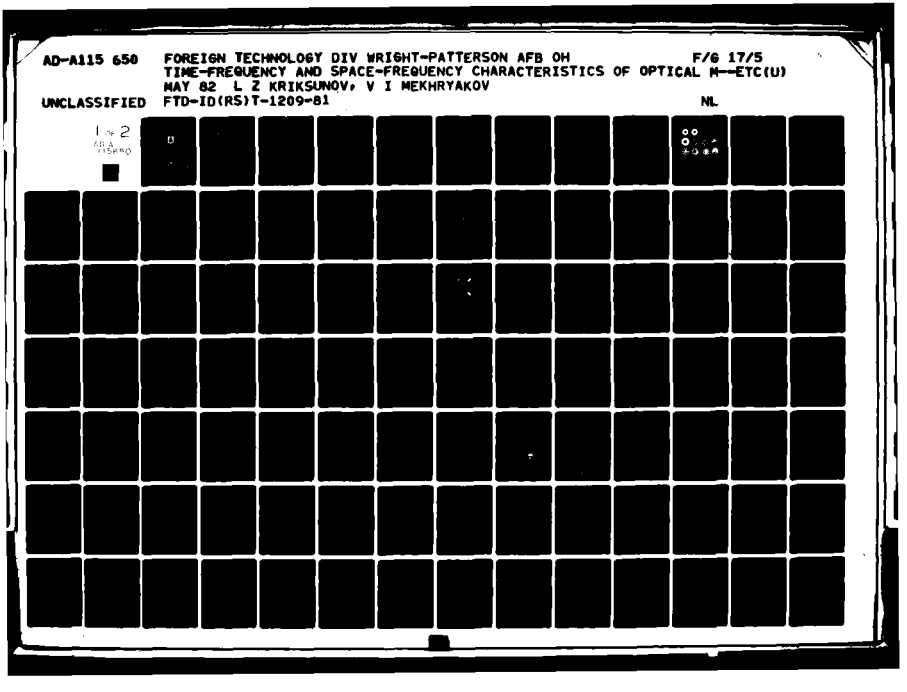
AD-A115 650
FOREIGN TECHNOLOGY DIV WRIGHT-PATTERSON AFB OH
F/G 17/5
TIME-FREQUENCY AND SPACE-FREQUENCY CHARACTERISTICS OF OPTICAL M--ETC(U)
MAY 82 L Z KRIKSUNOV, V I MEKHRYAKOV
UNCLASSIFIED
FTD-ID(RS)T-1209-81
NL
1 OF 2
AD A115650

AD A115650

FTD-ID(RS)T-1209-81

FOREIGN TECHNOLOGY DIVISION

TIME-FREQUENCY AND SPACE-FREQUENCY CHARACTERISTICS OF OPTICAL MODULATORS

by

L.Z. Kriksunov, V.I. Mekhryakov, and O.I. Naygovzin

DTIC
ELECTE
JUN 16 1982
S D
D

Approved for public release;
distribution unlimited.

DTIC FILE COPY

82 06 16 049

Accession For
NTIS GRA&I
DTIC TAB
Unannounced
Justification
By
Distribution/
Availability Codes
Dist | Avail and/or Special
A

DTIC COPY INSPECTED 2

EDITED TRANSLATION

FTD-ID(RS)T-1209-81 20 May 1982

MICROFICHE NR: FTD-82-C-000633

TIME-FREQUENCY AND SPACE-FREQUENCY CHARACTERISTICS OF OPTICAL MODULATORS

By: L.Z. Kriksunov, V.I. Mekhryakov, and O.I. Naygovzin

English pages: 128

Source: Chastotno-Vremennyye i Prostranstvenno-Chastotnyye Kharakteristiki Opticheskikh Moduliruyushchikh Ustroystv, Publishing House "Mashinostroyeniye", Moscow 1972, pp. 1-131

Country of origin: USSR
Translated by: LEO KANNER ASSOCIATES
F33657-81-D-0264
Requester: USAMICOM
Approved for public release; distribution unlimited.

THIS TRANSLATION IS A RENDITION OF THE ORIGINAL FOREIGN TEXT WITHOUT ANY ANALYTICAL OR EDITORIAL COMMENT. STATEMENTS OR THEORIES ADVOCATED OR IMPLIED ARE THOSE OF THE SOURCE AND DO NOT NECESSARILY REFLECT THE POSITION OR OPINION OF THE FOREIGN TECHNOLOGY DIVISION.

PREPARED BY:

TRANSLATION DIVISION
FOREIGN TECHNOLOGY DIVISION
WP-AFB, OHIO.

TABLE OF CONTENTS

U. S. BOARD ON GEOGRAPHIC NAMES TRANSLITERATION SYSTEM

Block	Italic	Transliteration	Block	Italic	Transliteration
А а	*А а*	A, a	Р р	*Р р*	R, r
Б б	*Б б*	B, b	С с	*С с*	S, s
В в	*В в*	V, v	Т т	*Т т*	T, t
Г г	*Г г*	G, g	У у	*У у*	U, u
Д д	*Д д*	D, d	Ф ф	*Ф ф*	F, f
Е е	*Е е*	Ye, ye; E, e*	Х х	*Х х*	Kh, kh
Ж ж	*Ж ж*	Zh, zh	Ц ц	*Ц ц*	Ts, ts
З з	*З з*	Z, z	Ч ч	*Ч ч*	Ch, ch
И и	*И и*	I, i	Ш ш	*Ш ш*	Sh, sh
Й й	*Й й*	Y, y	Щ щ	*Щ щ*	Shch, shch
К к	*К к*	K, k	Ъ ъ	*Ъ ъ*	"
Л л	*Л л*	L, l	Ы ы	*Ы ы*	Y, y
М м	*М м*	M, m	Ь ь	*Ь ь*	'
Н н	*Н н*	N, n	Э э	*Э э*	E, e
О о	*О о*	O, o	Ю ю	*Ю ю*	Yu, yu
П п	*П п*	P, p	Я я	*Я я*	Ya, ya

*ye initially, after vowels, and after ъ, ь; e elsewhere.
When written as ё in Russian, transliterate as yё or ё.

RUSSIAN AND ENGLISH TRIGONOMETRIC FUNCTIONS

Russian	English	Russian	English	Russian	English
sin	sin	sh	sinh	arc sh	$\sinh^{-1}$
cos	cos	ch	cosh	arc ch	$\cosh^{-1}$
tg	tan	th	tanh	arc th	$\tanh^{-1}$
ctg	cot	cth	coth	arc cth	$\coth^{-1}$
sec	sec	sch	sech	arc sch	sech^{-1}
cosec	csc	csch	csch	arc csch	csch^{-1}

Russian	English
rot	curl
lg	log

GRAPHICS DISCLAIMER

All figures, graphics, tables, equations, etc. merged into this translation were extracted from the best quality copy available.

Annotation

This monograph examines frequency methods of analysis of modulators used in optical systems for determining the angular coordinates of moving objects and for automatic tracking. The feasibility of modeling optical systems for determining the angular coordinates of moving objects by means of analog computers is demonstrated. A method is given for experimental determination of the spatial frequency responses of modulators. The method is based on the use of a laser. The results of experimental and theoretical studies are covered.

This book is aimed at specialists engaged in the development of optical equipment. It may prove useful to students at higher educational institutions oriented toward instrument-making specialties.

There are 42 illustrations, 5 tables, and 31 bibliographic entries.

FOREWORD

In recent years several important works have been published on optical information-processing systems which make extensive use of operational problem-solving methods based on Fourier transforms. These methods have opened up the potential for far-reaching analogies between optics and communication theory. Communication systems, like systems which produce optical images, are designed for the processing and transmission of information. In the former case the information is temporal, and in the latter spatial. However, this difference is insignificant from the standpoint of using common mathematical techniques. This is especially important to both the analysis and synthesis of optical systems.

One of the most important elements of optoelectronic designed to measure angular coordinates and automatically track moving objects is the unit that modulates the light beam. Combined with other components of the device, it converts the values of luminous fluxes from different regions of the thermal field being scanned into corresponding signals. These signals are used to determine the angular coordinates of an object that differs from surrounding objects (the background) in its radiation characteristics. Moreover, the modulator performs spatial filtering which enhances the contrast between the object and the background and which is a powerful tool for improving the noise immunity and operating range of an optoelectronic device.

In this book we present the mathematical foundations of the theories of Fourier transforms and spatial filtering and the basic theorems and Fourier transforms that are used later to solve various problems. We introduce the concept of the spatial frequency transfer function and define it for the most widely used optical filters.

We also examine analytical methods of determining the frequency-versus-time characteristics of optical modulators and demonstrate the feasibility of computer simulation of optoelectronic devices that contain modulators.

Theoretical and experimental methods are presented for determining the spatial frequency transfer functions of modulators used in optical (infrared) systems for angular-coordinate determination and automatic tracking of moving objects.

Chapter 1 was written by Prof. L. Z. Kriksunov, honored scientist and engineer of the Ukrainian SSR and a doctor of technical sciences. Chapter 2 was written by O. N. Naigovzin, candidate of technical sciences. Chapter 3 was written by Assoc. Prof. V. I. Mekhryakov, candidate of technical sciences. The overall arrangement of the book and editing were handled by L. Z. Kriksunov.

The authors thank G. M. Mosyagin, candidate of technical sciences, for reviewing the book and for his constructive advice, which was taken into consideration in preparing the book for press.

The authors ask that all comments and requests be addressed to Mashinostroeniye Publishing House, Bldg. 3, Pervyy Basmannyy Pereulok, B-66, Moscow, USSR.

CHAPTER 1

THE FUNCTION OF MODULATORS AND FREQUENCY METHODS OF ANALYSIS

1.1. The Function and Types of Modulators

Optical (infrared) systems for angular-coordinate measurement and automatic tracking of moving objects make extensive use of modulation of the light flux that passes through an optical system. The modulating disks or modulators Used for this purpose (which also are known as analyzing diaphragms in the foreign literature) are thin sheets having some specific law of transparency distribution which are located in the focal plane of an objective.

When the modulating disk moves relative to the optical image of an object, current pulses that bear information on the object's location in the system's field of view periodically occur in the circuit of the radiant-energy detector located behind the modulating disk. Electronic processing of these pulses is used to identify signals that depend on the angular coordinates of the moving object. These signals are used for automatic tracking based on the angular coordinates.

An optical system accepts radiation not only from an object, but also from the surrounding background. The radiant characteristics and the linear dimensions of the object and the background generally differ. Modulation of the light flux that passes through the optical system makes it possible to discriminate between signals due to a small (point) object and the extended background.

Thus, the following three tasks are handled by a modulator:

(1) conversion of light fluxes from different regions of the scanned thermal field into corresponding signals that are functions of time;

(2) determination of the angular coordinates of an object that differs in radiant characteristics from the surrounding background by electronic processing of signals resulting from modulation of the light flux;

(3) spatial filtering, which helps discriminate signals from a small (point) object and an extended background.

The modulating disk performs these functions together with other components of the optical system and of the entire optoelectronic device.

A modulating unit usually is implemented as a modulating disk (a modulator) that is placed in rotation at a constant angular velocity by an electric or pneumatic motor. Schemes using a fixed modulating disk relative to which the image of the object moves are encountered less often.

The configuration and combination of transparent and opaque elements of the modulating disk determine the type of modulation of the light beam. Shown in Fig. 1.1 are scandard schemes of the modulating disks of infrared systems for determining the angular coordinates of moving objects [14].

A disk with two series of opaque bands applied with different frequencies (a) provides frequency modulation of the light beam and makes it possible to determine the location of a radiating object in some half-plane from the change in signal frequency at the output of the radiant-energy detector of photocurrent amplifier. By changing the character of the placement of the modulating strips on the disk, it is possible to obtain frequency modulation of a light beam such that the modulation frequency is linearly dependent on the coordinate of the object in the plane being analyzed (b), or such that the frequency varies according to a meander law with arm ratios determined by the present position of the radiating object (c).

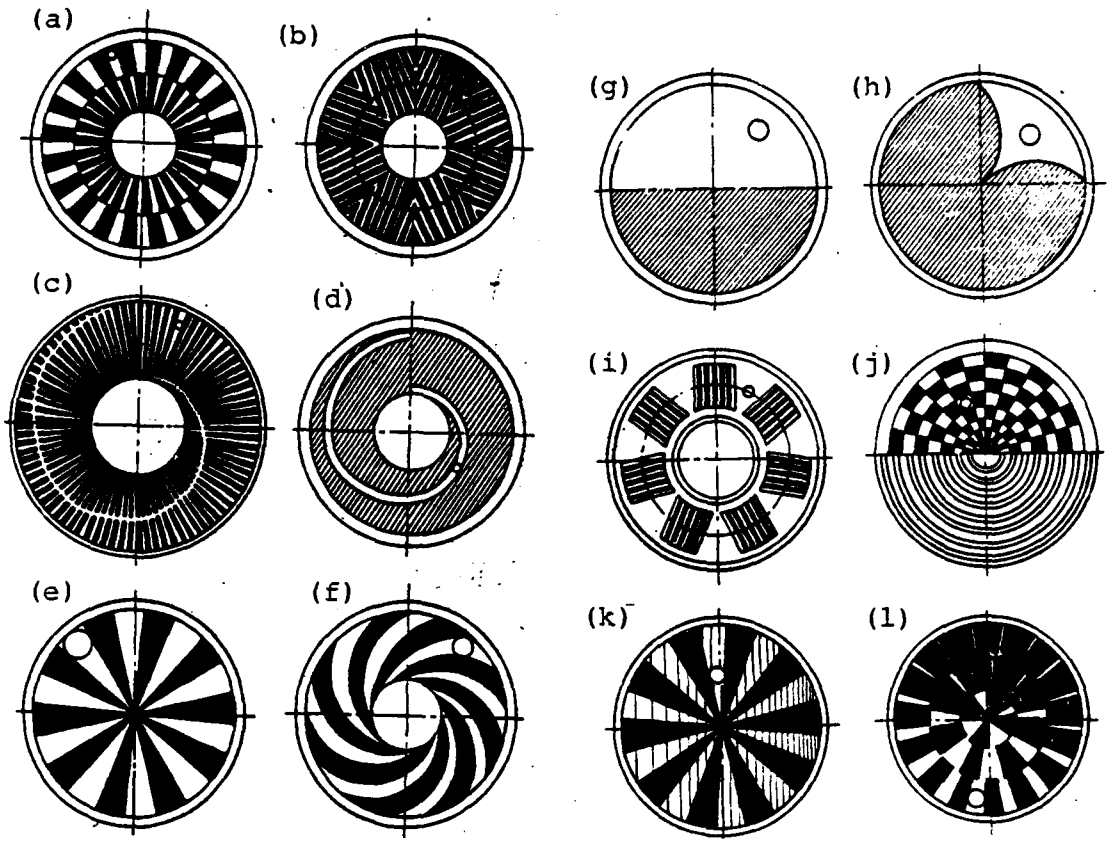

Fig. 1.1. Standard schemes of modulating disks: a, b, c - disks that provide frequency modulation of a light beam; d, e, f - disks designed for phase or amplitude modulation; g, h, i - disks that provide pulse position modulation; j, k, l - disks for pulse amplitude modulation.

A modulating disk with a spiral cutout (d) successively scans the image of a given field. If, when the disk is rotated by some angle, the cutout intersects the image of an object, then a current pulse appears at the output of the radiant-energy detector located behind the modulating disk. The position (phase) of this pulse relative to the selected origin of coordinates characterizes the coordinates of the image of the radiating object in the image plane of the field being scanned (phase modulation).

A radial sector disk (e) produces amplitude modulation of a light beam. The percentage modulation is the parameter that determines an

object's position in the plane being analyzed. A disk with spiral-type modulating strips (f) performs an analogous function.

During one half-rotation a modulating disk with a sector cutout (g) transmits radiation from the object to the radiant-energy detector, and during the other half-rotation it obscures it. The phase of the photocurrent pulse depends on the object's location in some quadrant of the field of view. If the cutout in the disk is made shaped (h), then the pulse length moreover turns out to be proportional to the displacement of the object (and its image in the focal plane) from the position adopted as the zero position. A variable pulse length also can be obtained by using a disk (i) that has a certain number of windows with parallel transparent and opaque modulating strips.

The most widely used disks in modern optical systems for determining the angular coordinates of moving objects are modulating disks that produce light-beam modulation in which the signal at the output of an electronic circuit is sinusoidal. The signal amplitude is proportional to the movement of the object's image from the zero point, and the phase determines the direction of motion (the plane of displacement). Such disks are shown in Figs. 1.1j, 1.1k, and 1.1l. In particular, the transparent elements of disk j are arranged in a checkerboard pattern, and their dimensions are equal to the image of a point emitter in the plane of analysis of the radiating field. As a result, the light flux from the object is modulated and a signal is transmitted from the output of the radiant-energy detector by an electronic circuit, while the light flux from the spatially extended background is not modulated and does not cause a signal to appear at the circuit's output.

These examples show how important a modulator is in forming the working signal of an optical system designed to determine the angular coordinates of moving objects. Hence particular attention is paid to the modulator in the development of new systems, as this selection

largely predetermines the block diagram and specifications of the system.

In recent years the frequency-versus-time and spatial frequency responses of modulators, based on Fourier transforms, have been used for analysis and synthesis. The use of multidimensional Fourier transforms makes possible the solution of a number of important problems that arise in the design of optoelectronic systems. These include:

--the determination of the characteristics of signals when they are converted by different optical elements;

--the synthesis of optical filters that filter legitimate signals in the presence of noise signals;

--the determination of the characteristics of electrical signals at the output of the optoelectronic system when it converts optical signals into electrical signals, and so forth.

Before moving on to the solution of some of the problems listed, let us examine the block diagram of a standard optoclectronic device designed to determine the angular coordinates of radiating objects (Fig. 1.2). The input element of the device is a lens- or mirror-type objective in whose focal plane there is a rotating modulating disk 6. If we assume that the modulating disk is implemented after the diagram in Fig. 1.1k, then a sinusoidal signal with a period $T=(2\pi)/\Omega$, where Ω is the angular rotational velocity of the disk, periodically appears in the circuit of the radiant-energy detector located behind the modulating disk.

This signal carries a "high-frequency filler" that is a sequence of square current pulses $t_u=\pi/\omega$ long with a period $t=(2\pi)/\omega$, where ω is the modulation frequency of the light beam, with $\omega=z\Omega$, where z is the number of transparent (or opaque) sectors of the modulating disk.

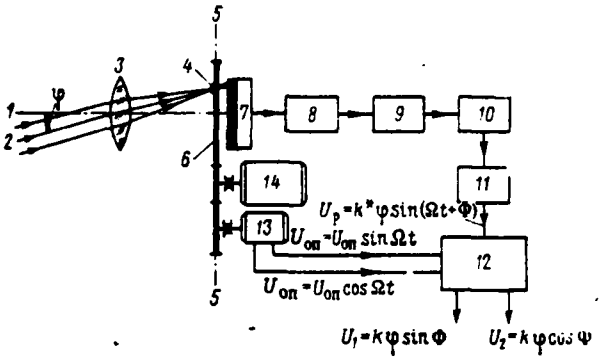

Fig. 1.2. Block diagram of an optical system for determining the angular coordinates of radiating objects: (1) optical axis of objective; (2) direction to object; φ - error angle; (3) objective; (4) image of object; (5) focal plane of objective; (6) modulating disk; (7) radiant-energy detector; (8) preamplifier; (9) tuned amplifier; (10) detector; (11) error signal amplifier; (12) phase detector and filter; U_p - error voltage; U_{on} - reference voltages; (13) reference generator (ГОН); (14) drive motor of modulating disk and reference generator.

The signal from the output of radiant-energy detector 7 is amplified by electronic preamplifier 8 and tuned amplifier 9, which is tuned to a frequency ω. Then the signal is detected and the frequency envelope Ω is isolated. This is a sinusoidal voltage with an amplitude proportional to the error angle (the angle φ between the optical axis of the objective and the direction to the object) and the phase, which is determined by the plane in which the object is located.

Reference generator (ГОН) 13 and phase detector (ФД) 12 are used to determine signals proportional to the components of the error angle in two mutually perpendicular planes. The rotor of the reference generator rotates synchronously and in phase with the modulating disk (one motor); two sinusoidally varying voltages (of frequency Ω) that are phase-shifted by an angle of $2/\pi$ are picked up from the terminals

of the reference generator. These voltages are supplied to the phase detector and are the reference voltages, since the phase of the error voltage from the output of the photcurrent amplifier, which also is fed to the phase detector, is determined with respect to them. DC voltages proportional to the components of the error angle in two mutually perpendicular planes are picked up from the filter of the phase detector.

Basic data for some foreign optoelectronic devices are presented in Table 1.1 [31].

1.2. The Fourier Series and Integral

Any periodic function f(x) of a variable x of the period T which satisfies the Dirichlet conditions (i.e., the function is bounded, piecewise continuous, and has a finite number of extrema over the period) is known to be representable as a sum of trigonometric functions:

$$f(x)=a_0+\sum_{k=1}^{\infty}\left(a_k\cos 2\pi k\frac{x}{T}+b_k\sin 2\pi k\frac{x}{T}\right), \quad (1.1)$$

where

$$a_0=\frac{1}{T}\int_{-\frac{T}{2}}^{\frac{T}{2}} f(x)\,dx; \quad (1.2)$$

$$\left.\begin{matrix}a_k\\ b_k\end{matrix}\right|=\int_{-\frac{T}{2}}^{\frac{T}{2}} f(x)\left|\begin{matrix}\cos\\ \sin\end{matrix}\right|2\pi k\frac{x}{T}\,dx$$

$$(k=1,\ 2,\ 3,\ldots). \quad (1.3)$$

This series is called the Fourier series of the function f(x); the quantity a_0 expresses the average value of the function over the period and is called the constant component; the individual terms are called harmonics and have frequencies that are multiples of the fundamental frequency 1/T.

Table 1.1. Basic Data on Foreign Optoelectronic Devices with Modulators

(a) Модель, фирма	(b) Подвижный элемент	(c) Диаметр апертуры мм	(d) Поле зрения	(e) Тип ПЛЭ	(f) Диапазон длин волн мкм	(g) Облученность, соответствующая шумам Вт/см²	(h) Полоса частот Гц	(i) Оптическая система	(j) Способ фильтрации и пространственная частота 1/рад
EM-2 Baird—Atomic	(k) Модулирующий диск	305	30′	PbS PbTe (охл.) (r)	0,5—2,7 1,3—1,5	10^{-12} $5\cdot10^{-11}$	30	(l) Первичное параболическое зеркало, вторичное плоское зеркало и полевая линза	(m) Пространственная, 20
Redstone Arsenal	Плоское зеркало (n)	127	1°,3	PbS	0,6—2,7	$1,7\cdot10^{-11}$	1,2	Катодиоптрическая (o)	Пространственная, 250 (p)
T-8 Aerojet General	Германиевая пластина (q)	89	5°,75	PbS (охл.) (r) InSb (охл.) (r)	2—3 3—5	$7\cdot10^{-12}$ $7\cdot10^{-11}$	10	Кассегреновская, Ge пластина и полевая линза (s)	Спектральная и пространственная (t)
Bendix—Scyscraper	Зеркало, модулирующий диск (u)	254 254	30′ 6′	PbS Ge:Cu (охл.) (z)	1,2—2,7 1,8—14	$1,6\cdot10^{-9}$ $7,4\cdot10^{-10}$	2	(v) Кассегреновская и полевая линза	Спектральная и пространственная, 6000 (w)
Gmb H. Heidelberg	(k) Модулирующий диск	166	2°	PbS (r) PbSe (охл.)	1,7—2,7 3—5	$1,5\cdot10^{-12}$ $5\cdot10^{-13}$	1	(v) Кассегреновская и полевая линза	Спектральная и пространственная, 1000 (x)
T-51A Aerojet General	(k) Модулирующий диск	153	30′—1°	PbS	0,7—2,7	$4\cdot10^{-12}$	1	(v) Кассегреновская и полевая линза	Спектральная и пространственная, 1360 (y)
21-110 Barnes	(k) Модулирующий диск	51	4°	PbS	1,8—2,7	$1,5\cdot10^{-10}$	500	(z) Две 50 мм линзы и полевая линза	Спектральная и пространственная, 125 (aa)
		51	8 мрад (bb)	PbS	1,8—2,7	$2,0\cdot10^{-11}$	500	То же (cc)	Пространственная (dd)

Key: (a) model, company; (b) movable element; (c) aperture diameter, mm; (d) field of view; (e) type of PLE [expansion unknown]; (f) wavelength interval, microns; (g) irradiance; corresponding to noise, W/cm²; (h) frequency band, Hz; (i) optical system; (j) filtering method and spatial frequency, 1/rad; (k) modulating disk; (l) primary parabolic mirror, secondary plane mirror, and field lens; (m) spatial, 20; (n) plane mirror; (o) catodioptric; (p) spatial, 250; (q) germanium sheet; (r) cooled; (s) Cassegrain, Ge sheet, and field lens; (t) spectral and spatial; (u) mirror, modulating disk; (v) Cassegrain and field lens; (w) spectral and spatial, 6000; (x) spectral and spatial, 1000; (y) spectral and spatial, 1360; (z) two 50-mm lenses and a field lens; (aa) spectral and spatial, 125; (bb) mrad; (cc) the same; (dd) spatial. [Table continued on p. 9.]

If the function f(x) is even, i.e., if f(-x)=-f(x), then

$$a_k=\frac{4}{T}\int_0^{\frac{T}{2}} f(x)\cos 2\pi k\frac{x}{T}dx;$$

$$b_k=0.$$

For an odd function [f(x)=-f(-x)], we have

Table 1, continued

(a) Модель, фирма	(b) Подвижный элемент	(c) Диаметр апертуры мм	(d) Поле зрения	(e) Тип ПЛЭ	(f) Диапазон длин волн мкм	(g) Облученность, соответствующая шумам Вт/см²	(h) Полоса частот Гц	(i) Оптическая система	(j) Способ фильтрации и пространственная частота 1/рад
21-111 Barnes	(k) Модулирующий диск	25	1°	PbS	1,8—2,7 0,45—0,6	$8\cdot10^{-11}$	500	(ee) Две 25 мм линзы и полевая линза	(ff) Пространственная, двухцветная, 62
21-112 Barnes	(k) Модулирующий диск	305	4°	PbS	1,8—2,7	$1\cdot10^{-13}$	20	(gg) 300 мм кассегреновская и полевая линза	(hh) Спектральная и пространственная, 70 (140)
ATR-1 ACF Electronics	—	140	12 мрад (bb)	(r) PbS (охл.) InSb (охл.)	2—3 3—5	$3\cdot10^{-13}$ $2\cdot10^{-12}$	0,6	(v) Кассегреновская и полевая линза	(ii) Спектральная, мгновенное поле зрения 6 мрад
TGA-4 ITT	(k) Модулирующий диск	76	70 мрад (bb)	(r) PbS	2,1—2,7	$1\cdot10^{-10}$	—	—	(jj) Спектральная и пространственная, 357
21-120 Barnes	(k) Модулирующий диск	180 84	10°×20° 2°	PbS	1,8—2,6 0,45—0,6	$9\cdot10^{-10}$ $9\cdot10^{-11}$	5	(kk) Рефракционная Максутовская	(ll) Пространственная, двухцветная, 210
21-122 Barnes	(k) Модулирующий диск	204	2° (mm) или 30'	(r) PbS (охл.) (nn) ФЭУ PbSe (охл.) (r)	0,7—2,7 0,35—0,65 2,7—6,5	$1,5\cdot10^{-13}$ $2\cdot10^{-16}$ $3\cdot10^{-11}$	25	(oo) 200 мм кассегреновская и полевая линза	(pp) Пространственная, трехцветная, 270 и 1080

Key: (a) model, company; (b) movable element; (c) aperture diameter, mm; (d) field of view; (e) type of PLE [expansion unknown]; (f) wavelength interval, microns; (g) irradiance corresponding to noise, W/cm²; (h) frequency band, Hz; (i) optical system; (j) filtering method and spatial frequency, 1/rad; (k) modulating disk; (ee) two 25-mm lenses and a field lens; (ff) spatial, two-color, 62; (gg) 300-mm Cassegrain and a field lens; (hh) spectral and spatial, 70 (140); (r) cooled; (v) Cassegrain and a field lens; (bb) mrad; (ii) spectral, instantaneous field of view 6 mrad; (jj) spectral and spatial, 357; (kk) Maksutov refraction system; (ll) spatial, two-color, 210; (mm) or; (nn) photomultiplier [FEU]; (oo) 200-mm Cassegrain and a field lens; (pp) spatial, three-color, 270 and 1080.

$$a_k=0;$$

$$b_k=\frac{4}{T}\int_0^{\frac{T}{2}} f(x)\sin 2\pi k\frac{x}{T}\,dx.$$

Let us consider as an example the expansion into a Fourier series of a rectangular sawtooth function f(x) that assumes values of "+1" or "-1" with a period τ (Fig. 1.3a).

We find

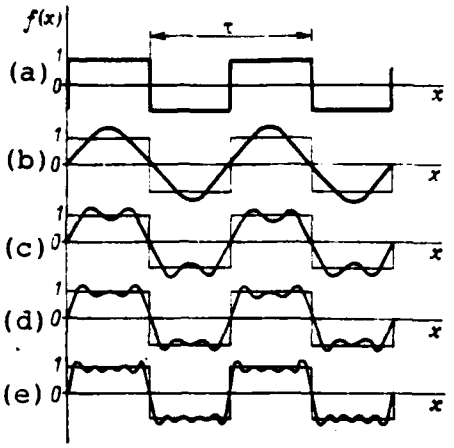

Fig. 1.3. Expansion of a rectangular sawtooth function f(x) into a Fourier series: (a) f(x); (b) first harmonic; (c), (d), and (e) - curves calculated from the first two, first three, and first four terms of the expansion.

$$a_0=\frac{1}{\tau}\int_{-\frac{\tau}{2}}^{\frac{\tau}{2}} f(x)\,dx=0,$$

$$a_k=\frac{2}{\tau}\int_{-\frac{\tau}{2}}^{\frac{\tau}{2}} f(x)\cos 2\pi k\frac{x}{\tau}\,dx=0,$$

$$b_k=\frac{2}{\tau}\int_{-\frac{\tau}{2}}^{\frac{\tau}{2}} f(x)\sin 2\pi k\frac{x}{\tau}\,dx=$$

$$=\begin{cases}0, & \text{if } k=2n \text{ (even)}\\ \frac{4}{k\pi}, & \text{if } k=2n+1 \text{ (odd)}\end{cases}$$

Thus, the function f(x) can be represented by the following series:

$$f(x)=\frac{4}{\pi}\left(\sin\frac{2\pi x}{\tau}+\frac{1}{3}\sin 3\frac{2\pi x}{\tau}+\right.$$
$$\left.+\frac{1}{5}\sin 5\frac{2\pi x}{\tau}+\frac{1}{7}\sin 7\frac{2\pi x}{\tau}+\ldots\right).$$

As the number of terms in the series increases, the representation of the function becomes increasingly accurate, as we can see from Fig. 1.3, which shows curves corresponding to the first term of the series (b), to the sum of the first two terms (c), to the sum of the first three terms (d), and to the sum of the first four terms (e).

A Fourier series also may be written in a different form:

$$f(x)=a_0+\sum_{k=1}^{\infty} c_k \cos\left(2\pi k \frac{x}{T}-\varphi_k\right), \qquad (1.4)$$

where

$$c_k=\sqrt{a_k^2+b_k^2}, \qquad (1.5)$$

$$\varphi_k=\operatorname{arctg}\frac{b_k}{a_k}. \qquad (1.6)$$

The aggregate of the amplitudes of the frequency components c_k is called the amplitude spectrum, and the aggregate of the phases φ_k is called the phase spectrum. In most cases the values of c_k are only real or only imaginary. This makes it possible to describe the function as just a single spectrum.

The spectrum of a periodic function can be represented graphically in a coordinate system $(c_k;\ \omega=\pm(\frac{2\pi k}{T}))$. The amplitudes of individual frequency components commonly are marked by vertical lines of the appropriate length. Thus, the spectrum of a periodic function is discrete (or, as we say, it is a line spectrum, by analogy with an optical spectrum). The individual components of a discrete spectrum are separated from each other by $\frac{2\pi}{T}$. The spectrum is symmetric relative to the vertical axis, which passes through the origin.

Let us examine a frequently encountered complex formula for writing a Fourier series. Using Euler's formulas, we can represent a Fourier series as

$$f(x)=\sum_{-\infty}^{\infty} \dot{c}_k e^{i2\pi k \frac{x}{T}}, \qquad (1.7)$$

where

$$\bar{c}_k = \frac{1}{T}\int_{-\frac{T}{2}}^{\frac{T}{2}} f(x)e^{-i2\pi k\frac{x}{T}}dx; \qquad (1.8)$$

$$\bar{c}_k = c_k e^{i\varphi_k}$$

$$(k = \pm 1, \pm 2, \pm 3, \ldots). \qquad (1.9)$$

The quantity $\bar{c}_k$ is called the complex amplitude of the k-th harmonic, and the aggregate of the quantities $\bar{c}_k$ is called the complex spectrum of the function f(x). The quantity c_k, which is the modulus of $\bar{c}_k$, is called the amplitude of the k-th harmonic; as noted above, the aggregates of the quantities c_k and φ_k are called the amplitude spectrum and the phase spectrum.

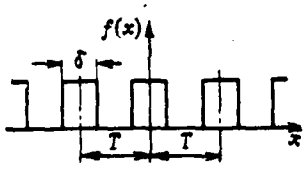

Fig. 1.4. A rectangular periodic function.

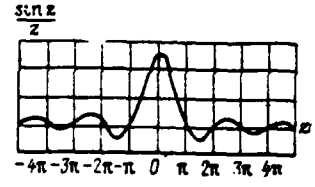

Fig. 1.5. Graph of the function (sin z)/z.

As an example, let us expand the periodic function shown in Fig. 1.4, which has a width δ and a repetition period T, into an exponential Fourier series. On a one-period interval this function may be written as

$$f(x) = \begin{cases} A \text{ when } -\frac{\delta}{2} < x < \frac{\delta}{2}, \\ 0 \text{ when } \frac{\delta}{2} < x < T - \frac{\delta}{2}. \end{cases}$$

Selecting limits of integration from $-\frac{\delta}{2}$ to $T-\frac{\delta}{2}$, we find

$$\bar{c}_k = \frac{1}{T}\int_{-\frac{\delta}{2}}^{T-\frac{\delta}{2}} f(x)e^{-i2\pi k\frac{x}{T}}dx = \frac{1}{T}\int_{-\frac{\delta}{2}}^{\frac{\delta}{2}} Ae^{-i2\pi k\frac{x}{T}}dx = \frac{A}{k\pi}\frac{e^{ik\frac{\pi\delta}{T}} - e^{-ik\frac{\pi\delta}{T}}}{2i} = \frac{A\delta}{T}\left[\frac{\sin\left(\frac{k\pi\delta}{T}\right)}{\frac{k\pi\delta}{T}}\right].$$

A square-bracketed function of the type (sin z)/z is shown in Fig. 1.5. It oscillates with a period 2π, decreasing in amplitude with increasing z and passing through zero at the points $z=\pm\pi$, $\pm 2\pi$, $\pm 3\pi$, etc.

Thus,

$$\bar{c}_k = \frac{A\delta}{T} \frac{\sin\left(\frac{\pi k\delta}{T}\right)}{\frac{\pi k\delta}{T}}, \qquad (1.10a)$$

$$f(x) = \frac{A\delta}{T} \sum_{k=-\infty}^{\infty} \frac{\sin\left(\frac{\pi k\delta}{T}\right)}{\frac{\pi k\delta}{T}} e^{i\frac{2\pi kx}{T}}. \qquad (1.10b)$$

It follows from formula (1.10a) that $\bar{c}_k$ is real; therefore, a single spectrum (the amplitude spectrum) suffices for a frequency representation of the function f(x). Since k can assume values ±1, ±2, ±3, etc., the spectrum found is a discrete function that only exists at frequencies $\omega=0$, $\pm\frac{2\pi}{T}$, $\pm\frac{4\pi}{T}$, $\pm\frac{6\pi}{T}$, etc. with the corresponding amplitudes:

$$\frac{A\delta}{T}, \quad \frac{A\delta}{T}\frac{\sin\frac{\pi\delta}{T}}{\frac{\pi\delta}{T}}, \quad \frac{A\delta}{T}\frac{\sin\frac{2\pi\delta}{T}}{\frac{2\pi\delta}{T}} \quad \text{etc.}$$

Shown in Fig. 1.6 are the spectra for the following values of T and δ:

(a) $T=\frac{1}{4}$, $\delta=\frac{1}{20}$; (b) $T=\frac{1}{2}$, $\delta=\frac{1}{20}$; (c) $T=1$, $\delta=\frac{1}{20}$.

It follows from an inspection of Fig. 1.6 that the frequency $\frac{2\pi}{T}$ decreases with increasing period T. As a result, the number of frequency components per unit frequency increases. In other words, as the period T increases, the spectral lines converge but the amplitudes of the frequency components decrease. The shape of the frequency spectrum remains unchanged, i.e., the envelope of the spectrum depends solely on the pulse shape, but not on the repetition period T.

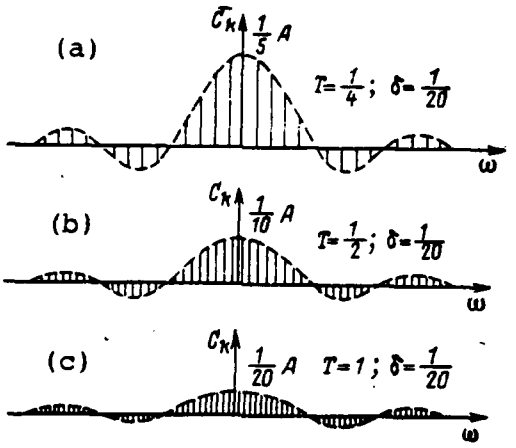

Fig. 1.6. Spectra of a rectangular periodic function for various repetition periods.

Expressions for the Fourier series may be written analogously for a function of several variables. For example, if the function f(x, y, z) satisfies the periodicity criterion, i.e.,

$$f(x, y, z)=f(x+kT_x,\ y+mT_y,\ z+nT_z),$$

where T_x, T_y, and T_z are the signal repetition periods, then the Fourier series assumes the form

$$f(x, y, z)=a_{000}+\sum_{k=1}^{\infty}\sum_{m=1}^{\infty}\sum_{n=1}^{\infty}\left[a_{kmn}\cos\left(\frac{2\pi k}{T_x}x+\frac{2\pi m}{T_y}y+\right.\right.$$
$$\left.\left.+\frac{2\pi n}{T_z}z\right)+b_{kmn}\sin\left(\frac{2\pi k}{T_x}x+\frac{2\pi m}{T_y}y+\frac{2\pi n}{T_z}z\right)\right]. \quad (1.11)$$

The coefficients of the series are determined by the formulas

$$\left.\begin{matrix}a_{kmn}\\ b_{kmn}\end{matrix}\right| =\frac{8}{T_xT_yT_z}\int_{-\frac{T_x}{2}}^{\frac{T_x}{2}}\int_{-\frac{T_y}{2}}^{\frac{T_y}{2}}\int_{-\frac{T_z}{2}}^{\frac{T_z}{2}} f(x, y, z)\left|\begin{matrix}\cos\\ \sin\end{matrix}\right|\left(\frac{2\pi k}{T_x}x+\right.$$
$$\left.+\frac{2\pi m}{T_y}y+\frac{2\pi n}{T_z}z\right)dx\,dy\,dz \quad (1.12)$$

$$\left(\begin{matrix} k \\ m \\ n \end{matrix} \right| = 1, 2, 3, \ldots \Bigg).$$

The Fourier series is written in complex form as follows:

$$f(x, y, z) = \sum_{k=-\infty}^{\infty} \sum_{m=-\infty}^{\infty} \sum_{n=-\infty}^{\infty} c_{kmn} e^{i\left(\frac{2\pi k}{T_x} x + \frac{2\pi m}{T_y} y + \frac{2\pi n}{T_z} z\right)}, \tag{1.13}$$

where

$$c_{kmn} = \frac{1}{T_x T_y T_z} \int_{-\frac{T_x}{2}}^{\frac{T_x}{2}} \int_{-\frac{T_y}{2}}^{\frac{T_y}{2}} \int_{-\frac{T_z}{2}}^{\frac{T_z}{2}} f(x, y, z) \times$$

$$\times e^{-i\left(\frac{2\pi k}{T_x} x + \frac{2\pi m}{T_y} y + \frac{2\pi n}{T_z} z\right)} dx\, dy\, dz. \tag{1.14}$$

The real coefficients a_{kmn} and b_{kmn} of series (1.11) are related to the complex coefficients c_{kmn} of series (1.13) by the equation

$$2c_{kmn} = a_{kmn} - ib_{kmn}. \tag{1.15}$$

A Fourier expansion also can be applied to nonperiodic functions. Any one-dimensional nonperiodic function f(x) that satisfies the Dirichlet conditions and that is integrable over an infinite range can be represented as the sum of an infinite set of harmonic components:

$$f(x) = \sum_{-\infty}^{\infty} \bar{c}_k e^{i 2\pi k \frac{x}{T}} =$$

$$= \sum_{-\infty}^{\infty} \frac{1}{T} \left[\int_{-\frac{T}{2}}^{\frac{T}{2}} f(x) e^{-i 2\pi k \frac{x}{T}} dx \right] e^{i 2\pi k \frac{x}{T}}. \tag{1.16}$$

Replacing the repetition period of the function by the first harmonic frequency ($u_1=1/T$), we have

$$f(x)=\sum_{-\infty}^{\infty}\left[\int_{-\frac{T}{2}}^{\frac{T}{2}} f(x)e^{-i2\pi ukx}\,dx\right]e^{i2\pi ukx}u_1. \qquad (1.17)$$

Upon passage to the limit, when $T\to\infty$, the discrete values of the frequencies ku are converted to the present frequencies u, and the first harmonic frequency is converted to a differential; hence,

$$f(x)=\int_{-\infty}^{\infty}\left[\int_{-\infty}^{\infty} f(x)\varkappa(-2\pi ux)\,dx\right]\varkappa(2\pi ux)\,du, \qquad (1.18)$$

where $e^{ix}=\varkappa(x)$.

The inner integral of expression (1.18)

$$g(iu)=\int_{-\infty}^{\infty} f(x)\varkappa(-2\pi ux)\,dx \qquad (1.19)$$

is the direct Fourier transform of the function f(x), designated $\Phi[f(x)]$, and the outer integral

$$f(x)=\int_{-\infty}^{\infty} g(iu)\varkappa(2\pi ux)\,du \qquad (1.20)$$

is the inverse Fourier transform, symbolized $\Phi^{-1}[f(x)]$. Let us note that the mathematical operations of the direct and inverse transformations differ only in the sign of the exponent in the integrand.

The difference between a Fourier series and a Fourier integral is that a Fourier series is a periodic function in the form of a sum of an infinite number of sinusoids with frequencies that have defined discrete values, whereas a Fourier integral is an aperiodic function of a sum of periodic components with a continuous sequence of frequencies.

The function g(iu) is called the complex spectrum of an aperiodic function; it may be written as the sum of two functions:

$$g(iu)=A(u)+iB(u) \qquad (1.21)$$

or as the product

$$g(iu)=g(u)e^{i\psi(u)} \qquad (1.22)$$

where A(u), B(u), g(u), and $\psi(u)$ are the real, imaginary, amplitude, and phase characteristics of the spectrum, respectively.

It follows from the formula

$$f(x)=\int_{-\infty}^{\infty} g(iu)e^{i2\pi ux}du$$

that the aperiodic function f(x) may be considered as the continuous sum of exponential functions having frequencies from $-\infty$ to $+\infty$. The amplitude of the component at any frequency is proportional to g(iu); hence g(iu) is the spectrum of the function f(x) and is called the spectral density function. Let us note that the spectrum of an aperiodic function is depicted as a continuous curve, and not as discrete points or lines, and is said to be a continuous spectrum.

The Fourier transform enables us to represent a given signal in terms of exponential components. The function g(iu), the direct Fourier transform of a signal f(x), characterizes the relative amplitudes of different frequency components, i.e., it represents the signal f(x) in the frequency domain. In the general case the function g(iu) is complex, and graphs of the amplitude spectrum g(u) and phase spectrum $\psi(u)$ are needed to represent it. In many cases, however, g(iu) is either a real or an imaginary function, so its representation is limited to a single graph of the spectrum.

It follows from the formula for a Fourier transform that it exists if the integral $\int_{-\infty}^{\infty} f(x)\kappa(-2\pi ux)dx$ has a finite value. Since

the modulus of $\kappa(-2\pi ux)$ is equal to unity, the condition for the existence of a Fourier transform of the function f(x) is that the integral $\int_{-\infty}^{\infty} |f(x)|dx$ have a finite value. This condition is sufficient but not necessary. Such functions as the sine, cosine, and Heaviside's function do not meet this criterion and strictly speaking do not have a Fourier transform. However, in the limit there also is a Fourier transform for these functions [16, 20].

For a two-dimensional aperiodic function f(x, y) the Fourier transforms are expressed by the following relations:

$$g(iu, iv) = \iint_{-\infty}^{\infty} f(x, y) e^{-2\pi i(ux+vy)}\, dx\, dy^*, \qquad (1.23)$$

$$f(x, y) = \iint_{-\infty}^{\infty} g(iu, iv) e^{2\pi i(ux+vy)} du\, dv. \qquad (1.24)$$

A number of theorems that are used extensively in solving various practical problems stem from basic definition (1.19) of a Fourier transform [3, 16, 20].

Theorem of Linearity:

$$\Phi[af_1(x, y)+bf_2(x, y)] = a\Phi[f_1(x, y)]+ \\ +b\Phi[f_2(x, y)], \qquad (1.25)$$

i.e., the Fourier transform of the sum of two functions is equal to the sum of their transforms.

Similarity Principle

If $\Phi[f(x, y)]=g(iu, iv)$,

* When only one limit of integration is indicated above or below the double integral symbol, this limit applies to integration over both variables.

then

$$\Phi[f(ax, by)] = \frac{1}{|ab|} g\left(i\frac{u}{a}, i\frac{v}{b}\right), \qquad (1.26)$$

i.e., stretching of coordinates in the space domain (x, y) leads to contraction of coordinates in the frequency domain (u, v) and to a change in the overall amplitude of the spectrum.

Translation Property

If $\Phi[f(x, y)] = g(iu, iv)$, then

$$\Phi[f(x-a, y-b)] = g(iu, iv) \times (-2\pi au - 2\pi bv), \quad (1.27)$$

i.e., a shift of a function in the space domain causes a linear frequency shift in the frequency domain.

Parseval's Theorem

If $\Phi[f(x, y)] = g(iu, iv)$, then

$$\int_{-\infty}^{\infty}\int |f(x, y)|^2 dx\, dy = \int_{-\infty}^{\infty}\int |g(iu, iv)|^2 du\, dv. \qquad (1.28)$$

Convolution Theorem

If $\Phi[f_1(x, y)] = g_1(iu, iv)$ and $\Phi[f_2(x, y)] = g_2(iu, iv)$, then

$$\Phi[f_1(x, y) f_2(x, y)] =$$
$$= \int_{-\infty}^{\infty}\int g_1(u-u', v-v') g_2(u', v')\, du'\, dv', \qquad (1.29)$$

i.e., the Fourier transform of the product of two functions $f_1(x, y)$ $f_2(x, y)$ is expressed in terms of the transforms $g_1(iu, iv)$ and $g_2(iu, iv)$ by means of an integration operation called the convolution of the functions g_1 and g_2.

In frequency analysis the convolution theorem is an important theorem. Let us recall that the convolution of two given functions $f_1(t)$ and $f_2(t)$ is defined by an integral

$$f(t)=\int_{-\infty}^{\infty} f_1(\tau) f_2(t-\tau)\, d\tau,$$

which is symbolically written as

$$f(t)=f_1(t) * f_2(t).$$

By analogy with multiplication algebra, we can derive the following laws of convolution algebra:

commutative law:

$$f_1(t) * f_2(t)=f_2(t) * f_1(t);$$

distributive law:

$$f_1(t) * [f_2(t)+f_3(t)]=f_1(t) * f_2(t)+f_1(t) * f_3(t);$$

associative law:

$$f_1(t) * [f_2(t) * f_3(t)]=[f_1(t) * f_2(t)] * f_3(t).$$

To provide a graphic illustration of the convolution operation, we will assume that the function $f_1(t)$ has a rectangular form, while $f_2(t)$ has a triangular form (Fig. 1.7a). Let us find the convolution of these functions graphically. By definition,

$$f_1(t) * f_2(t)=\int_{-\infty}^{\infty} f_1(\tau) f_2(t-\tau)\, d\tau.$$

Here τ is an independent variable.

The functions $f_1(\tau)$ and $f_2(-\tau)$ are shown in Fig. 1.7b. The graph of the function $f_2(t-\tau)$ for $t=t_1$ is the function $f_2(-\tau)$ shifted by an amount $t=t_1$ in the positive direction (Fig. 1.7c). The convolution of

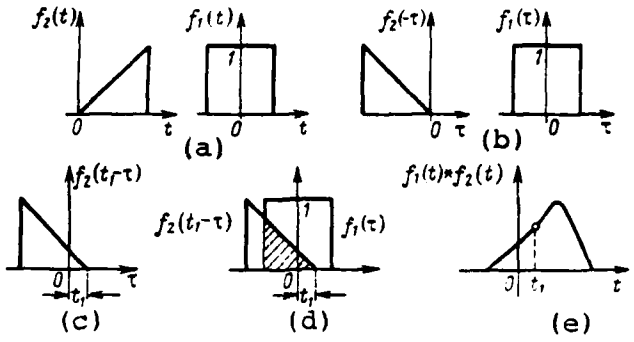

Fig. 1.7. Graphic representation of the convolution operation.

the functions $f_1(t)$ and $f_2(t)$ for $t=t_1$ is determined by the area under the curve of $f_1(\tau)f_2(t_1-\tau)$. This area is hatched in Fig. 1.7d and is plotted as a dashed line in Fig. 1.7e. The values of the convolution can be obtained in an analogous fashion for different t. As a result we obtain the graph shown in Fig. 1.7e.

Let us also note that the convolution of a function f(t) with a Heaviside function gives the function f(t) itself, i.e.,

$$f(t) * \delta(t) = \int_{-\infty}^{\infty} f(t)\delta(t-\tau)d\tau = f(t).$$

The Fourier transforms of some functions are presented in Table 1.2, and the values of the functions $\sin c(x)=\frac{\sin \pi x}{x}$ and $\frac{2I_1(z)}{z}$ that are needed to calculate the Fourier transforms are given in Tables 1.3 and 1.4 [16, 20, 27].

Let us recall that the first-order Bessel function $I_1(z)$ is defined by the relation

$$I_1(z)=\frac{1}{\pi}\int_0^{\pi}\cos(z\sin\varphi-\varphi)d\varphi,$$

and can be calculated by using the series

$$I_1(z)=\frac{z}{2}-\frac{z^3}{16}+\frac{z^5}{384}-\frac{z^7}{18432}+\ldots,$$

Table 1.2. Fourier Transforms of Frequently Encountered Functions

(a) Функция	(b) Преобразование Фурье
Прямоугольная (ступенчатая) функция (c) $f(x)=\begin{cases}1 \text{ (d) при } \lvert x\rvert<\frac{a}{2},\\ 0 \text{ при } \lvert x\rvert>\frac{a}{2}\end{cases}$ 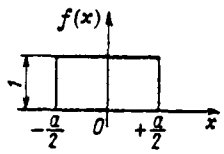	$g(u)=a\,\frac{\sin \pi a u}{\pi a u}$ 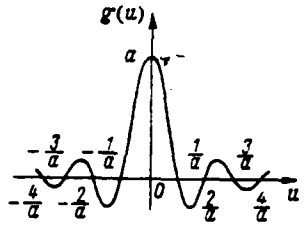
Двумерная прямоугольная функция (e) $f(x,y)=\begin{cases}1 \text{ (d) при } \lvert x\rvert<\frac{a}{2};\ \lvert y\rvert<\frac{b}{2},\\ 0 \text{ (f) в остальных точках}\end{cases}$ 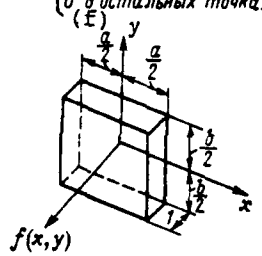	$g(u,v)=ab\,\frac{\sin \pi a u}{\pi a u}\cdot\frac{\sin \pi b v}{\pi b v}$ 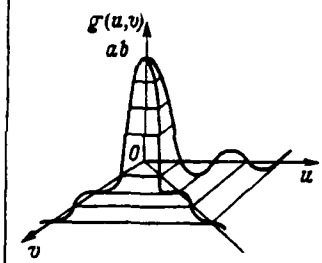
(g) Круговая функция $f(x,y)=\begin{cases}1 \text{ (d) если } x^2+y^2=z^2\begin{cases}\leqslant R^2\\ >R^2\end{cases}\\ 0,\end{cases}$ 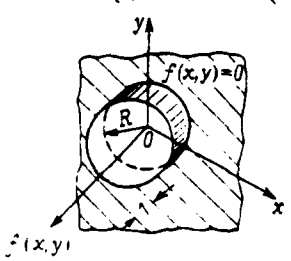	$g(u,v)=2\pi R^2\,\frac{J_1(2\pi R\sqrt{u^2+v^2})}{2\pi R\sqrt{u^2+v^2}}$ 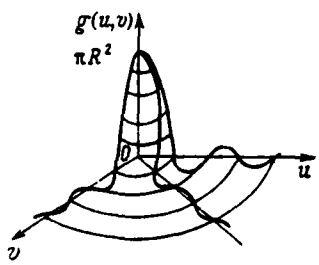

Key: (a) function; (b) Fourier transform; (c) rectangular (step) function; (d) if; (e) two-dimensional rectangular function; (f) elsewhere; (g) circular function.

while for large values of z,

$$J_1(z)\approx\frac{\sin\left(z-\frac{\pi}{4}\right)}{\sqrt{\frac{\pi}{2}z}}.$$

Table 1.2, continued

(a) Функция	(b) Преобразование Фурье
(c) Треугольная функция $f(x)=\begin{cases}1-\lvert x\rvert & \lvert x\rvert\leqslant 1;\\ 0 & \text{(d) в остальных точках}\end{cases}$ 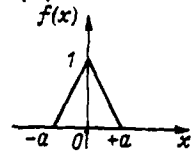	$g(u)=a\left(\frac{\sin\pi au}{\pi au}\right)^2$ 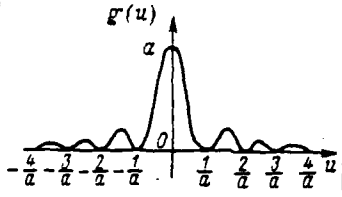
(e) Функция Гаусса $f(x)=e^{-x^2/2\sigma^2}$ 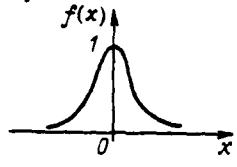	$g(u)=\sigma\sqrt{2\pi}\,e^{-2\sigma^2\pi^2u^2}$ 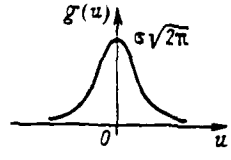
(f) Экспоненциальная функция $f(x)=e^{-a\lvert x\rvert}$ 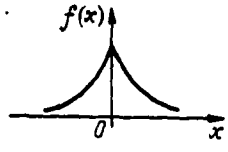	$g(u)=\frac{2a}{a^2+4\pi^2u^2}$ 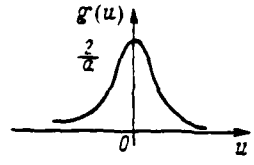
(g) Функция знака $f(x)=\begin{cases}1 & \text{при } x>0,\\ -1 & \text{при } x<0\end{cases}$ (h) 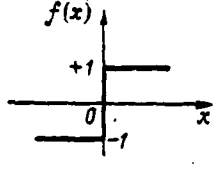	$g(u)=\frac{1}{i\pi u}$ 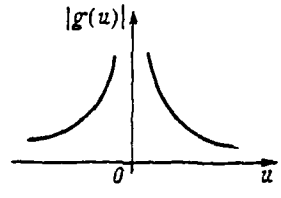

Key: (a) function; (b) Fourier transform; (c) triangular function; (d) elsewhere; (e) Gaussian function; (f) exponential function; (g) sign function; (h) if.

The zero-order Bessel function is expressed by the formula

$$I_0(z)=\frac{1}{\pi}\int_0^{\pi}\cos(z\cos\varphi)\,d\varphi.$$

Table 1.2, continued

(a) Функция	(b) Преобразование Фурье
(c) Дельта-функция Дирака $f(x)=\delta(x)=0$ при $t\neq 0$ $\int_{-\infty}^{\infty}\delta(x)\,dx=1$ 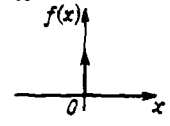	$g(u)=1$ 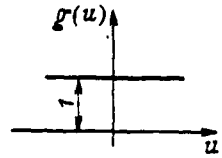
(d) Гребенчатая функция $f(x)=\sum_{n=-\infty}^{\infty}\delta(x-nT)$ 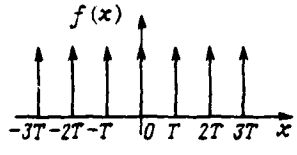	$g(u)=\frac{2\pi}{T}\sum_{k=-\infty}^{\infty}\delta\left(u-\frac{2\pi k}{T}\right)$ 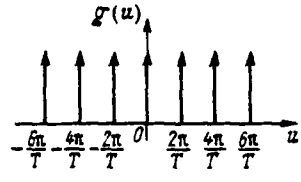
Косинусоидальная функция (e) $f(x)=\cos\omega x$ 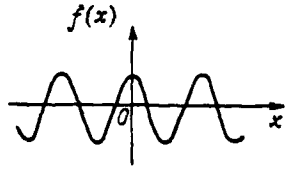	$g(u)=\pi\left[\delta(2\pi u-\omega)+\delta(2\pi u+\omega)\right]$ 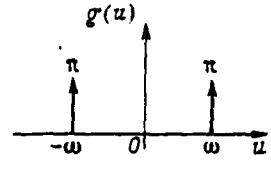
(f) Синусоидальная функция $f(x)=\sin\omega x$ 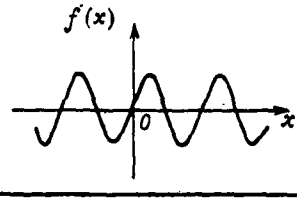	$g(u)=i\pi\left[\delta(2\pi u-\omega)-\delta(2\pi u+\omega)\right]$ 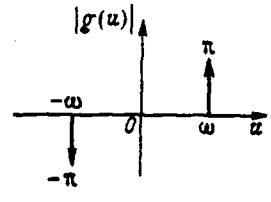

Key: (a) function; (b) Fourier transform; (c) Dirac delta function; (d) comb function; (e) cosine function; (f) sine function.

The function $I_0(z)$ can be calculated by using the series

$$I_0(z)=1-\frac{z^2}{4}+\frac{z^4}{64}-\frac{z^6}{2304}+\ldots,$$

Table 1.3. Values of the Functions sinc x and $\text{sinc}^2 x$

x	$\text{sinc}\, x$	$\text{sinc}^2 x$	$\text{sinc}(x+\pi)$	$\text{sinc}^2(x+\pi)$	$\text{sinc}(x+2\pi)$	$\text{sinc}^2(x+2\pi)$
0	1,0	1,0	0,0	0,0	0,0	0,0
$\frac{\pi}{4}$	0,9003	0,8105	—0,1801	0,0324	0,1001	0,0100
$\frac{\pi}{2}$	0,6366	0,4053	—0,2122	0,0450	0,1274	0,0162
$\frac{3}{4}\pi$	0,3001	0,0901	—0,1286	0,0165	0,0819	0,0067

Table 1.4. Values of the Functions $\frac{2I_1(z)}{z}$ and $\left[\frac{2I_1(z)}{z}\right]^2$

z	$\frac{2I_1(z)}{z}$	$\left[\frac{2I_1(z)}{z}\right]^2$	z	$\frac{2I_1(z)}{z}$	$\left[\frac{2I_1(z)}{z}\right]^2$
0	1,0	1,0	5,0	—0,1310	0,0172
1,0	0,08801	0,7746	6,0	—0,0922	0,0085
2,0	0,5767	0,3326	7,0	—0,0013	0,0000
3,0	0,2260	0,0511	8,0	0,0587	0,0034
3,832	0,0	0,0	9,0	0,0545	0,0030
4,0	—0,0330	0,0011	10,0	0,0087	0,0001

while for large values of z

$$I_0(z) \approx \frac{\cos\left(z-\frac{\pi}{4}\right)}{\sqrt{\frac{\pi}{2}z}}.$$

The functions $I_1(z)$ and $I_0(z)$ are interrelated by the equation

$$2\int_0^n \frac{I_1^2(z)}{z}dz = 1-\left[I_0^2(n)+I_1^2(n)\right].$$

1.3. Spatial Frequency Spectra of Radiating Objects and Backgrounds

Let there be a flat emitter that has a radiance distribution B(y, z). The variables y and z are the coordinates of some point of

of the object in a Cartesian coordinate system yOz selected so that the plane yOz is perpendicular to a specified direction.

For objects with noncoherent self-radiation, by radiance we mean the power per unit area of emitting surface in a solid angle of 1 steradian that corresponds to a unit wavelength interval near the wavelength λ.

The Fourier transform of the function B(y, z) will be written as

$$b(iu, iv)=\int\limits_{-\infty}^{\infty}\int B(y, z)\times[-2\pi(uy+vz)]\,dy\,dz; \quad (1.30)$$

$$B(y, z)=\int\limits_{-\infty}^{\infty}\int b(iu, iv)\times[2\pi(uy+vz)]\,du\,dv. \quad (1.31)$$

The quantities u and v, the inverse periods of the harmonics that describe the distribution of an object's radiance along the directions y and z, are called the spatial frequencies by analogy with frequency in the generally accepted sense of the word which we obtained [sic] if the function depended on just one variable--time. If the dimension of the temporal frequency is 1/s, then the dimension of the spatial frequency is a unit of length to the power -1.

Thus, the distribution of an object's radiance may be represented as the superposition of an infinite set of various harmonic components each of which can be characterized in terms of amplitude, phase, and spatial frequency. Such a representation of a two-dimensional function of radiance makes it possible to bring into consideration the notion of the spatial frequency spectrum, which plays an important part in the analysis of modulators.

Let us examine the main differences between spatial and temporal harmonic oscillations. The frequencies of temporal oscillations may range from 0 to $+\infty$, since time cannot be negative; spatial frequencies can assume values from $-\infty$ to $+\infty$.

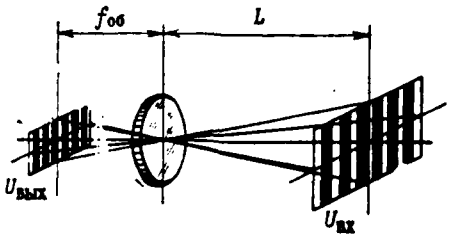

Fig. 1.8. Change in the frequency of a spatial harmonic upon passage through an optical element.

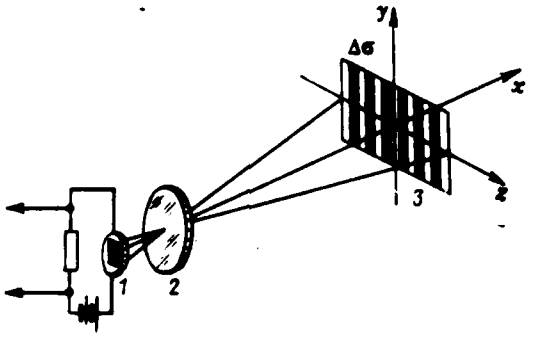

Fig. 1.9. Diagram illustrating the conversion of a spatial frequency into a temporal frequency of changing electrical current. (1) radiant-energy detector; (2) objective; (3) plane of object.

Upon passing through linear dynamic sections, temporal (electrical) harmonics undergo a change in amplitude and phase while maintaining unchanged frequencies. Upon passing through optical elements, spatial harmonics may undergo a change in both amplitude and phase on the one hand, and spatial frequency on the other. For example, if the magnification of an optical element is β, and the spatial frequency at its input is $u_{вх}$, then the value of the spatial frequency at the output of the element will be

$$u_{вых}=u_{вх}\frac{1}{\beta} \qquad (1.32)$$

where $\beta=\frac{f_{об}}{L}$ according to the symbols used in Fig. 1.8.

The spatial frequency u can be converted into the temporal frequency f* of an electrical current, as shown in Fig. 1.9. At every instant a section of the image having an area $\Delta\sigma$ is projected by the optical system onto a radiant-energy detector [PLE]. The load resistance of the radiant-energy detector will cause an electrical current to flow with a frequency

$$f^*=Vu \qquad (1.33)$$

where V is the scan rate.

The spatial frequencies of different regions of the spatial frequency spectrum play different parts in the construction of images of radiating objects. The low-frequency components carry primary information on extended distributions of radiance, on large details, and on uniformly radiating regions of the object. Medium-frequency components of the spatial frequency spectrum of signals are important for correct reproduction of tones, and high-frequency components are important in the construction of small details, sharp transitions, and image contours. If low- and medium-frequency components are reproduced without distortion while the high-frequency components are attenuated, small details and sharp borders of the object will be conveyed poorly in the resultant images.

Returning to formulas (1.30) and (1.31), let us note that the function b(iu, iv) is a complex function of the spatial frequencies. The aggregate of the moduli of b(iu, iv) is called the spatial frequency spectrum of the function B(y, z).

The function b(iu, iv) is the spectral density of the function B(y, z) and is expressed by a direct Fourier transform. The expression of the function B(y, z) in terms of its spectrum is the inverse Fourier transform.

The function B(y, z) often may be assumed symmetric relative to the origin; in this case, assuming

$$z=\varrho\cos\psi,\quad y=\varrho\sin\psi,$$
$$2\pi u=w\cos\varphi,\quad 2\pi v=w\sin\varphi$$

and inserting the new variables into Fourier integral (1.30),, we obtain

$$b(lw,\varphi)=\int_0^{\infty}\int_0^{2\pi}B(\varrho,\psi)\times[-\varrho w(\cos\varphi\cos\psi+\sin\varphi\sin\psi)]\times \times\varrho d\varrho d\psi. \qquad (1.34)$$

We write

$$\psi-\varphi=\theta,\ b(lw,\varphi)=b(w)e^{in\varphi},$$
$$B(\varrho,\psi)=l^{-n}s(\varrho)e^{in\psi},$$

then

$$b(w)=l^{-n}\int_0^{\infty}\int_0^{2\pi}s(\varrho)\times(-\varrho w\cos\theta+n\theta]\,\varrho d\varrho\,d\theta, \qquad (1.35)$$

or

$$b(w)=2\pi\int_0^{\infty}\varrho J_n(\varrho w)s(\varrho)d\varrho, \qquad (1.36)$$

where

$$J_n(\varrho w)=\frac{i^{-n}}{2\pi}\int_0^{2\pi}e^{-i\varrho w\cos\theta+in\theta}d\theta$$

is the integral representation of a Bessel function.

Expression (1.36) is called the Hankel transform of the function $s(\rho)$. The inverse Hankel transform is defined by the integral

$$s(\varrho)=\int_0^{\infty}wJ_n(\varrho w)b(w)dw, \qquad (1.37)$$

or

$$B(\varrho,\psi)=l^ne^{-in\psi}\int_0^{\infty}wJ_n(\varrho w)b(w)dw. \qquad (1.38)$$

If the function B(y, z) is symmetric with respect to the origin, then n=0, $s(\rho)=B(\rho)$, and a zero-order Bessel function must be inserted into the Hankel integral. We obtain

$$b(w)=2\pi\int_0^\infty \varrho J_0(\varrho w)B(\varrho)d\varrho, \qquad (1.39)$$

$$B(\varrho)=2\pi\int_0^\infty \varrho J_0(\varrho w)b(w)dw. \qquad (1.40)$$

The Hankel transform is distinguished by the following property:

$$b\left(\frac{w}{a}\right)=a^2 2\pi\int_0^\infty \varrho J_0(\varrho w)B(a\varrho)d\varrho, \qquad (1.41)$$

whence it follows that when the function B is expanded in space, its spectrum narrows.

If the object's radiance varies not only in space, but also in time (as is characteristic of "flashing" or fast-moving objects), then it is described as a function of three variables, B(y, z, t), for which a Fourier transform can be found. In the particular case where the function B depends only on time, we have

$$b(f^*)=\int_{-\infty}^{\infty} B(t)e^{-2\pi f^* t}dt. \qquad (1.42)$$

The function b(f*) is the spectral relation that describes a temporal spectrum.

Now let us consider the spatial frequency spectra of backgrounds. The radiation of clouds and of topographic details of the relief of the earth's surface, inhomogeneous atmospheric radiation, and reflected or scattered radiation from various sources have the feature that the radiation field they produce can only be represented as a random function of radiance that obeys some statistical laws. Therefore, isolating useful information on an object that is against a radiating background entails major difficulties.

The full diversity of backgrounds usually is divided into "ensembles" (e.g., forest or steppe landscapes, large urban areas, continuous cloud cover, etc.) which have certain statistical characteristics of a random two-dimensional radiance function. Moreover, a random radiance function is assumed stationary in many cases in order greatly to simplify the mathematical conversions. For example, it has been established that the random function that describes a bright background is nonstationary in the general case. However, the background of a cloudy sky nonetheless may be assumed steady at small angles from the directions to the sun and horizon [18, 25].

A peculiarity of random functions that must be dealt with in the design of optoelectronic devices is the fact that they usually are not sign-alternating, and their values always are positive. The corresponding signals at the output of the radiant-energy detector also are unipolar.

The set of statistical characteristics of a random function that is simplest for mathematical processing includes the mathematical expectation, the dispersion, and the correlation function.

The mathematical expectation of a random two-dimensional radiance function $B(y, z)$ when there are several realizations of the function is the "average" function about which specific realizations of the random radiance function vary in different ways:

$$m(y, z)=M[B_n(y, z)] \qquad (1.43)$$

where n is the number of the realization.

The dispersion of a random two-dimensional function characterizes the spread of possible realizations of the random function with respect to the mathematical expectation:

$$D(y, z)=M[B_n(y, z)-m(y, z)]^2 \qquad (1.44)$$

The correlation function shows the degree of interrelation of the quantities of a two-dimensional radiance function at two adjacent points having coordinates (y, z) and $(y+\Delta y, z+\Delta z)$:

$$K[(y, z)(y+\Delta y, z+\Delta z)]=M\{[B(y, z)-m(y, z)]\times$$
$$\times[B(y+\Delta y, z+\Delta z)-m(y+\Delta y, z+\Delta z)]\}. \quad (1.45)$$

When $\Delta y=0$ and $\Delta z=0$, the correlation function becomes the dispersion of a random function. Thus, the need vanishes for the dispersion as a separate characteristic of a random function; the mathematical expectation and correlation function may be adopted as its basic characteristics.

If the random function is stationary, then its correlation function depends solely on the quantities Δy and Δz and is independent of y and z.

The spatial frequency properties of stationary random functions are characterized by a so-called Khinchine-Wiener spectrum (X-B), which is the dependence of the spectral density of the dispersion of a random function on the spatial frequency.

The Khinchine-Wiener spectrum of a random function B(y, z) of the spatial distribution of radiance is defined as follows. Let the random function B(y, z) be defined in the domain

$$|y|\leq A; \quad |z|\leq C$$

The Fourier transform of this function

$$b(u, v)=\int_{-A}^{A} dy \int_{-C}^{C} B(y, z)\times[-2\pi(uy+vz)]\,dz \quad (1.46)$$

has a property defined by the equation:

$$\int_{-A}^{A}\int_{-C}^{C}|B(y, z)|^2\,dy\,dz=\int_{-\infty}^{\infty}\int_{-\infty}^{\infty}|b(u, v)|^2\,du\,dv, \quad (1.47)$$

i.e., the integral of the square of the function in question over its domain is equal to the integral of the square of the modulus of the amplitude spectrum over the entire spatial frequency domain.

The correlation function $K_B(\Delta y, \Delta z)$ of a random function B(y, z) is defined by the expression

$$K_B(\Delta y, \Delta z)=\lim_{\substack{A\to\infty\\ C\to\infty}} \frac{1}{4AC}\int_{-A}^{A}\int_{-C}^{C} B(y, z)\times$$
$$\times \tilde{B}(y+\Delta y, z+\Delta z)\,dy\,dz, \qquad (1.48)$$

where $\tilde{B}(y+\Delta y, z+\Delta z)$ is the complex-conjugate function of the function $B(y+\Delta y, z+\Delta z)$.

The inverse Fourier transform of the function b(u, v) has the form:

$$B(\Delta y, \Delta z)=\int_{-\infty}^{\infty} b(u, v)\times[2\pi(u\Delta y+v\Delta z)]\,du\,dv. \qquad (1.49)$$

Inserting expression (1.49) into (1.48), we obtain

$$K_B(\Delta y, \Delta z)=\lim_{\substack{A\to\infty\\ C\to\infty}} \frac{1}{4AC}\int_{-A}^{A}\int_{-C}^{C} B(y, z)\,dy\,dz\times$$
$$\times\int_{-\infty}^{\infty}\int \tilde{b}(u, v)\times\{-2\pi[u(y-\Delta y)+v(z-\Delta z)]\}\,du\,dv. \qquad (1.50)$$

Since the function B(y, z) is square-integrable, the integration order in equation (1.50) may be changed:

$$K_B(\Delta y, \Delta z)=\lim_{\substack{A\to\infty\\ C\to\infty}} \frac{1}{4AC}\int_{-\infty}^{\infty}\int \tilde{b}(u, v)\times\{2\pi[u\Delta y+v\Delta z]\}\,du\,dv$$
$$\times\int_{-A}^{A}\int_{-C}^{C} B(y, z)\times[-2\pi(uy+vz)]\,dy\,dz. \qquad (1.51)$$

Using equation (1.46), we find

$$K_B(\Delta y,\ \Delta z)=\lim_{\substack{A\to\infty\\C\to\infty}}\frac{1}{4AC}\int\limits_{-\infty}^{\infty}\int b(u,v)\,\tilde{b}(u,\ v)\times$$

$$\times\times[2\pi(u\Delta y+v\Delta z)]\,du\,dv=$$

$$=\lim_{\substack{A\to\infty\\C\to\infty}}\frac{1}{4AC}\int\limits_{-\infty}^{\infty}\int|b(u,\ v)|^2\times[2\pi(u\Delta y+v\Delta z)]\,du\,dv. \qquad (1.52)$$

The limit $\lim\limits_{\substack{A\to\infty\\C\to\infty}}\frac{1}{4AC}|b(u,\ v)|^2=b_{X-B}(u,\ v)$ is the Khinchine-Wiener spectrum or the spectral density of the dispersion of the random spatial distribution of radiance.

Obviously,

$$K_B(\Delta y,\ \Delta z)=\int\limits_{-\infty}^{\infty}b_{X-B}(u,\ v)\times[2\pi(u\Delta y+v\Delta z)]\,du\,dv, \qquad (1.53)$$

$$b_{X-B}(u,\ v)=\frac{1}{(AC)}\int\int[K_B(\Delta y,\Delta z)\times$$

$$\times\times[-2\pi(u\Delta y+v\Delta z)]\,d(\Delta y)\,d(\Delta z), \qquad (1.54)$$

i.e., there exists a relation describable by a Fourier transform between the Khinchine-Wiener spectrum of a random function B(y, z) and its correlation function; the correlation function of a random function B(y, z) can be obtained as the inverse Fourier transform of the Khinchine-Wiener spectrum.

Formula (1.54) can be used to determine the Khinchine-Wiener spectrum of an ergodic background process, i.e., when the correlation function can be obtained from one realization of the random function B(y, z) for a sufficiently large area in which it is defined.

For stationary and isotropic random radiance functions, the correlation functions and Khinchine-Wiener spectra are expressed by functions of two variables that have circular symmetry in the coordinate systems $(\Delta y, \Delta z)$ and (u, v). This makes it possible to depict

these functions graphically as corresponding one-dimensional cuts. A complete two-dimensional representation of the functions can be obtained by rotating the one-dimensional cuts about the vertical axis.

Examples can be cited of functions $b_{X-B}(u, v)$ that are encountered in infrared equipment design practice [5, 25]. A spectrum of the following type is used to represent an anisotropic cloud background:

$$b(u, v)=4\pi\Delta y\,\Delta z D^2(1+u^2\Delta y^2+v^2\Delta z^2)^{-3/2}. \quad (1.55a)$$

where Δy and Δz are the so-called correlation intervals for the y and z axes, i.e., the distances at which the correlation function amounts to 37% of the dispersion D^2 of the background luminance.

In a polar coordinate system we have

$$b(w, \gamma)=2\pi\Delta\rho^2 D^2 \sin 2\vartheta\,[1+w^2F(\gamma)]^{-3/2}, \quad (1.55b)$$

where

$$\Delta y=\Delta\rho\cos\vartheta; \quad \Delta z=\Delta\rho\sin\vartheta;$$
$$F(\gamma)=2(\sin^2\gamma\sin^2\vartheta+\cos^2\gamma\cos^2\vartheta);$$
$\Delta\rho=\sqrt{\Delta x^2+\Delta y^2}$ is the correlation radius (a quantity analogous to the correlation interval).

The deviation of the angle θ from $\pi/4$ characterizes the degree of anisotropy of the background for a constant passband with respect to the modulus w of the vector of spatial frequencies.

When $\Delta y=\Delta z=\frac{\Delta\rho}{2}$ (or when $\theta=\pi/4$ in a polar system), equation (1.55b) reduces to the form

$$b(w)=2\pi\Delta\rho^2 D^2(1+w^2\Delta\rho^2)^{-\frac{3}{2}}, \quad (1.55c)$$

which corresponds to an isotropic cloud background. The formula given in Ref. 30 has an analogous form:

$$b(w)=2\pi\Delta\rho^2 D^2(1+w^2\Delta\rho^2)^{-1}. \quad (1.55d)$$

At high frequencies function (1.55d) tends asymptotically toward the quadratic hyperbola

$$b \approx 2\pi D^2 w^{-2}$$

whose parameters are independent of the correlation radius.

It proves convenient to use the Khinchine-Wiener spectrum of a heuristic model background to estimate the noise immunity of optoelectronic devices [4.18]:

$$b(u, v) = 8D^2 \Delta y \Delta z (1 + 2u^2 \Delta y^2)^{-1} (1 + 2v^2 \Delta z^2)^{-1}, \quad (1.55e)$$

When $\Delta y \neq \Delta z$, this approximately gives background anisotropy, while when $\Delta y = \Delta z = \frac{\Delta \rho}{2}$ it corresponds to a quasi-isotropic background.

1.4. Optical Signal Conversion by Multidimensional Filters

Signal conversion in optoelectronic systems is carried out by means of various elements called filters. A distinction is made between one-dimensional and multidimensional filters. One-dimensional filters transform the spectral composition of transmitted radiation. Multidimensional filters are used to change the spatiotemporal form of signals. Below we will consider only multidimensional filters. These include lenses, condensers, diaphragms, modulating disks, and other components used to focus, change the direction of, cut off, modulate, separate, and add light beams.

A signal that carries information on an object or the surrounding background is represented by a two-dimensional radiance function; the components listed above therefore are called spatial filters as well.

Spatial filters differ essentially from electrical filters. One of the differences is that the independent variable of functions that describe processes in electrical circuits is time, which always is greater than zero in real processes, whereas in spatial filters the

independent variables of the functions are the space coordinates, which are unbounded to either side of zero. The second difference is that electrical filters are characterized by both amplitude parameters and energy parameters of signal transmission; the description of processes by means of amplitude parameters is used more often. Only the energy parameters of a signal can be registered, by contrast, in spatial filters, which work with noncoherent radiation. Finally, the signal at the output of an electrical filter is time-delayed with respect to the input signal; no such delay (in space) occurs in spatial filters.

Despite these differences, the methods employed in the study of electrical filters can be used in the theoretical investigation of spatial filters.

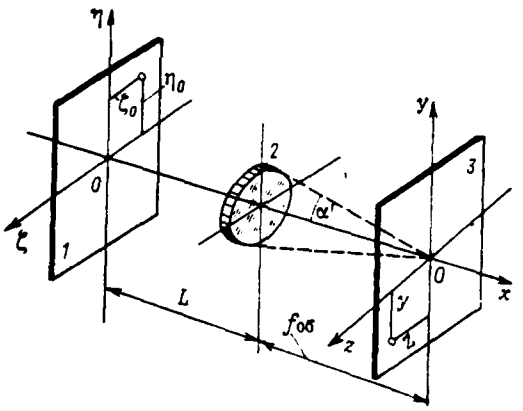

Fig. 1.10. Toward the determination of the weighting and spatial frequency transfer functions of a very simple optical system: (1) object plane; (2) objective; (3) image plane (focal plane).

The most important characteristics of multidimensional filters are the weight function, the unit step function, and the spatial frequency transfer function. We will give the definitions of these functions by using as an example a very simple optical system that consists of an objective which converts the radiance distribution

function for the object plane $\eta O\zeta$ into the irradiance distribution function for the image plane yOz (Fig. 1.10).

Let η_0, ζ_0 and y, z respectively be the coordinates of some point of the object and of its ideal image. For numerous reasons (aberration, diffraction, etc.), the image of the point extends to some small region whose irradiance distribution can be represented by the function $E_\delta(y, z)$ if the object point in question is located at the origin O, and by the function $E_\delta(y-\beta\eta_0, z-\beta\zeta_0)$ if the object point is not located at the origin; $\beta=f_{об}/L$.

The function $E_\delta(y, z)$, which describes the irradiance distribution in the image of an isolated point, is the optical system's reaction to a point source; it is called the weighting function. To avoid the difficulty associated with the presence of a point source that has a finite radiance, we use the concept of the spatial delta function (also called the Dirac function):

$$\delta(y-y_0, z-z_0)=\begin{cases}\infty \text{ if } & y=y_0 \text{ and } z=z_0;\\ 0 \text{ if } & y\neq 0 \text{ or } z\neq 0.\end{cases}$$

The spatial delta function is distinguished by the following properties:

$$\iint_{-\infty}^{\infty}\delta(y-y_0, z-z_0)\,dy\,dz=1; \qquad (1.56)$$

$$\iint_{-\infty}^{\infty}\delta(y-y_0, z-z_0)f(y, z)\,dy\,dz=f(y_0, z_0). \qquad (1.57)$$

where f(y, z) is a continuous, bounded function.

Depending on the type of weighting function, multidimensional filters are divided into stationary and nonstationary types. Whereas the weighting function of a stationary filter is independent of its movement along the coordinate axes, a nonstationary filter has such a dependence.

The function $E_\delta(y, z)$ is an important characteristic of an optical system. If we know how an optical system converts the radiance of a point source, then we can determine how it alters the object's radiance distribution function, as the object can be represented as an infinite number of point sources that have a radiance equal to the radiance of the corresponding point of the object.

By writing $\beta\eta_0=y'$ and $\beta\zeta_0=z'$ and representing the object's radiance distribution function as $B(\eta_0, \zeta_0)=B^*(y', z')$, we can obtain the irradiance distribution function of the object image $E(y, z)$ as the sum of the irradiances of the images obtained from different points of the object:

$$E(y, z)=\iint B^*(y, z)E_\delta(y-y', z-z')dy'dz'. \quad (1.58)$$

Relation (1.58) shows that $E(y, z)$ is the convolution of the functions B^* and E_δ, which may be conditionally written as

$$E(y, z)=B^* \ast E_\delta. \quad (1.59)$$

The limits of integration of (1.58) are determined by the borders of the object, i.e., by the range of real values of $B^*(y, z)$ or by the system's field of view.

We will use a Fourier transform to solve equation (1.59). Introducing the variables μ and ν, which are spatial frequencies, we may write the Fourier transform $\mathcal{G}(\mu, \nu)$ of the function $E(y, z)$ as

$$\mathcal{G}(\mu, \nu)=\iint E(y, z)\times[-2\pi(\mu y+\nu z)]dydz; \quad (1.60)$$

$$E(y, z)=\iint \mathcal{G}(\mu, \nu)\times[2\pi(\mu y+\nu z)]d\mu d\nu. \quad (1.61)$$

Replacing $E(y, z)$ by its value according to (1.58), we find

$$\mathcal{G}(\mu, \nu)=\iiiint B^*(y', z')E_\delta(y-y', z-z')\times$$
$$\times\times[-2\pi(\mu y+\nu z)]dy'dz'dydz, \quad (1.62)$$

or, using the new variables $Y=y-y'$ and $Z=z-z'$,

$$\mathcal{S}(\mu, \nu)=\iiiint B^*(y', z')\varkappa[-2\pi(\mu y'+\nu z')]\times$$
$$\times E_\delta(Y, Z)\varkappa[-2\pi(\mu Y+\nu Z)]\,dy'dz'dYdZ. \quad (1.63)$$

This expression can be easily reduced to the form

$$\mathcal{S}(\mu, \nu)=b^*(\mu, \nu)\mathcal{S}_\delta(\mu, \nu), \quad (1.64)$$

i.e., the Fourier transform of the irradiance distribution function of the object image is equal to the product of the Fourier transform of the object's radiance distribution function by the Fourier transform of the weighting function.

The direct Fourier transform of the irradiance distribution function of the image of an isolated point (of the weighting function) is called the spatial frequency transfer function [ПЧПФ] of the optical system. If the weighting function $E_\delta(y, z)$ depends on two coordinates, then the spatial frequency transfer function is

$$W(i\mu, i\nu)=\int_{-\infty}^{\infty}\int E_\delta(y, z)e^{-2\pi i(\mu y+\nu z)}dy\,dz. \quad (1.65)$$

The spatial frequency transfer function, which is the analog of the transfer function used in automatic control theory, can be represented as

$$W(i\mu, i\nu)=P(\mu, \nu)+iQ(\mu, \nu), \quad (1.66)$$

or

$$W(i\mu, i\nu)=W(\mu, \nu)e^{-\Psi(\mu, \nu)}, \quad (1.67)$$

where $P(\mu, \nu)$, $Q(\mu, \nu)$, $W(\mu, \nu)$, and $\Psi(\mu, \nu)$ respectively are the real, imaginary, amplitude, and phase frequency responses. The following relationships exist among these characteristics:

$$W(\mu, \nu)=\sqrt{[P(\mu, \nu)]^2+[Q(\mu, \nu)]^2}; \quad (1.68)$$
$$\Psi(\mu, \nu)=\operatorname{arctg}\frac{Q(\mu, \nu)}{P(\mu, \nu)}. \quad (1.69)$$

If the weighting function is axisymmetric, then the amplitude frequency response can be found by using a Hankel transform:

$$W(\omega)=2\pi\int_0^\infty \varrho J_0(\varrho\omega)\omega(\varrho)\,d\varrho,$$

where $\varrho=\sqrt{y^2+z^2}$; $\omega=2\pi\sqrt{\mu^2+\nu^2}$.

In this case $W(\omega)$ has rotational symmetry.

When the optical signal depends on three variables (the space coordinates y and z and the time t), the spatial frequency transfer function of a multidimensional filter is

$$W(i\mu, i\nu, i\xi)=\int_{-\infty}^{\infty}\int\int E_\delta(y, z, t)e^{-2\pi i(\mu y+\nu z+\xi t)}dy\,dz\,dt. \quad (1.70)$$

In order to give a physical interpretation of the spatial frequency transfer function, let us examine the expressions for the input and output signals of a multidimensional filter. As noted above, the light signal $\varphi_0(y, z)$ at the filter's input can be represented as an infinite sequence of spatial delta functions. Based on property (1.57) of the delta function, we have

$$\varphi_0(y, z)=\int_{-\infty}^{\infty}\int\delta(y-m, z-n)\varphi_0(m, n)\,dm\,dn. \quad (1.71)$$

To find the signal at the filter's output, let us recall that the weighting function E_δ is its reaction to a signal in the form of the spatial delta function. Therefore, each of the infinitesimal light signals

$$\varphi_0(m, n)\,\delta(y-m, z-n)\,dm\,dn$$

causes an elementary signal at the filter's output:

$$\varphi_0(m, n)E_\delta(y-m, z-n)\,dm\,dn$$

The resultant output signal is

$$\varphi_1(y, z)=\int_{-\infty}^{\infty}\int E_\delta(y-m, z-n)\varphi_0(m, n)\,dm\,dn. \quad (1.72)$$

The integral in the right side of expression (1.72) is a two-dimensional integral of convolution, which is written as follows in vector form:

$$\varphi_1(\vec{Q}) \int_{-\infty}^{\infty} E_\delta(\vec{Q}-\vec{r})\varphi_0(\vec{r})\,d\vec{r}. \qquad (1.73)$$

Taking the Fourier transforms from both sides of equation (1.73), we find

$$F_1(i\vec{\omega}) = \int_{-\infty}^{\infty} e^{-i\vec{\omega}\vec{Q}} \left[\int_{-\infty}^{\infty} E_\delta(\vec{Q}-\vec{r})\,\varphi_0(\vec{r})\,d\vec{r} \right] d\vec{Q}. \quad (1.74)$$

Introducing the new variable $\vec{\Delta}=\vec{\rho}-\vec{r}$, we have

$$F_1(i\vec{\omega}) = \int_{-\infty}^{\infty} e^{-i\vec{\omega}\vec{Q}} E_\delta(\vec{r})\,d\vec{\Delta} \int_{-\infty}^{\infty} e^{-i\vec{\omega}\vec{r}}\,\varphi_0(\vec{r})\,d\vec{r}, \quad (1.75)$$

Hence it follows that

$$F_1(i\vec{\omega}) = W(i\vec{\omega})F_0(i\vec{\omega}),$$

or

$$W(i\vec{\omega}) = \frac{F_1(i\vec{\omega})}{F_0(i\vec{\omega})}, \qquad (1.76)$$

i.e., the spatial frequency transfer function of a multidimensional filter is the ratio of the Fourier transform of the output signal to the Fourier transform of the input signal.

Before moving on to a description of some properties of spatial frequency transfer functions, let us make two remarks. The first pertains to the optical system's reaction to the spatial delta function. Because of diffraction effects, even an ideal optical system in which there are no aberrations produces the image of an isolated radiating point in the form of a spot of finite dimensions whose irradiance decreases rapidly from its center to its periphery.

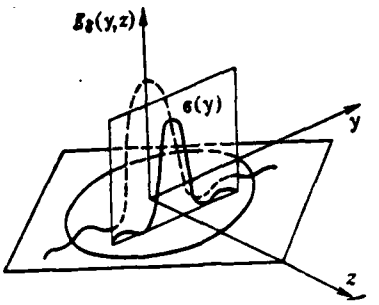

Fig. 1.11. Irradiance distribution function for the image of an isolated point.

The distribution of the irradiance in the image of an isolated point that is produced by an ideal instrument is described by the function [19, 22]:

$$E_\delta(y, z)=E_M\frac{4J_1^2(n)}{n^2}, \qquad (1.77)$$

where

$$n=\frac{2\pi a'}{\lambda}\sqrt{y^2+z^2};$$

α'--half the angle at the vertex of the cone of rays that forms the image (Fig. 1.10);

λ--the wavelength;

I_1--a first-order Bessel function of the first kind;

E_M--the maximum value of the function $E_\delta(y, z)$ that corresponds to the values of the coordinates y=0 and z=0.

The function $E_\delta(y, z)$ can be represented as a surface (Fig. 1.11) which bounds a volume called the "diffraction body." If the function $E_\delta(y, z)$ is symmetric, then it is represented as a one-dimensional cut. Table 1.5 gives the values of E_δ/E_M for various n. The function E_δ vanishes for n equal to 3.83, 7.02, 10.17, 13.32, 16.47, etc., and has a maximum at the following values of n: 5.13, 8.42, 11.62, 14.80,

Table 1.5. Values of E_δ/E_M for Various n

n	$\frac{E_\delta}{E_M}$	n	$\frac{E_\delta}{E_M}$	n	$\frac{E_\delta}{E_M}$
0,0	1,000	2,8	0,0856	5,6	0,0153
0,4	0,961	3,2	0,0267	6,0	0,0085
0,8	0,850	3,6	0,0028	6,4	0,0032
1,2	0,690	4,0	0,0011	6,8	0,0004
1,6	0,507	4,4	0,0085	7,2	0,0003
2,0	0,333	4,8	0,0155	7,6	0,0018
2,4	0,188	5,2	0,0174	8,0	0,0034

17.96, etc. Ratios E_δ/E_M of 100% are respectively equal to 1.75, 0.416, 0.160, 0.078, and 0.044 [22].

The function $E_\delta(y, z)$ has no analytical expression for real optical systems. As a result, experimental methods of determining this function and approximate theoretical methods that take into account the effect of spherical and chromatic aberrations only have been under development recently.

The second remark relates to the optical system's response to a signal in the form of a unit step function. If the object plane contains a sharp boundary between an illuminated quarter of the plane and the other quarters, which are dark, i.e., if B*(y, z) is equal to unity when y>0 and z>0 and to zero otherwise, then the irradiance distribution in the image of this picture can be found from formula (1.58):

$$E_h(y, z)=\int_0^\infty\int_{-\infty}^{\infty} E_\delta(y-y', z-z')\,dy'\,dz'. \quad (1.78)$$

Integrating over y-y'=Y and noting that dy'=-dY, we obtain

$$\sigma_h(y, z)=\int_0^\infty \sigma(z-z')\,dz'. \quad (1.79)$$

The function $\sigma(z)$ is equal to the cross-sectional area of the diffraction body where it is intersected by a plane having an ordinate z (Fig. 1.11).

The function $g_h(y, z)$, which represents the reaction of a multidimensional filter to a unit light signal propagated in one quadrant, is called the unit step function (the Heaviside unit function). It is analogous to the unit step function of the linear section of an automatic control system--the section's reaction to a unit step.

Returning to our examination of spatial frequency transfer functions, let us note an important aspect that follows from its [sic] mathematical definition. If we know the complex spatial frequency spectrum $b_{вх}(i\mu, i\nu)$ of a signal at the input of the transfer section and its spatial frequency transfer function $W(i\mu, i\nu)$, then the signal $b_{вых}(i\mu, i\nu)$ at the output of the section is defined by the relation

$$b_{вых}(i\mu, i\nu) = b_{вх}(i\mu, i\nu) W(i\mu, i\nu). \qquad (1.80)$$

If several sections are connected in series, the signal at their output will be

$$b_{вых}(i\mu, i\nu) = b_{вх}(i\mu, i\nu) \prod_{n=1}^{n=m} W_n(i\mu, i\nu), \qquad (1.81)$$

where m is the number of series-connected sections.

Expression (1.81) follows directly from expression (1.80) if the output signal of each preceding section is considered the input signal of the next section.

In most cases we are concerned only with peak signals that can be represented by their amplitude spatial frequency spectra. In these cases expression (1.81) assumes the form

$$|b_{вых}(i\mu, i\nu)| = |b_{вх}(i\mu, i\nu)| \prod_{n=1}^{n=m} W_n(\mu, \nu). \qquad (1.82)$$

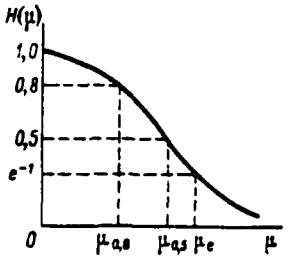

Fig. 1.12. Evaluation of the properties of a transfer section based on its spatial frequency transfer function.

The spatial frequency transfer function completely describes the transfer properties of individual sections and of an entire optical information transmission system. It also makes it possible to synthesize a system. Efforts are made to ensure that the curve of the spectral frequency transfer function comes as close to unity as possible in the range of spatial frequencies used. To compare two sections, we usually select characteristic points on the curve of the spatial frequency transfer function that correspond to the levels 0.8, 0.5, e^{-1}=0.37, and so forth (Fig. 1.12). The selection of a given level as a criterion for evaluating a section depends on its function.

In synthesizing two-dimensional systems from the spatial frequency transfer functions of individual sections, one should keep in mind that the spatial frequency transfer function of each section is defined in a certain plane; in recomputing the spatial frequency transfer function, allowance should be made for scale transformations of the sections.

The mathematical tools considered above for determining the spatial frequency transfer function of two-dimensional systems are valid only if these systems are linear and if the light beam that carries information regarding an object is produced by a source of

noncoherent radiation. Let us determine the spatial frequency transfer functions for some elementary filters.

In the absence of diffraction effects, an ideal nonaberrational lens is an amplifier section whose weighting function is expressed in terms of the spatial delta function as follows:

$$E_\delta(y, z)=k\delta(y, z).$$

Obviously,

$$W(l\mu, l\nu)=k\int_{-\infty}^{\infty}\int\delta(y, z)\,e^{-2\pi l(\mu y+\nu z)}\,dy\,dz. \qquad (1.83)$$

It is not hard to see that

$$W(l\mu, l\nu)=k. \qquad (1.84)$$

An optical shifter changes the direction of propagation of light rays without changing the waveform. It has the weighting function

$$E_\delta(y, z)=\delta(y-y_0, z-z_0).$$

Based on property (1.57) of the spatial delta function, we have

$$W(l\mu, l\nu)=e^{-2\pi l(\mu y_0+\nu z_0)}. \qquad (1.85)$$

A nonaberrational lens stretches the image of a point source of optical radiation into a line. Its weighting function is represented by a one-dimensional delta function:

$$E_\delta(y, z)=\delta(y-y_0),$$

where y_0 is the displacement along the y axis.

The Fourier transform of the weighting function is

$$W(l\mu, l\nu)=\delta(\nu)e^{-2\pi l\mu y_0}. \qquad (1.86)$$

A Diaphragm with a Rectangular Aperture. The weighting function in the form of a rectangular parallelipiped has the following analytical expressions:

$$E_\delta(y, z)=\begin{cases}1 \text{ when } -\frac{y_1}{2}<y<\frac{y_1}{2} \text{ and } -\frac{z_1}{2}<z<\frac{z_1}{2},\\ 0 \text{when } y>\frac{y_1}{2},\ y<-\frac{y_1}{2} \text{ or } z>-\frac{z_1}{2},\ z<-\frac{z_1}{2}.\end{cases}$$

In this case

$$W(i\mu, i\nu)=\int_{-\frac{y_1}{2}}^{\frac{y_1}{2}}\int_{-\frac{z_1}{2}}^{\frac{z_1}{2}} e^{-2\pi i(\mu y+\nu z)}\,dy\,dz. \qquad (1.87)$$

Separating the integrals and integrating, we find [7]:

$$W(i\mu, i\nu)=\frac{1}{\pi^2\mu\nu}\sin\pi\mu y_1 \sin\pi\nu z_1. \qquad (1.88)$$

A Diaphragm with a Round Aperture. Setting $E_\delta(\rho)=1$ and using the Hankel transform, we find

$$W(\omega)=2\pi\int_\delta^R \varrho I_0(\varrho\omega)\,d\varrho, \qquad (1.89)$$

where R is the radius of the circle.

Taking into consideration that

$$d[(\varrho\omega)^n I_n(\varrho\omega)]=(\varrho\omega)^n I_{n-1}(\varrho\omega)\,d(\varrho\omega),$$

we obtain

$$W(\omega)=2\pi R^2\frac{I_1(R\omega)}{R\omega}. \qquad (1.90)$$

A Lens with Aberrations. The light-scattering function for the aberrational point of a lens can be approximated as follows [6]:

$$E_i(y, z)=\frac{Q_1^2}{\pi r_1^2}e^{-Q_1^2\left(\frac{y^2+z^2}{r_1^2}\right)}, \qquad (1.91)$$

where ρ_1=0.4769--a constant

r_1--the radius within which 50% of the energy in the light signal is concentrated.

Obviously,

$$W(i\mu, i\nu)=\frac{Q_1^2}{\pi r_1^2}\int_0^{\infty} e^{-Q_1^2\frac{y^2}{r_1^2}-2\pi i\mu y}dy\int_{-\infty}^{\infty} e^{-Q_1^2\frac{z^2}{r_1^2}-2\pi i\nu z}dz. \quad (1.92$$

Without giving a detailed solution, we will present the final result [6, 7]:

$$W(i\mu, i\nu)=e^{-\frac{\pi^2 r_1^2}{Q_1^2}(\mu^2+\nu^2)}. \qquad (1.93)$$

A Filter with Complex Weighting Functions. If the weighting function of a filter has a complex expression or is determined experimentally, then it may be divided approximately into regions whose frequency responses are readily determined analytically. For example, when

$$E_i(y, z)=\sum_{r=1}^{n}\sum_{k=1}^{m}E_{ir_k}(y, z)$$

we have

$$W(i\mu, i\nu)=\sum_{r=1}^{n}\sum_{k=1}^{m}W_{r_k}(i\mu, i\nu). \qquad (1.94)$$

Dividing the complex weighting function into elementary rectangles (Fig. 1.13a), we find

$$W_{r_k}(i\mu, i\nu)=\frac{A_{r_k}}{\pi^2\mu\nu}\sin\pi\mu\Delta y\cdot\sin\pi\nu\Delta z\cdot e^{2\pi i(\mu y_r+\nu z_k)},$$

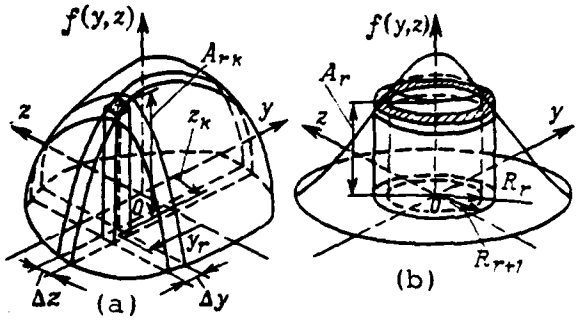

Fig. 1.13. Calculation of the spatial frequency transfer function of a filter with a complex weighting function.

where A_{rk}--the amplitudes of elementary components of the weighting function;

Δy, Δz--the dimensions of the elementary rectangles;

y_r, z_k--the coordinates of the centers of the rectangles.

Obviously,

$$W(i\mu, i\nu) = \frac{1}{\pi^2 \mu\nu} \sum_{r=1}^{n} \sum_{k=1}^{m} \sin \pi\mu\Delta y \cdot \sin \pi\nu\Delta z \times \times A_{rk} e^{2\pi i(\mu y_r + \nu z_k)}. \quad (1.95)$$

Since

$$\lim_{\substack{\Delta y \to 0 \\ \Delta z \to 0}} \frac{1}{\pi^2 \mu\nu} \sin \pi\mu\Delta y \cdot \sin \pi\nu\Delta z = \Delta y \cdot \Delta z,$$

we have

$$W(i\mu, i\nu) = \sum_{r=1}^{n} \sum_{k=1}^{m} A_{rk} e^{2\pi i(\mu y_r + \nu z_k)} \Delta y \, \Delta z. \quad (1.96)$$

If the weighting function has rotational symmetry, then it is advisable to divide the function into cylindrical rings (Fig. 1.13b), for each of which

$$\Delta W_r(\omega) = A_r 2\pi \left[R_{r+1}^2 \frac{I_1(R_{r+1}\omega)}{R_{r+1}\omega} - R_r^2 \frac{I_1(R_r\omega)}{R_r\omega} \right], \quad (1.97($$

where R_r and R_{r+1} are the radii of the ring.

In this case

$$W(\omega)=\frac{2\pi}{\omega}\sum_{r=0}^{n}A_r[R_{r+1}I_1(R_{r+1}\omega)-R_rI_1(R_r\omega)]. \quad (1.98)$$

Passing to the limit for small thickness of the cylindrical ring, we obtain

$$W(\omega)=2\pi\sum_{r=0}^{n}A_rI_0(R_r\omega)R_r\Delta R. \quad (1.99)$$

A Filter with Time-Varying Weighting Functions. First let us consider the case where the weighting function undergoes translation in space and has the form

$$E_3=E_3[\vec{\varrho}+\vec{r}(t)], \quad (1.100)$$

where $\vec{r}(t)$ is the displacement vector.

Based on the property of the Fourier transform of a displaced signal that if

$$f(\vec{\varrho})=f_1(\vec{\varrho}+\vec{r}),$$

then

$$F(i\vec{\omega})=F_1(i\vec{\omega})e^{-i\vec{\omega}\vec{r}},$$

we find

$$W(i\vec{\omega}, t)=W(i\vec{\omega})e^{-i\vec{\omega}\vec{r}(t)}, \quad (1.101)$$

where $W(i\vec{\omega})$ is the spatial frequency transfer function of a filter whose weighting function is found at rest.

If the weighting function is rotated by an angle $\gamma=\gamma(t)$, the spatial frequency transfer function of the filter has the form:

$$W(i\vec{\omega}, t) = W[iM_{\gamma(t)}\vec{\omega}], \qquad (1.102)$$

where

$$M_{\gamma(t)} = \begin{Vmatrix} \cos\gamma(t) & -\sin\gamma(t) \\ \sin\gamma(t) & \cos\gamma(t) \end{Vmatrix}$$

is the rotation matrix.

If we know the spectrum of the input signal and the spatial frequency transfer function of a multidimensional filter, then we can calculate the spectrum and spatial form of the output signal. As an example, let us calculate the spectrum and shape of the output signal of a multidimensional filter with a bell-shaped weighting function to whose input a unit signal propagated in a quadrant of the half-plane is supplied (Fig. 1.14a).

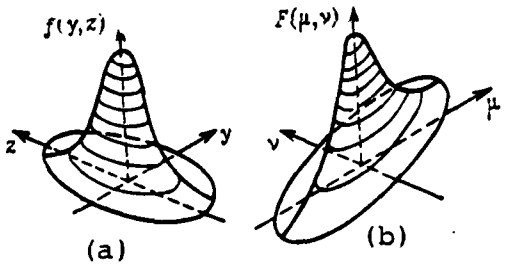

Fig. 1.14. Calculation of the spectrum and shape of the output signal of a multidimensional filter.

Analytically, such a signal is expressed in the following form:

$$f_0(y, z) = \begin{cases} 1 & \text{if } y>0 \text{ and } z>0; \\ 0 & \text{for other values of y and z} \end{cases}$$

The input-signal spectrum is

$$F_0(i\mu, i\nu) = \int_0^\infty\int_0^\infty e^{-2\pi i(\mu y+\nu z)}\,dy\,dz = \frac{1}{4\pi^2\mu\nu}. \qquad (1.103)$$

The amplitude characteristic of the spectrum is shown in Fig. 1.14b. By stipulation, the spatial frequency transfer function of a filter is defined by the relation

$$W(i\mu, i\nu)=e^{-\frac{\pi^2 r_1^2}{c_1^2}(\mu^2+\nu^2)}, \qquad (1.104)$$

Therefore, the output-signal spectrum is

$$F_1(i\mu, i\nu)=F_0(i\mu, i\nu)W(i\mu, i\nu), \qquad (1.105)$$

or

$$F_1(i\mu, i\nu)=\frac{1}{4\pi^2\mu\nu}e^{-\frac{\pi^2 r_1^2}{c_1^2}(\mu^2+\nu^2)}. \qquad (1.106)$$

The shape of the output signal is determined by the inverse Fourier transform:

$$f_1(y, z)=\frac{1}{(2\pi)^2}\int_{-\infty}^{\infty}\int\frac{1}{\mu\nu}e^{-\frac{\pi^2 r_1^2}{c_1^2}(\mu^2+\nu^2)}\times$$
$$\times e^{-2\pi i(\mu y+\nu z)}d\mu\, d\nu. \qquad (1.107)$$

Calculating the integral, we obtain

$$f_1(y, z)=\frac{1}{4}\left[1+\Phi_1\left(\frac{y}{r_1}\right)\right]\left[1-\Phi_1\left(\frac{z}{r_1}\right)\right], \qquad (1.108)$$

where $\Phi_1(x)=\frac{2c_1}{\sqrt{\pi}}\int_0^x e^{-c_1^2x^2}dx$ is the reduced error function.

As a second example, let us consider the passage of a rectangular signal through an optical shifter whose weighting function rotates at some constant angular speed [6, 7].

The spatial frequency transfer function of an optical shifter with a stationary weighting function according to (1.85) has the form

$$W(i\mu, i\nu) = e^{-2\pi i(\mu y_0 + \nu z_0)}.$$

Upon rotation of the weighting function,

$$W[i\mu'(t), i\nu'(t)] = e^{-2\pi i[y_0\mu'(t) + z_0\nu'(t)]}. \quad (1.109)$$

The component frequencies are determined by the rotation matrix and are

$$\left.\begin{aligned} \mu' &= \mu\cos\dot{\gamma}t - \nu\sin\dot{\gamma}t, \\ \nu' &= \mu\sin\dot{\gamma}t + \nu\cos\dot{\gamma}t, \end{aligned}\right\} \quad (1.110)$$

so that

$$W(i\mu, i\nu, t) = e^{-2\pi i[\cos\dot{\gamma}t(\mu y_0 + \nu z_0) + \sin\dot{\gamma}t(\mu z_0 - \nu y_0)]}. \quad (1.111)$$

The shape of the output signal is determined by the inverse Fourier transform:

$$f_1(t) = \frac{1}{(2\pi)^2}\int\limits_{-\infty}^{\infty}\int e^{-2\pi i[\cos\dot{\gamma}t(\mu y_0 + \nu z_0) + \sin\dot{\gamma}t(\mu z_0 - \nu y_0)]} \times$$

$$\times \frac{1}{\pi^2\mu\nu}\sin\pi\mu y_1 \cdot \sin\pi\nu z_1 d\mu\, d\nu. \quad (1.112)$$

After transformations which we omit, we find [7]:

$$f_1(t) = \phi_1(y_0\cos\dot{\gamma}t + z_0\sin\dot{\gamma}t)\,\phi_2(z_0\cos\dot{\gamma}t - y_0\sin\dot{\gamma}t), \quad (1.113)$$

where

$$\phi_1 = \begin{cases} 0 \text{ if } y_0\cos\dot{\gamma}t + z_0\sin\dot{\gamma}t < -\frac{y_1}{2} \text{ and} \\ \quad y_0\cos\dot{\gamma}t + z_0\sin\dot{\gamma}t > \frac{y_1}{2}; \\ 1 \text{ if } -\frac{y_1}{2} < y_0\cos\dot{\gamma}t + z_0\sin\dot{\gamma}t < \frac{y_1}{2}; \end{cases}$$

$$\phi_2 = \begin{cases} 0 \text{ if } z_0\cos\dot{\gamma}t - y_0\sin\dot{\gamma}t < -\frac{z_1}{2} \text{ and} \\ \quad z_0\cos\dot{\gamma}t - y_0\sin\dot{\gamma}t > \frac{z_1}{2}; \\ 1 \text{ if } -\frac{z_1}{2} < z_0\cos\dot{\gamma}t - y_0\sin\dot{\gamma}t < \frac{z_1}{2}. \end{cases}$$

At the filter's output the signal has the form of rectangular pulses.

CHAPTER 2

TIME-AND-FREQUENCY CHARACTERISTICS OF MODULATORS

2.1. Analytical Determination of the Time-and-Frequency Characteristics of Modulators

If a radiant flux $F_0(t)$ is incident on a modulating disk, then the value of the modulated radiant flux is

$$F(t)=F_0(t)\tau(t) \qquad (2.1)$$

where $\tau(t)$ is the tranmission function of the modulating disk.

The time-and-frequency characteristics of signals picked up from the radiant-energy detector depend on the configuration of the raster of the modulating disk. By expanding the transmission function of the modulating disk into a Fourier series, we can estimate the characteristics of signals going from the output of a radiant-energy detector to the selective elements of an optoelectronic device.

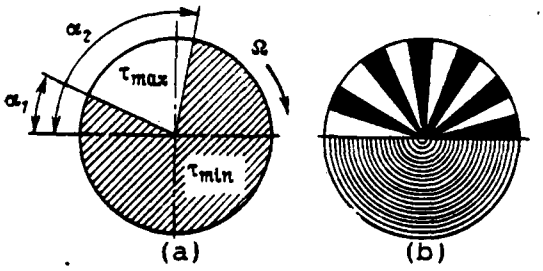

Fig. 2.1. Modulating disks: (a) with a transparent sector; (b) with alternating transparent and opaque sectors.

One of the simplest modulating disks is a slit modulator, which is implemented as a circle with a sector that differs in its transmission coefficient from the rest of the surface (Fig. 2.1a).

The transmission function of a slit modulator in relation to the angle of rotation can be represented as

$$\tau(\alpha)=\begin{cases}\tau_{max} \text{ if } & \alpha_1 \leqslant \alpha \leqslant \alpha_2, \\ \tau_{min} \text{ if } & 0<\alpha<\alpha_1,\ \alpha_2<\alpha<2\pi,\end{cases} \tag{2.2}$$

or

$$\tau(t)=\begin{cases}\tau_{max} \text{ if } & \frac{\alpha_1}{\Omega} \leqslant \frac{\alpha}{\Omega} \leqslant \frac{\alpha_2}{\Omega}, \\ \tau_{min} \text{ if } & 0<\frac{\alpha}{\Omega}<\frac{\alpha_1}{\Omega},\ \frac{\alpha_2}{\Omega}<\frac{\alpha}{\Omega}<T,\end{cases} \tag{2.3}$$

where Ω is the angular rotational velocity of the modulating disk.

Using the relations presented in Chapter 1, we can represent the coefficients of the expansion of a slit modulator's transmission function into a Fourier series by the following expressions:

$$\left.\begin{aligned}
&\frac{a_0}{2}=\tau_{min}+(\tau_{max}-\tau_{min})\frac{\alpha_2-\alpha_1}{2\pi}; \\
&a_k=\frac{\tau_{max}-\tau_{min}}{k\pi}(\sin k\alpha_2-\sin k\alpha_1); \\
&b_k=\frac{\tau_{max}-\tau_{min}}{k\pi}(\cos k\alpha_1-\cos k\alpha_2); \\
&c_k=\frac{2(\tau_{max}-\tau_{min})}{k\pi}\sin k\frac{\alpha_2-\alpha_1}{2}; \\
&\varphi_k=\operatorname{arctg}\ \frac{\cos k\alpha_1-\cos k\alpha_2}{\sin k\alpha_2-\sin k\alpha_1}=k\ \frac{\alpha_2+\alpha_1}{2}.
\end{aligned}\right\} \tag{2.4}$$

According to formulas (2.4), the transmission function of a slit modulator will assume the form

$$\tau(t)=\tau_{min}+(\tau_{max}-\tau_{min})\frac{\alpha_2-\alpha_1}{2\pi}+$$
$$+\frac{2(\tau_{max}-\tau_{min})}{\pi}\sum_{k=1}^{\infty}\frac{\sin k\frac{\alpha_2-\alpha_1}{2}}{k}\cos k\left(\Omega t+\frac{\alpha_2+\alpha_1}{2}\right). \tag{2.5}$$

For a modulating disk patterned after Fig. 1.1f, $\alpha_2-\alpha_1=\pi$. If we assume $\tau_{max}=1$, $\tau_{min}=0$, and $\alpha_1=0$, then the transmission function of the disk is

$$\tau(t)=\frac{1}{2}+\frac{2}{\pi}\sum_{k=1}^{\infty}\frac{\sin k\frac{\pi}{2}}{k}\cos\left(\Omega t+\frac{\pi}{2}\right). \tag{2.6}$$

For even k, sin $k\frac{\pi}{2}=0$, and expression (2.6) simplifies, assuming the form

$$\tau(t)=\frac{1}{2}+\frac{2}{\pi}\sum_{q=0}^{\infty}\frac{1}{2q+1}\sin(2q+1)\Omega t. \qquad (2.7)$$

A "uniform grating"-type modulating disk is shown in Fig. 1.1e. Depending on the angle α of rotation of the disk, its transmission function is determined by the relation

$$\tau(\alpha)=\begin{cases}1 \text{ if } \frac{2\pi}{z}(m-1)\leqslant\alpha\leqslant\frac{\pi}{z}(2m-1),\\ 0 \text{ if } \frac{\pi}{z}(2m-1)<\alpha<\frac{2\pi}{z}m,\end{cases} \qquad (2.8)$$

where z--the number of transparent (or opaque) sectors;
m--the sector number (m=1, 2, 3, ..., z).

Since the modulating disk rotates with a contant angular velocity Ω, the transmission function can be expressed by the formula

$$\tau(t)=\begin{cases}1 \text{ if } \frac{2\pi}{z\Omega}(m-1)\leqslant\frac{\alpha}{\Omega}\leqslant\frac{\pi}{z\Omega}(2m-1),\\ 0 \text{ if } \frac{\pi}{z\Omega}(2m-1)<\frac{\alpha}{\Omega}<\frac{2\pi}{z\Omega}m.\end{cases} \qquad (2.9)$$

The period of the function (t) is the quantity $T_H=\frac{2\pi}{z\Omega}$, and $z\Omega=\omega$ is the modulation frequency of the radiant flux. The expression for the transmission function of a modulating disk of the "uniform grating" type is analogous to expression (2.7), but with the difference that the angular frequency ω of modulation of the radiant flux will figure in this equation in place of the angular rotational velocity Ω of the disk.

The raster of the modulating disk shown in Fig. 2.1b has a more complex pattern. The disk consists of two halves each of which transmits 50% of the incident radiation, while the other half consists of alternating transparent and opaque sectors. The transmission function of such a disk is represented by the expression

$$\tau(\alpha)=\begin{cases}1 \text{ if } \frac{2\pi}{z}(m-1)\leqslant\alpha\leqslant\frac{\pi}{z}(2m-1),\\ 0 \text{ if } \frac{\pi}{z}(2m-1)<\alpha<\frac{2\pi}{z}m,\\ \frac{1}{2} \text{ if } \pi<\alpha<2\pi,\end{cases} \qquad (2.10)$$

where z--twice the number of sector pairs;

m--the number of a sector pair (m-1, 2, 3, ..., z/2).

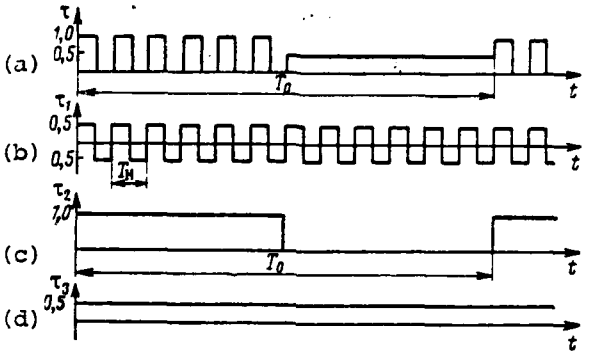

Fig. 2.2. Waveform at the output of a radiant-energy detector (a), and the type of auxiliary functions that allow representation of the transmission coefficient of a modulating disk as a linear combination (b, c, d).

The waveform at the output of a radiant-energy detector in front of which the modulating disk in question is positioned is shown in Fig. 2.2a. For Fourier expansion of the transmission function $\tau(t)$ of a modulating disk with a complex raster pattern, it is convenient to represent $\tau(t)$ as a linear combination of simple functions:

$$\tau(t)=\tau_1(t)\tau_2(t)+\tau_3(t) \qquad (2.11)$$

The form of the functions $\tau_1(t)$, $\tau_2(t)$, and $\tau_3(t)$ is shown in Figs. 2.2b, c, and d. The elementary functions in expression (2.11) have the form

$$\tau_1(t)=\frac{2}{\pi}\sum_{q=0}^{\infty}\frac{1}{2q+1}\sin(2q+1)\omega t; \qquad (2.12)$$

$$\tau_3(t)=\frac{1}{2}+\frac{2}{\pi}\sum_{q=0}^{\infty}\frac{1}{2q+1}\sin(2q+1)\Omega t; \quad (2.13)$$

$$\tau_3(t)=\frac{1}{2}. \quad (2.14)$$

The transmission function of the modulating disk is

$$\tau(t)=\frac{1}{2}+\frac{2}{\pi}\left[\sum_{q=0}^{\infty}\frac{1}{2q+1}\sin(2q+1)\omega t\right]\times$$
$$\times\left[\frac{1}{2}+\frac{2}{\pi}\sum_{q=0}^{\infty}\frac{1}{2q+1}\sin(2q+1)\Omega t\right]. \quad (2.15)$$

Some optoelectronic devices use a "uniform grating" modulating disk that has variable optical density over its diameter (Fig. 1.1k). This is accomplished by using a material whose transparency obeys a wedge law. The transmission function of such a modulating disk (provided that $\tau_{max}=1$ and $\tau_{min}=0$) is expressed by the series

$$\tau(t)=\left[\frac{1}{2}+\frac{2}{\pi}\sum_{q=0}^{\infty}\frac{1}{2q+1}\sin(2q+1)\omega t\right]\times$$
$$\times\left(\frac{1}{2}+\frac{1}{2}\sin\Omega t\right). \quad (2.16)$$

As we can see from formula (2.16), the factor in brackets is the transmission function of a "uniform grating" modulating disk, while the second factor determines the change in the optical density of the disk material according to a wedge law.

The problem of precision of modulator fabrication arises in solving practical problems of the design of optical apparatus for measuring angular coordinates. All changes in the configuration of the raster pattern can be reduced to a change in the dimensions of the transmitting (or nontransmitting) sectors or to a change in the transmission function.

The transmission function of a modulating disk with deviations from the specified raster pattern can be represented as follows:

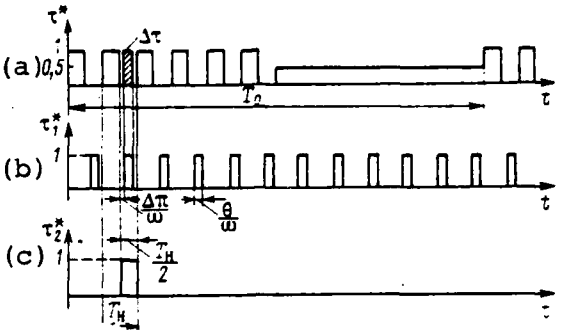

Fig. 2.3. Waveform at the output of a radiant-energy detector when a modulating disk having a nonideal raster pattern is used (a), and the form of auxiliary functions that produce $\Delta\tau(t)$.

$$\tau^*(t)=\tau(t)+\Delta\tau(t), \qquad (2.17)$$

where $\tau(t)$--the transmission function of an ideal modulating disk;

$\Delta\tau(t)$--the change in the transmission function due to deviations of the actual raster pattern from the ideal.

Fig. 2.3a shows the waveform at the output of a radiant-energy detector for a modulating disk implemented as in Fig. 2.1b that has an additional transmitting sector. Figs. 2.3b and 2.3c show the auxiliary functions $\tau_1^*(t)$ and $\tau_2^*(t)$ which are used to facilitate the representation of $\Delta\tau(t)$ as a Fourier expansion.

The width of the additional transmitting sector is assumed equal to θ, the distance between the primary transmitting sector and the secondary sector is $\Delta\pi$, and the secondary transmitting sector is located in a pair of (transmitting and nontransmitting) sectors numbered m.

Since

$$\Delta\tau(t)=\tau_1^*(t)\cdot\tau_2^*(t) \qquad (2.18)$$

by expanding each of the functions in the right side of expression (2.18) into a series, it is possible to determine the change in the

transmission function of the modulating disk.

For simplicity we will assume $\tau^*_{max}=1$ and $\tau^*_{min}=0$. Allowing for the notations introduced above, we have

$$\tau_1^*(t)=\left|\begin{array}{ll} 1 \text{ if} & \frac{\pi}{\omega}+\frac{\Delta\pi}{\omega}\leqslant t\leqslant\frac{\pi}{\omega}+\frac{\Delta\pi}{\omega}+\frac{\theta}{\omega}, \\ 0 \text{ if} & 0<t<\frac{\pi}{\omega}+\frac{\Delta\pi}{\omega},\ \frac{\pi}{\omega}+\frac{\Delta\pi}{\omega}+ \\ & \quad +\frac{\theta}{\omega}<t<\frac{2\pi}{\omega}; \end{array}\right\} \quad (2.19)$$

$$\tau_2^*(t)=\left|\begin{array}{ll} 1 \text{ if} & \frac{2\pi}{z\Omega}(m-1)+\frac{\pi}{z\Omega}\leqslant t\leqslant\frac{2\pi}{z\Omega}m, \\ 0 \text{ if} & \frac{2\pi}{z\Omega}(m-1)<t<\frac{2\pi}{z\Omega}(m-1)+ \\ & \quad +\frac{\pi}{z\Omega}. \end{array}\right\} \quad (2.20)$$

The change in the transmission function of a modulating disk due to deviations of the actual raster pattern from the ideal is represented by the Fourier series

$$\Delta\tau(t)=\left\{\frac{\theta}{2\pi}+\frac{2}{\pi}\sum_{k=1}^{\infty}\frac{\sin k\frac{\theta}{2}}{k}\cos k\left[\omega t-\left(\pi+\Delta\pi+\frac{\theta}{2}\right)\right]\right\}\times$$

$$\times\left\{\frac{1}{2z}+\frac{2}{\pi}\sum_{k=1}^{\infty}\frac{\sin k\frac{\pi}{2z}}{k}\cos k\left[\Omega t-\frac{\pi}{2z}(4m-1)\right]\right\}. \quad (2.21)$$

In analyzing expression (2.21) we should note that the additional signal generated at the radiant-energy detector carries information at the ω-carrier and Ω-envelope frequencies. This signal will be picked up by selective elements of information processors and will affect the output signals of the control elements of the equipment.

A modulating disk with nonuniform width of the transmitting and nontransmitting sectors (Fig. 1.11) is used in optoelectronic instrument making. To represent the transmission function of such a disk as a Fourier series, we must determine the expansion coefficients for

$\omega=\omega(t)$. Even in the simplest case where $\omega=\omega_0+\xi t\Big|_0^{t=T_0}$, finding the coefficients of the series reduces to calculating an integral of the type $\int_0^T \sin t^2\,dt$. This integral in turn is represented by a series of the type

$$\int_0^T \sin t^2\,dt=\frac{2}{\sqrt{2\pi}}\sum_{n=0}^{\infty}\frac{(-1)^n T^{4n+3}}{(2n+1)!(4n+3)}=$$

$$=\frac{2}{\sqrt{2\pi}}\left(\frac{T^3}{3}-\frac{T^7}{42}+\frac{T^{11}}{1320}-\frac{T^{15}}{83\,160}+\ldots\right). \qquad (2.22)$$

The need for a large volume of computations forces us to seek methods that make possible a reduction of the amount of time needed. Electronic simulation or modeling equipment, in particular, may be used for this purpose.

2.2. Simulation of the Time-and-Frequency Characteristics of Modulators Using Analog Computers

When analog computers are used to simulate the time-and-frequency characteristics of modulators, sine-wave voltages of different frequencies must be added. A sinusoidal voltage can be obtained in an analog computer [ABM] by solving the equation

$$y''+\alpha y=0 \qquad (2.23)$$

under certain initial conditions.

The solution of equation (2.23) is

$$y=A\sin(\omega t+\psi) \qquad (2.24)$$

where

$$\omega=\sqrt{\alpha},\quad \psi=\operatorname{arctg}\omega\frac{y_0}{y_0'},$$

$$y_0=y_{t=0},\qquad y_0'=y_{t=0}'.$$

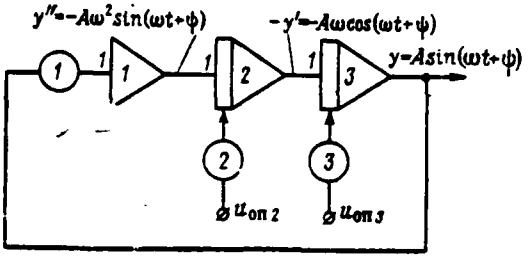

Fig. 2.4. Block diagram of the solution of the equation y"+ay=0.

Adder	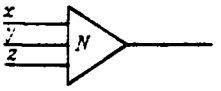
Inverter	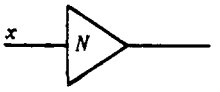
Integrator	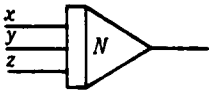
Potentiometer with grounded terminal Without grounded terminals	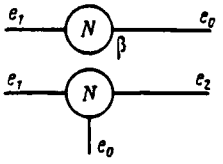
Multiplier-divider	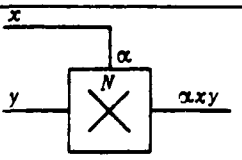
Nonlinearity of a special type	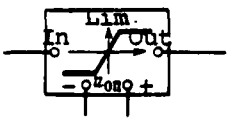

Fig. 2.5. Symbols for decision elements of an analog computer.

To solve equation (2.23) on an analog computer, we must have two integrators, one inverter, and three potentiometers. A block diagram of the solution is shown in Fig. 2.4. The symbols for the decision elements accord with Fig. 2.5. The transfer ratios of potentiometers 2 and 3 depend on the initial conditions, and the value of the transfer ratio of potentiometer 1 is determined by the value of ω^2.

There are two reasons why it is extremely difficult to use this method to add the components of a series. The first is that there must be a large number of decision units in the analog computer. The number N of integrators and inverters is

$$N=3n+1$$

where n is the number of terms in the expansion.

The second factor that determines the practical inapplicability of adding sinusoidal components is the fact that the addition of the sinusoidal components of a series is extremely difficult work that requires much experience and knowhow, even with large analog computers on which the operator can work without having to look for reserve decision elements. The sinusoidal components must have multiple frequencies; it is practically impossible to determine exactly the value of the transfer ratios of units and potentiometers. And if the operation of a modulator must be analyzed over a single period, the addition of sinusoidal components makes it difficult to correct the transfer ratios, which determine the accuracy with which the required sinusoidal voltage frequency is set.

In investigating the operation of a modulator over a time $t>>T_0$, the method of adding sinusoidal components cannot be used. Even slight inaccuracy (a fraction of a percent) in the setting of the coefficients that determine the frequencies of the sinusoids being added will lead to phase mismatch of the terms in a few periods. Therefore, a number of artificial procedures are used to simulate time-and-frequency

characteristics. The simplest signals to modulate are those which have passed through a modulating disk. This is done by using a set of nonlinear units and infralow-frequency equipment. For example, a low-frequency periodic oscillator (such as the NGPK-2 or the NGPK-3) is used to produce signals that simulate the operation of the modulating disks shown in Fig. 1.1f and 1.1e. [When such a generator] is combined with a multiplier, it is possible to construct the model modulator shown in Fig. 2.1b. A circuit that solves relation (2.11) is constructed for this purpose.

The use of infralow-frequency equipment imposes major constraints on the frequencies of the simulated signals. The actual frequency values are limited to a few tens of hertz. The introduction of a nonunity time scale during simulation eliminates the possibility of working with real signal processors on signals picked up from radiant-energy detectors.

A number of modern analog computers have frequency responses that allow the investigation of the operation of modulators without introducing a time scale. For example, type EMU-10 electronic simulation equipment can be used to obtain sinusoidal voltages at frequencies on the order of a few thousand hertz. Furthermore, the elementary logic operations that analog computers are capable of performing make it possible to construct model modulators without additional sets of equipment such as the NGPK [low-frequency periodic oscillator], the use of which always entails additional difficulties in trigger synchronization.

Electronic and electromechanical function generators make it possible to obtain models of very simple modulators relatively easily. For example, if a function corresponding to the signals picked up from a modulator of the "uniform grating" type is superposed on the field of an electromechanical function generator, signals corresponding to modulators of the "uniform grating" and "nonuniform grating" types can be obtained from the generator's output by varying the value of

the control voltage according to a prespecified law. If the control voltage obeys a linear law, the repetition period of rectangular voltage pulses that simulate the transmitting sectors of a modulating disk will be constant. When use is made of a control voltage whose variation is nonlinear, the voltage-pulse repetition period at the output of the function generator will not be constant and will be determined by the law that governs the control voltage.

Exact assembly of the transmission function of a modulating disk cannot be accomplished, even when the simplest raster pattern is used, because no function generator makes it possible to create a pulse edge close to a rectangular one. A way out of this situation can be found if a sinusoidal voltage at the fundamental of the maximum amplitude is produced in the analog computer by using equation (2.24) and a circuit after Fig. 2.4 (for most analog computers, the peak voltage amplitude is 100 V). By using output-voltage limiters it is possible to obtain rectangular pulses in practice.

A sweep-frequency generator circuit must be used to model disks of the "nonuniform grating" type. This circuit can be constructed on the basis of equation (2.24) and the circuit in Fig. 2.4. The only difference is that the law governing the variation of the coefficient a must be calculated according to the law $\omega=\omega(t)$, and this law must be implemented in a function generator. The quantity a (see Fig. 2.4) is represented by potentiometer 1; therefore, a function generator must be installed in place of the potentiometer. Since a change in a will lead to a change in the amplitude of the output voltage, we will need still another function generator to ensure a constant amplitude of the sinusoidal voltage.

In many cases the law governing the radiant flux need not be reproduced exactly by the modulator. For example, if selective converters operating on signals received from a radiant-energy detector are tuned to the fundamental frequency, then there is no need to achieve an exact match between the form of the simulating signal

and the theoretical form. It suffices to use only the first harmonic or a signal close to it in form.

2.3. Simulation of Optical Systems for Measuring the Angular Coordinates of Radiating Objects

The simulation of optical systems for measuring the angular coordinates of radiating objects can be carried out by two methods. The first consists in drawin up a general equation for a system and then simulating it. In the second method, the equations of individual elements in the system are put together, a model is constructed for each element, and the resultant schemes are switched according to a block diagram.

Each of these simulation methods has its own advantages and drawbacks. The first method makes it possible to get by with a minimal number of decision elements in the analog computer, but at the same time requires correction of the values of many coefficients of the model when even one parameter of the real device changes. Although less economical, the second method does makes it possible easily to compensate for the characteristics of individual elements and of an entire device, and simplifies the analysis and synthesis of the equipment as a whole. Simulation using the second method actually leads to an electronic breadboard model of the system and may be called electronic breadboarding.

The need to introduce a time scale due to the limited frequency responses of analog computers arises in the construction of a breadboard or a circuit for solving the overall equation of a system. The introduction of a time scale limits the use of actual selective nodes of a system,but all transients, like steady states, can not only be view with a cathode-ray display, but also recorded by means of mirror-galvanometer oscillographs or recorders.

Before undertaking simulation, we must determine the range of questions that must be answered by the investigation, for the circuit

depends on this. In many cases it is advisable to linearize the equations to be simulated. When linear equations are implemented, the need vanishes for strict scaling. This greatly expands the possibility of varying the parameters.

In simulating angular-coordinate measuring systems, one must have the block diagram of the system and the transfer functions of its individual elements or the transfer function of the entire system.

The modeling of high-frequency filters of tuned amplifiers and narrow-passband filters is based on the analogy of a parallel tuned circuit. The equation that describes the processes which occur in the circuit has the form:

$$pE_0+\Delta fE_0+f^2\frac{1}{p}E_0=k_yE_{вх}, \qquad (2.25)$$

where p--the derivative symbol;
$E_{вх}$ and E_0--the input and output signals;
k_y--the gain;
Δf--the circuit's passband;
f--the circuit's natural frequency.

The machine time $t_м=m_t t$ is determined by the time scale m_t, which varies over a broad range. For modeling optical tracking systems, m_t may have values of 10^2-10^4.

With allowance for the time scale, the equation of a parallel tuned circuit is

$$p\bar{E}_0+\frac{1}{m_t}\Delta f\bar{E}_0+\frac{1}{m_t^2}f^2\frac{1}{p}\bar{E}_0=\frac{k_y}{m_t}\bar{E}_{вх}, \qquad (2.26)$$

where $\bar{E}_0$ and $\bar{E}_{вх}$ are the output and input voltages.

A block diagram of the solution of equation (2.26) by an analog computer is presented in Fig. 2.6. The generally accepted procedure presented in Ref. 23, in particular, is used to calculate the

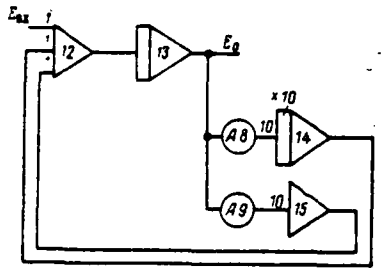

Fig. 2.6. Block diagram of the modeling of a tuned amplifier.

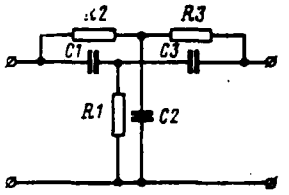

Fig. 2.7. Twin-T filter.

constants, which can be determined by using potentiometer-type voltage dividers, and to calculate the transfer ratios for each input of amplifiers.

Twin-T RC filters are widely used in optoelectronic devices. The transfer function of the filter shown in Fig. 2.7 has the form

$$W(p)=\frac{T_1T_2T_3p^3+T_1(T_{23}+T_3)p^2+(T_1+T_{13})p+1}{T_1T_2T_3p^3+[T_1(T_{23}+T_3)+T_2(T_1+T_{13}+T_3)]p^2+(T_1+T_{13}+T_{23}+T_3)p+1}, \quad (2.27)$$

where $T_1=R_1C_1$, $T_2=R_2C_2$, $T_3=R_3C_3$, $T_{13}=R_1C_3$, and $T_{23}=R_2C_3$.

To obtain the best selective properties in a filter, the relations between the parameters of branches of the bridge are selected as follows:

$$R_2=R_3=R,\ C_1=C_3=C,\ R_1=\frac{R}{2},\ C_2=2C$$

The nominal values of R and C are adopted on the basis of the condition $RC=1/\omega$. With allowance for the foregoing, the equation for a twin-T filter reduces to the form

$$(p^3+5\omega p^2+5\omega^2p+\omega^3)E_0=(p^3+\omega p^2+\omega^2p+\omega^3)E_{in}. \quad (2.28)$$

A block diagram of the modeling of equation (2.28) is shown in Fig. 2.8.

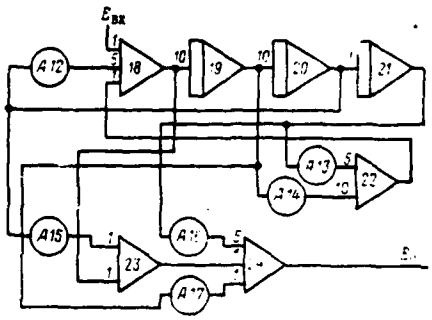

Fig. 2.8. Block diagram of the modeling of a twin-T filter.

Low-frequency filters usually contain only a capacitor and a resistor and are first-order inertial elements. The transfer function of a lf filter is

$$W(p)=\frac{1}{1+Tp} \qquad (2.29)$$

where T=RC.

Circuits of diode-type level limiters or the diodes found in most machines can be used as detectors in analog computers. The block diagram of the modeling of a detector and a lf filter is presented in Fig. 2.9.

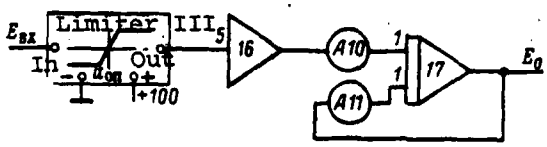

Fig. 2.9. Block diagram of the modeling of a detector and a lf filter.

Delay lines or constant-delay circuits can be implemented in special devices called time-delay units. The relation between the input and output quantities of a time-delay unit is given, in the ideal case, by the expression

$$E_0(t)=E_{вх}(t-T_0)$$

where T_0 is the delay time.

The output quantity of a delay unit usually exactly duplicates the input quantity, but with a time-shift of T_0. Recurrent networks consisting of passive and active two-terminal-pair networks that simulate long lines are used as time-delay units. Passive networks using RC elements have an extremely limited range of delay times and do not allow continuous variation of the delay time. Many analog computers are equipped with special delay devices based on capacitors. The present value of the output quantity is continuously stored in a capacitor-type memory, and is continuously pulled from it after a specified delay time T_0. The capacitors are switched by means of stepping switches.

It is advisable to use magnetic recording for delays of over 50 s. When the magnetic recording principle is used, the need arises for frequency modulation of the recorded signal and subsequent demodulation. This complicates the modeling circuit.

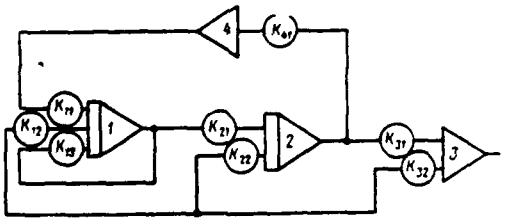

Fig. 2.10. Block diagram of the modeling of an adjustable delay.

A general-purpose delay circuit is shown in Fig. 2.10 [10]. In drawing up this circuit, use was made of a transfer function that reproduces the first two terms of the expansion of e^{-pT_0} into a fractional Pade series:

$$e^{-pT_0}\cong W(p)=1-\frac{12pT_0}{p^2T_0^2+6pT_0+12}. \qquad (2.30)$$

For the circuit shown, the transfer ratios of the amplifiers are related to the delay time by the equations $k_{22}=\frac{12}{T_0}$, $k_{13}=\frac{6}{T_0}$, $k_{21}k_{11}k_{41}=\frac{12}{T_0^2}$, $k_{21}k_{12}=k_{22}k_{13}$. The time delay T_0 can be changed by changing the transfer ratios of the amplifiers at different inputs. The circuit makes it possible to vary the delay time from 0.05 to 100 s.

A circuit that puts out a sinusoidal voltage at a frequency is used to simulate a reference generator. To do this, we construct a circuit for solving the equation $y''+\alpha y=0$ (see Fig. 2.4). If two reference voltages phase-shifted by an angle $\pi/2$ must be produced, then an additional inverting amplifier with a transfer ratio $1/\omega$ is used. A diagram of the simulation of a reference generator that puts out two voltages phase-shifted by an angle $\pi/2$ is shown in Fig. 2.11.

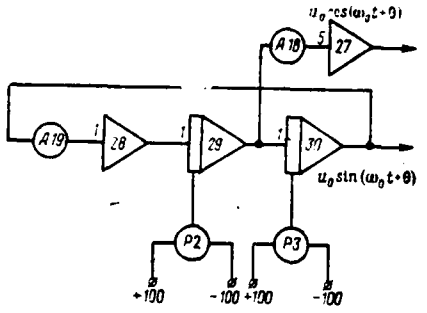

Fig. 2.11. Block diagram of the modeling of a reference generator.

Phase detectors convert the difference of two phases of harmonic oscillations into a voltage. The output voltage of a phase detector usually is expressed by a harmonic function of the phase difference having a maximum value proportional to the amplitude of one of the input signals:

$$E_0=E_{вх}\cdot U_0\sin\Phi. \qquad (2.31)$$

One multiplier unit is needed to implement equation (2.31) on an analog computer. In most computer electronic multipliers operate on the equation

$$z=-10^{2}xy$$

where 10^{2} is the transfer ratio of the multiplier unit.

A block diagram of the modeling of a phase detector and filter is presented in Fig. 2.12.

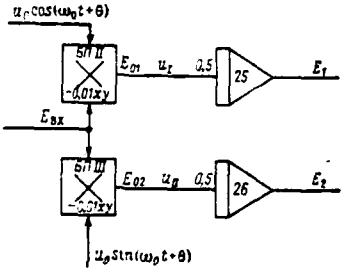

Fig. 2.12. Block diagram of the modeling of a phase detector and filter.

General recommendations for modeling the operation of modulators were given in the previous section. As an illustration, let us consider a model of an optical tracking system with the modulating disk shown in Fig. 2.1b. The purpose of the simulation is to determine the effect of the fabrication imprecision of the modulating disk on the output signals of the tracking system.

The initial data for modeling are:

--the number of pairs of sectors of the modulating disk is z=6;

--the rotational velocity is Ω=452 rad/s;

--the tuned amplifier is tuned to the first harmonic of the carrier frequency;

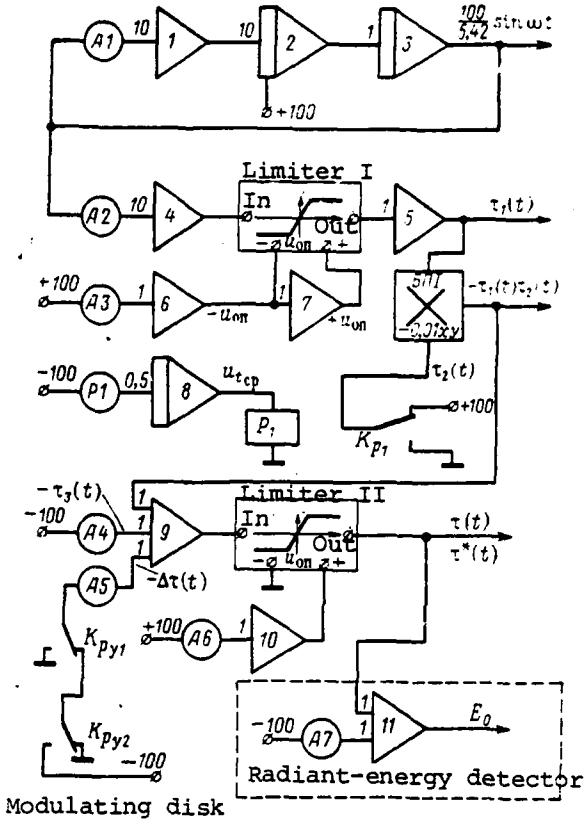

Fig. 2.13. Block diagram of a model of an optical tracking system.
Key: (a) limiter

--the passband of the tuned amplifier is $\Delta\omega=0.15\omega$;

--the radiant-energy detector and the preamplifier are no-lag elements;

--the error signal amplifier is equipped with a twin-T RC filter.

Since $\omega=2z\Omega=2\times6\times452=5420$ rad/s, the passband of the tuned amplifier is $\Delta f=2\Delta\omega\approx1630$ rad/s. The time scale $m_t=10^3$ was introduced during breadboarding of the optical tracking system.

The model of the modulating disk is created according to formula (2.11); it is shown in Fig. 2.13. The original relation for generating

$\tau_1(t)$ is realized at amplifiers 1, 2, and 3. When t=0, a quantity A_ω equal to 100 V is specified in the initial conditions at the output of amplifier 2. The amplitude of the sinusoid at the output of amplifier 3 will be $\frac{100}{\omega}m_t=\frac{100}{5.42}$. The value of the transfer ratio of potentiometer A_1 is $\alpha_1=0.294$, while the transfer ratios of amplifiers 1 and 2 are 10. This ensures that the specified frequency ω is produced.

Together with potentiometer A_2, amplifier 4 ensures the generation of a sinusoidal voltage with a 100-V amplitude ($\alpha_2=0.542$, and the transfer ratio of amplifier 4 is 10). A level limiter is used to produce near-rectangular signals. The limiting level is assumed to be 0.2, i.e., the reference voltages of amplifiers 6 and 7 respectively are -20 and +20 V. Amplifier 5 prevents the multiplier unit from having any effect on the operation of the level limiter.

The function $\tau_1(t)$, which is obtained by means of a relay circuit, is generated at the output of amplifier 5. Up to a time $t=\frac{T_0 m_t}{2}$, the machine unit, i.e., 100 V, is supplied to the input of multiplier unit БПИ; the relay is triggered at a time $t=\frac{T_0}{2}m_t$ and supplies a zero potential to the input of the multiplier. The actuation time of the relay is set by varying the voltage supplied to the input of the integrator that controls the relay winding. The voltage at the input of integrator 8 is set by means of potentiometer P_1.

The product of the functions $\tau_1(t)$ and $\tau_2(t)$ is generated at the output of multiplier unit БПИ. The function $\tau_3(t)$ is generated by potentiometer-type divider A_4 with a transfer ratio of 0.2. A voltage corresponding to $\tau_1(t)\tau_2(t)$ is supplied to one of the inputs of adding amplifier 9, while a voltage corresponding to $\tau_3(t)$ is supplied to the other input. The function $\tau(t)=\tau_1(t)\tau_2(t)+\tau_3(t)$ is produced at the input of amplifier 9.

A relay circuit consisting of two control relays P_{y1} and P_{y2} is used to introduce the function $\Delta\tau(t)$. The actuation time of each

relay can be set by means of time counters (some analog computers contain control relays whose actuation time is set in time counters) or by means of integrators. The time when $\Delta\tau(t)$ appears is determined by the actuation of relay P_{y2}, and the time when it disappears is determined by the actuation of relay P_{y1}. Limiter II prevents the possible appearance of an elevated voltage due to inaccurate setting of the actuation time of relays P_{y2} and P_{y1}. The limiting level is assumed to be 40 V and is formed by means of potentiometer A_6 (α=0.4) and decoupling amplifier.10. The signal at the output of limiter II corresponds to the function $\tau(t)=\tau(t)+\Delta\tau(t)$.

The radiant-energy detector is represented by amplifier 11, which changes the phase of the input signal by 180°. The signal supplied from potentiometer A_7 (α=0.4) provides a zero level.

The circuit for simulating a tuned amplifier (see Fig. 2.6) uses four operational amplifiers. If we allow for the digital data and time scale adopted, the equation for the amplifier has the form

$$pE_0+1{,}63E_0+29.4\frac{1}{p}E_0=kE_{ax}. \qquad (2.32)$$

Potentiometer A_8 (α=0.294) regulates the tuning frequency ω, and potentiometer A_9 (α=0.163) ensures the required passband. The transfer ratio of integrator 14 is 100 (the transfer ratio for the input of 10 and the ratio 10 of the feedback circuit [sic]). Level limiter III with limiting levels 0 and +10 V was used as the detector.

The frequency responses of a low-frequency filter (a block diagram is presented in Fig. 2.9) are determined by potentiometer A_{11} (α=0.904), while the gain is determined by the values of the transfer ratios of decoupling amplifier 16 and potentiometer A_{10} (α=0.452).

An error-signal amplifier with a twin-T RC filter is modeled after the scheme in Fig. 2.8. The settings of the transfer ratios α_i of potentiometers A_i are summarized in the following table:

A_i	A_{12}	A_{13}	A_{14}	A_{15}	A_{16}	A_{17}
α_i	0,296	0,321	0,272	0,295	0,321	0,544

The transfer ratios of the potentiometers and the operational amplifiers were calculated with consideration for the time scale m_i and the frequency Ω.

The phase detectors are two multiplier units to which a voltage is fed from the T filter and the reference generator. Integrators with a transfer ratio of 0.5 were used as the filters, while a circuit for producing two harmonic voltages phase-shifted by an angle $\pi/2$ (see Fig. 2.11) was used as the reference generator. The transfer ratio of potentiometer A_{19} is $\alpha=0.204$, corresponding to $\Omega/m_2=0.452$ rad/s. Amplifier 27 and potentiometer A_{18} ($\alpha=0.442$) ensure that the quantity $\cos(\Omega t+\psi)$ is generated. Potentiometers P_2 and P_3 are used to introduce the initial conditions; the voltage across P_2 must correspond to $\Omega \cos \psi$, while that across P_3 must correspond to $\sin \psi$. Potentiometers P_2 and P_3 phase the reference generator.

The simulation and investigation of an optical tracking system are based on the output signals of each channel (the system remains open) successively. First a system with an ideal modulating disk is studied. Phasing of the reference generator ensures that a signal corresponding to the position of the radiation source in one of the measuring planes is generated at the output of the tracking system. In this case the voltage from one of the integrators (25 or 26) corresponds to a unit error (mismatch) signal, while the voltage from the other integrator is zero. The variation of the signals at the output of the terminal integrators (filters) characterizes the effect of the precision of fabrication of the modulating disk on the operation of the optical tracking system.

The availability of a breadboard of an optical system makes it possible to utilize relatively simply the methods of the theory of

accuracy of computing devices to investigate the accuracy of the operation of a system as a whole and to synthesize such a system, since the physical processes under study and the processes that occur in a breadboard are described by the same equations. The theory of the accuracy of computers manipulates the following basic concepts:

--An Ideal Device--a device that can reproduce a specified relation between output and input quantities with absolute accuracy.

--A Real Device--any actual device that is designed to implement a specified relation.

--The Error of a Computing Device--the difference between the output quantities of a real device and an ideal device when the input quantities have absolutely precise values. The total error due to the error of the computing device and to errors in the input of the initial data is called the total error in the output quantity.

Device errors due to the limited accuracy of the input of initial data and to errors associated with the limited precision of fabrication and operation of components are called primary errors.

If we are given an equation of the following type

$$y=f(x_i) \qquad (2.33)$$

where y is the sought function and x_i (i=1, 2, 3, ..., n) is the argument of the sought function, and the equation is to be used for solution by means of a computing device, then the structure of the computing device is selected so that the processes that occur within it are described by an equation analogous to the specified equation. A breadboard model of an equation or a system of equations is precisely such a device.

The equation of a computing device is represented as

$$\varphi=\varphi(\psi_f, q_s), \qquad (2.34)$$

where ψ_i--independent variables of the computing device which represent x_i;

q_s--constants of the computing device.

The input quantities ψ_i cannot be determined exactly. Moreover, the constants q_s also cannot be sustained exactly in the implementation of computing devices.

For a real computing device, equation (2.34) may be written as

$$\varphi' = \varphi(\psi_i + \Delta\psi_i,\ q_s + \Delta q_s), \qquad (2.35)$$

where φ' is the value of the function φ that corresponds to the actual ψ_i and q_s, and $\Delta\psi_i$ and Δq_s are the primary errors of the computing device. The difference between the functions φ and φ' by definition represents the error of the computing device:

$$\Delta\varphi = \varphi' - \varphi. \qquad (2.36)$$

Equation (2.36) is unsuitable for practical use because φ' is a nonlinear function of a large number of primary errors. This leads to a large volume of computations. The calculations use an approximate formula for $\Delta\varphi$ obtained by linearizing equation (2.36) with respect to the primary errors $\Delta\psi_i$ and Δq_s. Let us write the expression for the error $\Delta\varphi$ in expanded form:

$$\Delta\varphi = \varphi'(\psi_i + \Delta\psi_i,\ q_s + \Delta q_s) - \varphi(\psi_i, q_s). \qquad (2.37)$$

Since $\Delta\psi_i$ and Δq_s are small compared with ψ_i and q_s, by expanding the function $\varphi'(\psi_i+\Delta\psi_i,\ q_s+\Delta q_s)$ into a Taylor series and confining ourselves to the zero and first terms of the expansion, we can write the equation for a real computing device as follows:

$$\varphi'(\psi_i + \Delta\psi_i,\ q_s + \Delta q_s) = \varphi(\psi_i, q_s) + \sum_{i=1}^{n} \left(\frac{\partial\varphi'}{\partial\psi_i}\right)_0 \Delta\psi_i + \sum_{s=1}^{m} \left(\frac{\partial\varphi'}{\partial q_s}\right)_0 \Delta q_s. \qquad (2.38)$$

Hence, the error of the computing device is

$$\Delta\varphi=\sum_{i=1}^{n}\left(\frac{\partial\varphi'}{\partial\psi_i}\right)_0\Delta\psi_i+\sum_{s=1}^{m}\left(\frac{\partial\varphi'}{\partial q_s}\right)_0\Delta q_s, \qquad (2.39)$$

where $\left(\frac{\partial\varphi'}{\partial\psi_i}\right)_0$, $\left(\frac{\partial\varphi'}{\partial q_s}\right)_0$ are the partial derivatives of the function φ' into which the exact values of ψ_i and q_s are inserted.

The primary errors and partial derivatives must be known in order to use formula (2.39) for calculations. In most cases the primary errors are random quantities or random functions of time. As far as the partial derivatives are concerned, the presence of a breadboard makes it possible to seek them out extremely simply. A finite increment of the i-th independent variable or of the s-th parameter must be specified to determine the partial derivatives from the independent variables ψ_i and the constants q_s. The increment in the function φ' that is due to a change in ψ_i or q_s and that is referred to the value of the increment in the variable or parameter will be the approximate value of the partial derivative:

$$\left.\begin{aligned}\left(\frac{\partial\varphi'}{\partial\psi_i}\right)_0&\cong\left(\frac{\Delta\varphi'}{\Delta\psi_i}\right)_0;\\ \left(\frac{\partial\varphi'}{\partial q_s}\right)_0&\cong\left(\frac{\Delta\varphi'}{\Delta q_s}\right)_0.\end{aligned}\right\} \qquad (2.40)$$

Knowing the partial derivative makes it possible numerically to estimate the degree of influence of a change in design parameters and independent variables on an output quantity. Furthermore, if the partial derivatives and the static characteristics of the independent variables and design parameters are known, then it is possible to obtain probabilistic characteristics of automatic devices without constructing a probabilistic model of the system, by investigating a deterministic model alone--in this case, the breadboard.

CHAPTER 3

SPATIAL FREQUENCY CHARACTERISTICS OF MODULATORS

3.1. Analytical Determination of the Spatial Frequency Transfer Functions of Modulators

In using the spatial frequency method to investigate the transmission of information through modulators, we will assume that they are linear components. The linearity condition presupposes that the reaction of a given element to the sum of two two-dimensional signals is equal to the sum of the two-dimensional reactions to each signal separately. For example, if the input signal has the form

$$F(y, z)=aF_1(y, z)+bF_2(y, z) \qquad (3.1)$$

then the output signal for all values of a and b, including zero, will be

$$F(\eta, \xi)=aF_1(\eta, \xi)+bF_2(\eta, \xi) \qquad (3.2)$$

The frequency-shift theorem also can be applied to spatial filters. For a known weighting function $E_{\delta_0}(y, z)$ of a "zero" element located at the origin and a transparent element $E_{\delta_1}(y, z)$ shifted by amounts Δy and Δz respectively relative to the "zero" element, and provided that

$$E_{\delta}(y, z)=E_{\delta_0}(y+\Delta y, z+\Delta z) \qquad (3.3)$$

the Fourier transform will be defined by the expression

$$W_1(i\mu, i\nu)=\int_{-\infty}^{\infty}\int E_{\delta_1}(y, z)e^{-2\pi i(\mu y+\nu z)}\,dy\,dz. \qquad (3.4)$$

After replacing the variables

$$u=y+\Delta y,\ du=dy,\ v=z+\Delta z,\ dz=dv$$

equation (3.4) reduces to the form

$$W_1(l\mu, l\nu)=W_0(l\mu, l\nu)\times[2\pi(\mu\Delta y+\nu\Delta z)], \qquad (3.5)$$

where

$$W_0(l\mu, l\nu)=\int_{-\infty}^{\infty}\int E_{\delta_0}(y, z)\times[-2\pi(\mu y+\nu z)]\,dy\,dz,$$

$$\times(x)=e^{lx}.$$

The exponential term in formula (3.5) defines the spatial shift of the weighting function $E_{\delta_1}(y, z)$ relative to the function $E_{\delta_0}(y, z)$.

Rotation of the weighting function in image space leads to an analogous rotation of the transform of this function in frequency space.

Let the following weighting function be given in polar coordinates:

$$E_{\delta_1}(\varrho, \varphi+\alpha)=E_{\delta_0}(\varrho, \varphi), \qquad (3.6)$$

where $\rho=\sqrt{y^2+z^2}$ and $\varphi=\text{arctg } z/y$ respectively are the modulus and phase of the vector $\bar{\rho}$; and α is an angle that defines the location of a transparent element having a weighting function E_{δ_1} relative to the "zero" element.

The Fourier transform of the function E_{δ_1} will be defined as

$$W_1(l\theta, \psi-\varphi-\alpha)=W_0(l\theta, \psi-\varphi), \qquad (3.7)$$

where $\theta=\sqrt{\mu^2+\nu^2}$ and $\psi=\text{arctg } \nu/\mu$ respectively are the modulus and phase of the spatial frequency vector $\bar{\theta}$.

These properties, which can be used in the analysis of electronic filters, facilitate the process of analytical determination of the spatial frequency transfer functions [ПЧПФ] of spatial filters.

The spatial frequency transfer function of a modulating disk, like that of any multidimensional filter, is determined by the direct

Fourier transform of the disk's weighting function, which in this case corresponds to its transmission function $\tau(y, z)$. In general, the spatial frequency transfer function of modulating disks can be determined directly by calculating the two-dimensional Fourier transforms of the transmission function $\tau(y, z)$ of the entire disk:

$$W(l\mu, l\nu)=\int_{-\infty}^{\infty}\int\tau(y, z)\times[-2\pi(\mu y+\nu z)]\,dy\,dz \qquad (3.8)$$

in a cartesian coordinate system, and

$$W(l\theta, \psi)=\int_{0}^{R}\int_{0}^{2\pi}\tau(\varrho, \varphi)\times[-2\pi\theta\varrho\cos(\varphi-\psi)]\,\varrho d\varrho\,d\varphi \qquad (3.9)$$

in a polar coordinate system.

To do this we must know the function $\tau(y, z)$ or $\tau(\rho, \varphi)$, which depend on the transmission coefficient and the size, shape, number, and relative location of the transparent and nontransparent elements of the modulating disk.

In the general case, the function $\tau(y, z)$ varies according to a specific law along the y and z coordinates; however, it usually is a step function of the coordinates and is expressed by the relation

$$\tau(y,\ z)=\begin{cases}1 & \text{in the region of transparent elements;}\\ 0 & \text{in an opaque region;}\\ 1/2 & \text{in a semitransparent region.}\end{cases}$$

Therefore, a periodic transmission function is represented by the Fourier series

$$\tau(y, z)=\sum_{n=0}^{N}\sum_{m=0}^{M}C_{nm}\times[2\pi(n\mu y+m\nu z)], \qquad (3.10)$$

where

$$C_{nm}=\frac{1}{L_yL_z}\int_{0}^{L_y}\int_{0}^{L_z}\tau(y, z)\times[-2\pi(n\mu y+m\nu z)]\,dy\,dz;$$

Here L_y and L_z are the repetition periods (spacings) of transparent elements of the modulating disk along the y and z coordinates, respectively.

In many cases the solutions of integrals (3.8) and (3.9) turn out to be cumbersome, even when one harmonic component is determined; furthermore, this solution often is expressed in terms of special functions (cylindrical functions, gamma functions, etc.) which are inconvenient to deal with in spectral spatial analysis.

A method of determining the spatial frequency transfer function by using the transform properties considered above is the most convenient for modulating disks that have a periodic structure, i.e., when the transparent element are periodically repeated on the disk surface. In this case we determine the Fourier transform of the transmission function of one elementary transparent region, and then, using the frequency-shift theorem and the superposition principle, we determine the spatial frequency transfer function of the entire modulating disk. For example, if the Fourier transform of the transmission function $\tau_0(y, z)$ of a transparent element located at the origin yOz is $W_0(i\mu, i\nu)$ and the other transparent elements are separated from the "zero" element by $n\Delta y$ and $m\Delta z$, respectively (where n=1, 2, 3,..., N; m=1, 2, 3, ..., M), then the Fourier transform of the transmission function n of the m-th element will be

$$W_{nm}(i\mu, i\nu)=W_0(i\mu, i\nu)\times[2\pi(\mu n\Delta y+\nu m\Delta z)]. \quad (3.11)$$

According to the superposition principle, the spatial frequency transfer function of the entire modulating disk will be given by the expression

$$W(i\mu, i\nu)=W_0(i\mu, i\nu)\sum_{n=0}^{N-1}\sum_{m=0}^{M-1}\times[2\pi(\mu n\Delta y+\nu m\Delta z)]. \quad (3.12)$$

Let us consider several examples of the determination of the spatial frequency transfer functions of different types of modulating

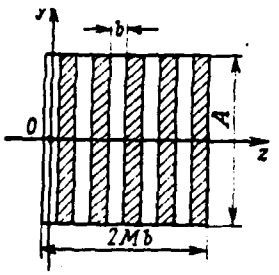

Fig. 3.1. Modulating disk with alternating transparent and opaque bands or strips.

disks, assuming that they are linear elements with known transmission functions $\tau(y, z)$ or $\tau(\rho, \varphi)$.

A modulating disk that consists of alternating equidistant transparent and opaque strips (Fig. 3.1) has a transmission function

$$\tau_0(y, z) = \begin{cases} 1 & |y| \leqslant \frac{A}{2}; \quad |z| \leqslant \frac{b}{2}, \\ 0 & |y| > \frac{A}{2}; \quad |z| > \frac{b}{2}, \\ & z - \text{any value} \quad y - \text{any value} \end{cases} \tag{3.13}$$

within a single transparent strip.

The Fourier transform of the transmission function of an axisymmetric transparent element located at the origin yOz will be defined as

$$W_0(l\mu, l\nu) = \int_{-\frac{A}{2}}^{\frac{A}{2}} \int_{-\frac{b}{2}}^{\frac{b}{2}} \varkappa[-2\pi(\mu y + \nu z)]\, dy\, dz = Ab \frac{\sin \pi\mu A}{\pi\mu A} \frac{\sin \pi\nu b}{\pi\nu b}. \tag{3.14}$$

Expression (3.14) is the modulus of the complex transfer function of the given transparent element, i.e.,

$$W_0(l\mu, l\nu) = [|W_0(l\mu, l\nu)|^2]^{\frac{1}{2}}. \tag{3.15}$$

Each successive transparent element of the disk is shifted by a distance 2b along the Oz axis relative to the preceding element. Based on relation (3.12), we find the spatial frequency transfer function of the modulating disk as a whole:

$$W(l\mu, l\nu) = W_0(l\mu, l\nu) \sum_{m=0}^{M-1} \varkappa(2\pi\nu m 2b) =$$
$$= W_0(l\mu, l\nu)\{1 + \varkappa(2\pi\nu 2b) + \varkappa(2\pi\nu 4b) + \ldots + \varkappa[2\pi\nu(M-1)2b]\}, \quad (3.16)$$

where the expression in brackets is a geometric progression the sum of whose terms is

$$\sum = \frac{1 - \varkappa[2\pi\nu(M-1)2b]}{1 - \varkappa(2\pi\nu 2b)} =$$
$$= \frac{\varkappa[-2\pi\nu b(M-1)] - \varkappa[2\pi\nu b(M-1)]}{\varkappa(-2\pi\nu b) - \varkappa(2\pi\nu b)} \cdot \frac{\varkappa[2\pi\nu b(M-1)]}{\varkappa(2\pi\nu b)} =$$
$$= \frac{\sin 2\pi\nu b(M-1)}{\sin 2\pi\nu b} \varkappa[2\pi\nu b(M-2)]. \quad (3.17)$$

With consideration for (3.14) and (3.17), the spatial frequency transfer function of the modulating disk is

$$W(l\mu, l\nu) = \sigma_0 \frac{\sin 2\pi\nu Mb}{2\pi\nu Mb} \cdot \frac{\sin \pi\mu A}{\pi\mu A} \times$$
$$\times \frac{1}{\cos \pi\nu b} \varkappa[2\pi\nu b(M-2)], \quad (3.18)$$

where σ_0=MAB [sic] is the area of the transparent portion of the modulating disk, and the exponential factor indicates that the origin Oyz does not coincide with the center of the modulating disk.

One quadrant of the modulus of the spatial frequency transfer function of a modulating disk with alternating transparent and opaque band is shown in Fig. 3.2. It follows from an examination of this figure that in space-frequency coordinates the maxima of the disk's spatial frequency response lie along the Oν coordinate axis at

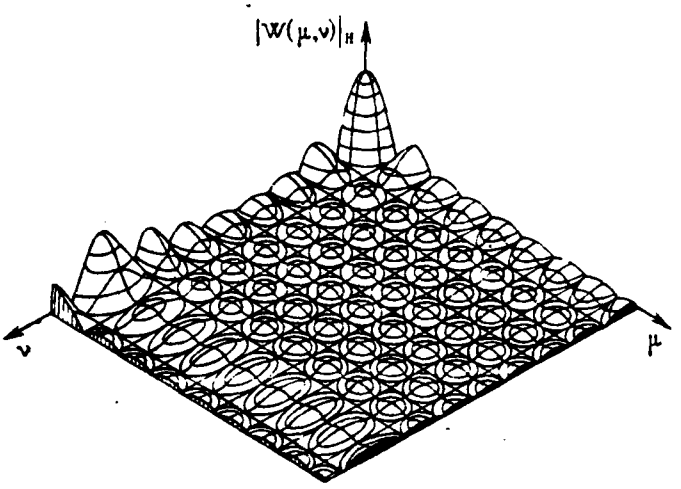

Fig. 3.2. Modulus of the spatial frequency transfer function of a modulating disk with alternating transparent and opaque bands (one quadrant).

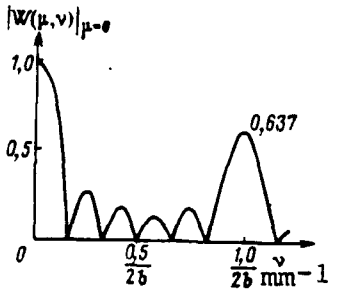

Fig. 3.3. One-dimensional cut of the modulus of the spatial frequency transfer function of a modulating disk with alternating transparent and opaque bands along the Oν coordinate axis.

$\nu=0$ and $\nu=\pm\frac{1}{2b}$, and respectively are equal to $|W(\mu, \nu)|_{\mu=\nu=0}=\sigma_0$ and $|W(\mu, \nu)|_{\mu=0,\ \nu=1/(2b)}=0.6376\sigma_0$. This is illustrated by Fig. 3.3.

The maximum at the origin of the frequency coordinates characterizes the sensitivity of the transfer function to a uniform

distribution of the radiant flux over the entire plane of the modulating disk. The other maxima (at $\mu=0$ and $\nu=\pm\frac{1}{2b}$) determine the sensitivity of the transfer function to a radiant-flux distribution such that the edge of the image of the thermal field runs parallel to the strips on the disk.

In order to improve the spatial discrimination of extended backgrounds with sharply defined edges, the transfer function of the modulating disk must not have maxima along the $O\mu$ or $O\nu$ frequency axes, but maxima that are shifted relative to them by some phase angle. This requirement is met by a modulating disk with a checkerboard arrangement of transparent and opaque squares, the dimensions of each of which are commensurate with the diameter of the optical system's circle of confusion.

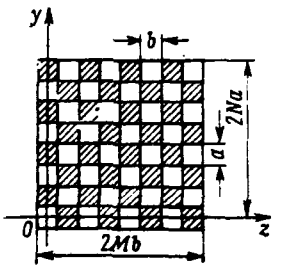

Fig. 3.4. Modulating disk with a checkerboard pattern of equal-sized transparent and and opaque elements.

For a modulating disk with a checkerboard pattern of equal-sized transparent and opaque elements (Fig. 3.4), the transmission function of a "zero" transparent element is

$$\tau_0(y, z)=\begin{cases} 1 \text{ when } |y|\leqslant\frac{a}{2};\ |z|\leqslant\frac{b}{2}; \\ 0 \text{ when } |y|>\frac{a}{2};\ |z|>\frac{b}{2}. \end{cases}$$

The spatial frequency transfer function of the element is a two-dimensional Fourier transform:

AD-A115 650 FOREIGN TECHNOLOGY DIV WRIGHT-PATTERSON AFB OH F/G 17/5
TIME-FREQUENCY AND SPACE-FREQUENCY CHARACTERISTICS OF OPTICAL M--ETC(U)
MAY 82 L Z KRIKSUNOV, V I MEKHRYAKOV
UNCLASSIFIED FTD-ID(RS)T-1209-81 NL

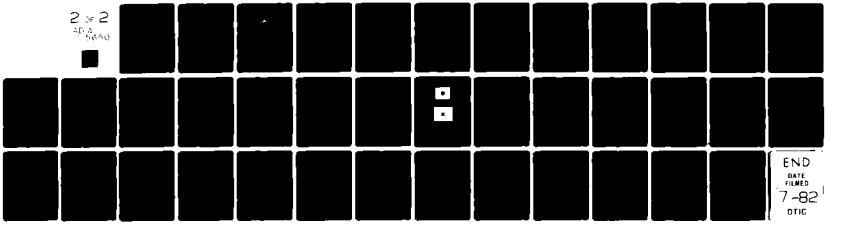

$$W_0(i\mu, i\nu) = \int_{-\frac{a}{2}}^{\frac{a}{2}} \int_{-\frac{b}{2}}^{\frac{b}{2}} \varkappa[-2\pi(\mu y + \nu z)]\, dy\, dz =$$

$$= ab \frac{\sin \pi\mu a}{\pi\mu a} \frac{\sin \pi\nu b}{\pi\nu b} \qquad (3.19)$$

and is the modulus of the spatial frequency transfer function of this element.

Transparent elements are shifted by distances 2mb, where m=0, 1, 2, ..., M, along the Oz axis relative to the zero element. Therefore, based on the frequency shift theorem, the Fourier transform of the transmission function of a row of transparent elements with center coordinates y=0 and z=2mb will be defined as

$$W_1(i\mu, i\nu) = Mba \frac{\sin 2\pi\nu Mb}{2\pi\nu Mb} \frac{\sin \pi\mu a}{\pi\mu a} \times$$

$$\times \frac{1}{\cos \pi\nu b} \varkappa[2\pi\nu b(M-1)]. \qquad (3.20)$$

by analogy with relation (3.18).

Transparent elements of the second row are shifted by an amount b along the Oz axis relative to the first row, and by an amount a relative to the Oy axis. The Fourier transform of the transmission function of two rows of a modulating disk will be written as

$$W_2(i\mu, i\nu) = W_1(i\mu, i\nu)\{1 + \varkappa[2\pi(\mu a + \nu b)]\}. \qquad (3.21)$$

Let us transform the expression in brackets:

$$1 + \varkappa[2\pi(\mu a + \nu b)] = \varkappa[\pi(\mu a + \nu b)] \times$$

$$\times \frac{\varkappa[-\pi(\mu a + \nu b)] + \varkappa[\pi(\mu a + \nu b)]}{2} 2 =$$

$$= 2\cos\pi(\mu a + \nu b)\varkappa[\pi(\mu a + \nu b)]. \qquad (3.22)$$

The spatial frequency transfer function of two rows of a modulating disk is

$$W_2(i\mu, i\nu)=2Mba\,\frac{\sin 2\pi\nu Mb}{2\pi\nu Mb}\,\frac{\sin \pi\mu a}{\pi\mu a}\times$$
$$\times\frac{\cos\pi(\mu a+\nu b)}{\cos\pi\nu b}\times[\pi\mu a+\pi\nu b(2M+1)]. \qquad (3.23)$$

The first two rows of transparent and opaque elements of the modulating disk repeat along the Oy axis with a period $2a$. Hence, the spatial frequency transfer function of the modulating disk as a whole will be

$$W(i\mu, i\nu)=W_2(i\mu, i\nu)\{1+\varkappa(2\pi\mu 2a)+\varkappa(2\pi\mu 4a)+$$
$$+\ \ldots\ +\varkappa[2\pi\mu(N-1)2a]\}. \qquad (3.24)$$

After inserting the value of the function $W_2(i\mu, i\nu)$ and performing some simple transformations, we get the final form of the spatial frequency transfer function of a modulating disk with a checkerboard pattern of transparent and opaque sectors:

$$W(i\mu, i\nu)=\sigma_0\,\frac{\sin 2\pi\mu Na}{2\pi\mu Na}\,\frac{\sin 2\pi\nu Mb}{2\pi\nu Mb}\times$$
$$\times\frac{\cos\pi(\mu a+\nu b)}{\cos\pi\mu a\cdot\cos\pi\nu b}\times\{\pi[\mu(2N+1)a+\nu(2M+1)b]\}, \qquad (3.25)$$

where $\sigma_0=2MNab$ is the area of the transparent portion of the modulating disk.

One quadrant of the modulus of the spatial frequency transfer function of the modulating disk in question is shown in Fig. 3.5. The maxima of the spatial frequency transfer function correspond to the spatial frequencies $\mu=0$, $\nu=0$, and $\mu=\pm\frac{1}{2a}$, $\nu=\pm\frac{1}{2b}$ and have values of σ_0 and $0.405\sigma_0$. The normalized amplitude spatial-frequency response is shown in Fig. 3.6 in a cross section with respect to the $O\nu$ axis, which is at an angle $\alpha=\text{arctg}\ a/b$ to the $O\mu$ axis.

As for the previous modulating disk, the transfer function of a disk with a checkerboard pattern of transparent and opaque squares is very sensitive to a uniform distribution of the radiant flux over the entire area of the modulating disk. The presence of maxima at $\mu=\pm\frac{1}{2a}$ and $\nu=\pm\frac{1}{2b}$ indicates the good sensitivity of the transfer

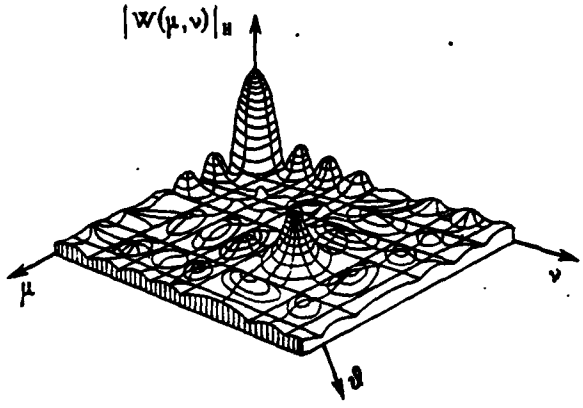

Fig. 3.5. Modulus of the spatial frequency transfer function of a modulating disk with a checkerboard pattern of equal-sized transparent and opaque elements (one quadrant).

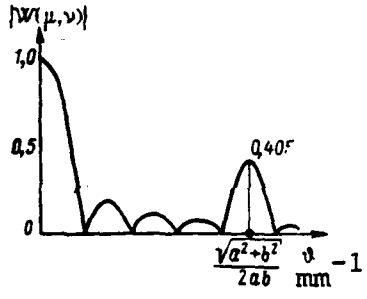

Fig. 3.6. One-dimensional cut of the modulus of the spatial frequency transfer function of a modulating disk with a checkerboard pattern of transparent and opaque elements along the Oϕ coordinate axis, directed at an angle of 45° to the Oμ and Oν axes.

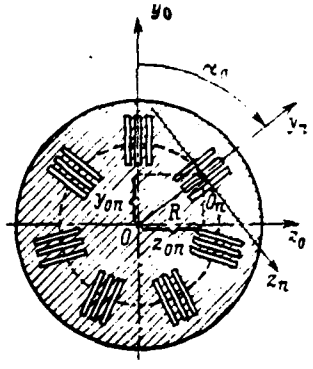

Fig. 3.7. A specially shaped modulating disk.

function to sharply defined edges of the background formation, which are positioned at an angle α=arctg a/b to the axis of the image plane.

If the modulating disk considered above scans along the Oy or Oz axis, then the incidence of a radiant flux from an extended background with clearly defined edges parallel to these axes does not lead to modulation of this flux. This cannot be said of a modulating disk with alternating transparent and opaque bands.

The modulating disk shown in Fig. 3.7 can be represented as a set of N modulating disks with transparent and opaque bands. These bands are expanded by an angle α_0 with respect to each other and are at the following distance from the center of the disk:

$$R=\sqrt{y_{0n}^2+z_{0n}^2},$$

where y_{0n} and z_{0n} are the coordinates of the coordinate centers of the n-th set of bands.

In Oy_nz_n coordinates, the transfer function of the n-th set of bands will be given by the expression

$$W_{0n}(i\mu, i\nu)=MbA\frac{\sin 2\pi\nu Mb}{2\pi\nu Mb}\frac{\sin \pi\mu A}{\pi\mu A}\times$$
$$\times\frac{1}{\cos \pi\nu b}\times[2\pi\nu b(M-1)]. \qquad (3.26)$$

In the Oyz coordinate system, the spatial frequency transfer function of the same n-th set of bands is

$$W_n(i\mu, i\nu)=W_{0n}(i\mu', i\nu')\times[-2\pi R(\mu'+\nu')], \quad (3.27)$$

where

$$\mu'=\mu\sin n\alpha_0, \quad \nu'=\nu\cos n\alpha_0.$$

According to the superposition principle, the spatial frequency of the entire modulating disk is defined by the sum

$$W(i\mu, i\nu)=\sum_{n=1}^{N}W_n(i\mu, i\nu)=\sum_{n=1}^{N}W_{0n}(\mu\sin n\alpha_0+\nu\cos n\alpha_0)\times$$
$$\times\times[-2\pi R(\mu\sin n\alpha_0+\nu\cos n\alpha_0)]. \qquad (3.28)$$

For N=6 the spatial frequency transfer function of the modulating disk is expressed by a modulus and has the form

$$W(l\mu, l\nu)=2\sigma_0\left(\frac{\sin \pi\mu A}{\pi\mu A}\cos 2\pi\mu R+2\,\frac{\sin \sqrt{3}\,\pi\nu Mb}{\sqrt{3}\,\pi\nu Mb}\times\right.$$

$$\left.\times\frac{\sin\frac{\pi}{2}\mu A}{\frac{\pi}{2}\mu A}\,\frac{\cos \sqrt{3}\,\pi\nu R\cos \pi\mu R}{\cos\frac{\sqrt{3}}{2}\pi\nu b}\right), \qquad (3.29)$$

where σ_0=MbA is the total transparent area of one n-th set of bands.

For odd N, the spatial frequency transfer function of the modulating disk is a complex function. For example, for N=7 we have

$$W(i\mu, l\nu)=\sigma_0\left[\frac{\sin \pi A\mu}{\pi A\mu}\times(-2\pi\mu R)+\right.$$

$$+2\left(\frac{\sin 2a_1\pi Mb\nu}{2a_1\pi Mb\nu}\,\frac{\sin c_1\pi A\mu}{c_1\pi A\mu}\,\frac{\cos 2a_1\pi R\nu}{\cos a_1\pi b\nu}\times(-2c_1\pi R\mu)+\right.$$

$$+\frac{\sin 2a_2\pi Mb\nu}{2a_2\pi Mb\nu}\,\frac{\sin c_2\pi A\mu}{c_2\pi A\mu}\,\frac{\cos 2a_2\pi R\nu}{\cos a_2\pi b\nu}\times(-2c_2\pi R\mu)+$$

$$\left.+\frac{\sin 2a_3\pi Mb\nu}{2a_3\pi Mb\nu}\,\frac{\sin c_3\pi A\mu}{c_3\pi A\mu}\,\frac{\cos 2a_3\pi R\nu}{\cos a_3\pi b\nu}\times(-2c_3\pi R\mu)\right], \qquad (3.30)$$

where

$$a_1=\sin\frac{\alpha_0}{2}; \qquad c_1=\cos\frac{\alpha_0}{2};$$

$$a_2=\sin\alpha_0; \qquad c_2=\cos\alpha_0;$$

$$a_3=\sin\frac{3}{2}\alpha_0; \qquad c_3=\cos\frac{3}{2}\alpha_0.$$

In the general case, for any odd value of N the spatial frequency transfer function of the modulating disk in question is given by the relation

$$W(l\mu, l\nu)=\sigma_0\left\{\frac{\sin \pi A\mu}{\pi A\mu}\times(-2\pi\mu R)+\right.$$

$$\left.+\sum_{n=1}^{\frac{N-1}{2}}\left[\frac{\sin 2a_n\pi\nu Mb}{2a_n\pi\nu Mb}\,\frac{\sin\pi\mu c_n A}{\pi\mu c_n A}\,\frac{\cos 2\pi\nu a_n R}{\cos\pi\nu a_n b}\times(-2c_n\pi\mu R)\right]\right., \qquad (3.31)$$

where

$$a_n = \sin\frac{n\pi}{N}; \quad c_n = \cos\frac{n\pi}{N}; \quad n = 1, 2, \ldots, N.$$

The modulating disk considered differs favorably from a "checkerboard"-type modulating disk in that it has better spatial filtering. On this disk individual modulating bands are inclined toward the radii that pass through the centers at different angles; therefore, each band cuts off the target image at an angle somewhat different from its neighbor. When a straight edge of the background is incident on the plane of the disk, just one band in each group can turn out to be parallel to this edge, and the other bands will intersect it an inclined angles. This enhances the process of spatial discrimination, since the degree of background suppression is directly proportional to the angular deflection of the bands from the corresponding radial lines.

For circular modulating disks the analytical representation and transformations of the original transparency functions are carried out in a polar coordinate system. Since the image plane has coordinates ρ and φ, which are related to the cartesian coordinates by the equations

$$\rho = \sqrt{y^2 + z^2}; \quad \varphi = \operatorname{arctg}\frac{z}{y}, \qquad (3.32)$$

and the Fourier transform of the transmission function is expressed in terms of θ and φ, so that

$$\theta = \sqrt{\mu^2 + \nu^2}; \quad \phi = \operatorname{arctg}\frac{\nu}{\mu}, \qquad (3.33)$$

where θ and ψ are the modulus and phase of the spatial frequency vector $\bar{\theta}$, respectively.

As an example, let us determine the spatial frequency transfer function of a modulating disk with alternating transparent and opaque sectors (see Fig. 1.1e). The transmission function of the "zero" transparent sector is written as

$$\tau_0(\varrho, \varphi) = \begin{cases} 1 & |\varphi| \leqslant \frac{\varphi_0}{2};\ \varrho < R; \\ 0 & |\varphi| > \frac{\varphi_0}{2};\ \varrho > R, \end{cases} \qquad (3.34)$$

where R--the radius of the modulating disk;

φ_0--the central angle of a transparent sector.

The Fourier transform of the transmission function of a transparent sector having a central angle $\varphi_0 = \pi/N$ has the form

$$W_0(l\theta, \psi) = \int_0^R \varrho\, d\varrho \int_{-\frac{\varphi_0}{2}}^{\frac{\varphi_0}{2}} \varkappa[-2\pi\theta\varrho\cos(\varphi-\psi)]\, d\varphi. \qquad (3.35)$$

We know [2] that the function $\varkappa[-z \sin \alpha]$ is the generating function for the Bessel functions:

$$\varkappa[-z\sin\alpha] = I_0(z) + 2\sum_{k=1}^{\infty} I_{2k}(z)\cos 2k\alpha - 2l\sum_{k=1}^{\infty} I_{2k-1}(z)\sin(2k-1)\alpha, \qquad (3.36)$$

where $I_K(z)$ is a k-th-order Bessel function of the first kind.

For our example,

$$\varkappa[-2\pi\theta\varrho\cos(\varphi-\psi)] = \varkappa\left[-2\pi\theta\varrho\sin\left(\frac{\pi}{2}+\varphi-\psi\right)\right] = I_0(2\pi\theta\varrho) + 2\sum_{k=1}^{\infty} I_{2k}(2\pi\theta\varrho)\cos 2k\left(\frac{\pi}{2}+\varphi-\psi\right) - 2l\sum_{k=1}^{\infty} I_{2k-1}(2\pi\theta\varrho)\sin(2k-1)\left(\frac{\pi}{2}+\varphi-\psi\right). \qquad (3.37)$$

Inserting expression (3.37) into formula (3.35) and integrating over φ, we obtain

$$W_0(\delta\theta, \psi) = \varphi_0 R^2 \frac{J_1(2\pi\theta R)}{2\pi\theta R} +$$
$$+4\sum_{k=1}^{\infty}\left[\frac{(-1)^k}{k}\cos 2k\psi \cdot \sin k\varphi_0 \int_0^R I_{2k}(2\pi\theta\varrho)\varrho\, d\varrho - \right.$$
$$\left. - i\,\frac{(-1)^k}{2k-1}\cos(2k-1)\psi \sin(2k-1)\frac{\varphi_0}{2}\int_0^R I_{2k-1}(2\pi\theta\varrho)\varrho\, d\varrho.\right.$$
(3.38)

The integrals in formula (3.38) reduce to the tabular values [2] through substitution of the variable $\rho = Rx$.

$$J_1 = \int_0^R I_{2k}(2\pi\theta\varrho)\varrho\, d\varrho = R^2 \int_0^1 I_{2k}(2\pi\theta Rx)x\, dx =$$
$$= \frac{1}{(2\pi\theta R)^2}\left[2k(2\pi\theta R) I_{2k}(2\pi\theta R) + S_{0,2k-1}(2\pi\theta R) - \right.$$
$$\left. - 2\pi\theta R I_{2k-1}(2\pi\theta R) S_{1,2k}(2\pi\theta R) + 2\frac{\Gamma(1+k)}{\Gamma(k)}\right], \quad (3.39)$$
$$J_2 = \int_0^R I_{2k-1}(2\pi\theta\varrho)\varrho\, d\varrho = R^2 \int_0^1 I_{2k-1}(2\pi\theta Rx)x\, dx =$$
$$= \frac{1}{(2\pi\theta R)^2}\left[(2k-1)(2\pi\theta R) I_{2k-1}(2\pi\theta R) + S_{0,2k-2}(2\pi\theta R) - \right.$$
$$\left. - 2\pi\theta R I_{2k-2}(2\pi\theta R) S_{1,2k-1}(2\pi\theta R) + 2\frac{\Gamma\left(k+\frac{1}{2}\right)}{\Gamma\left(k-\frac{1}{2}\right)}\right], \quad (3.40)$$

where $S_{p,q}(x)$ are Lommel's functions, and $\Gamma(y)$ are the gamma functions.

The rotation of a function in image space is known to lead to an analogous rotation of the transform function in frequency space. Therefore, in determining the Fourier transform of the tranmission function of the n-th transparent sector from the origin, the arguments of the cosines of expression (3.38) must take into consideration the phase shift $2n\varphi_0$, where n=0, 1, 2, ..., N-1 and N is the number of transparent sectors. The quantity $2\varphi_0$ is the angular repetition period of transparent sectors and is measured between radii drawn through the centers of adjacent sectors.

The Fourier transform of any n-th transparent sector has the form:

$$W_n(l\theta, \psi)=\varphi_0 R^2 \frac{I_1(2\pi\theta R)}{2\pi\theta R}+4\sum_{k=1}^{\infty}\left[\frac{(-1)^k}{k}\sin k\varphi_0\cos 2k(\psi-\right.$$

$$\left.-2n\varphi_0)J_1-l\frac{(-1)^k}{2k-1}\sin(2k-1)\frac{\varphi_0}{2}\cos(2k-1)(\psi-2n\varphi_0)J_2\right], \tag{3.41}$$

where the integrals J_1 and J_2 are determines from formulas (3.39) and (3.40), respectively.

After applying the superposition principle, we obtain the spatial frequency transfer function of a modulating disk with alternating transparent and opaque sectors:

$$W(l\theta, \psi)=\sum_{n=0}^{N-1}W_n(l\theta, \psi)=N\varphi_0 R^2\ \frac{I_1(2\pi\theta R)}{2\pi\theta R}+$$

$$+4\sum_{k=1}^{\infty}\frac{(-1)^k}{k}\sin k\varphi_0\cos 2k[\psi-(N-1)\varphi_0]\frac{\sin 4kN\varphi_0}{\sin 4k\varphi_0}J_1-$$

$$-l\frac{(-1)^k}{2k-1}\sin(2k-1)\frac{\varphi_0}{2}\cos(2k-1)[\psi-(N-1)\varphi_0]\times$$

$$\times\frac{\sin(2k-1)2N\varphi_0}{\sin(2k-1)2\varphi_0}J_2. \tag{3.42}$$

The first term of expression (3.42) characterizes the sensitivity of the transfer function to a uniform distribution of the radiant flux over the entire area of the modulating disk and does not have a significant effect on the transmission of small signals. The most characteristic features for analysis of a transfer function are its maxima, which are at spatial frequencies θ that are remote from the center of the frequency coordinates and that are determined by the second and third terms of formula (3.42).

As we see from the calculations presented above, the process of determining spatial frequency transfer functions entails considerable difficulties, even for modulating disks that have transparent elements of comparatively simple configuration. Furthermore, the expressions obtained for the spatial frequency transfer function are not very convenient when used for further spectral analysis of the

transmission of information through optoelectronic devices. It will be shown below that the location of the maxima of the spatial frequency transfer function in frequency space must be known in analyzing the transmission of information on radiating objects through modulating disks. It is difficult to obtain such data from the theoretical expressions of the spatial frequency transfer functions of most modulating disks. Therefore, experimental methods are used to investigate the spatial frequency transfer functions of modulating disks having elements of complex configuration.

3.2. An Experimental Method of Determining the Spatial Frequency Transfer Functions of Modulators

According to the classical theory of radiation, a light field can be described by using the vectors of electric field strength $\mathcal{E}(\bar{r}, t)$ and magnetic field strength $B(\bar{r}, t)$. In experimental studies of a light field the instruments react to the electric field. A Fourier series or integral is used to identify the four-dimensional equation for electric field strength, and this strength is treated as the sum of two complex components:

$$\mathcal{E}(\bar{r}, t)=\mathcal{E}^{+}(\bar{r}, t)+\mathcal{E}^{-}(\bar{r}, t). \qquad (3.43)$$

Both components, which are complex-conjugate to each other

$$\mathcal{E}^{-}(\bar{r}, t)=\mathcal{E}^{+*}(\bar{r}, t),$$

contain equivalent physical information and are called the complex strength or the complex amplitude of the light wave. These definitions will be used below in examining diffraction effects when modulating disks are irradiated with a parallel beam from a monochromatic source of coherent radiation.

Let us imagine that the modulating disk is a very simple diaphragm with an aperture having an area σ_0 and that it is located in a plane Q_1 (Fig. 3.8). When a plane monochromatic wave from a point source is incident on the modulating disk, a diffraction pattern can be observed on a screen located in plane Q_2.

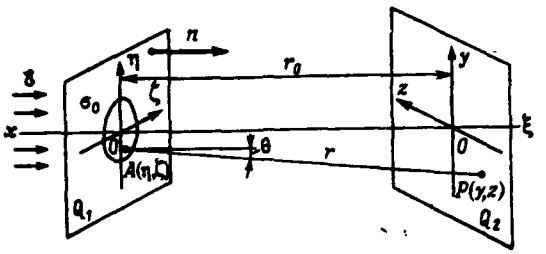

Fig. 3.8. Toward calculating the distribution of field strength in a diffraction pattern.

Kirchoff's formula [11] is used to calculate the complex strength $\mathcal{E}(x, y, z, t)$ in plane Q_2 for known strength of the light wave incident on the modulating disk:

$$\mathcal{E}(x, y, z, t)=\frac{1}{4\pi}\iint_{\sigma_0}\left\{\mathcal{E}(\xi, \eta, \zeta, t)\frac{\partial}{\partial n}\left[\varkappa(-kr)\frac{1}{r}\right]-\right.$$
$$\left.-\frac{\varkappa(-kr)}{r}\frac{\partial\mathcal{E}(\xi,\eta,\zeta,t)}{\partial n}\right\}d\sigma, \qquad (3.44)$$

where k=2π/λ--the wave number;

$\bar{n}$--the normal to the plane of the modulating disk;

r--the distance between points A and P.

This formula makes it possible to calculate the electromagnetic field at the observation point P when the field of the light wave is specified on an arbitrary surface.

Integral (3.44) is taken within the area of the transparent aperture on the assumption that the strength behind the opaque portion of the modulating disk is zero. It can be seen from Fig. 3.8 that the quantity r is defined by the expression

$$r^2=(x-\xi)^2+(y-\eta)^2+(z-\zeta)^2,$$

where

$$x^2+y^2+z^2=r_0^2.$$

In view of the fact that observation is done at a considerable distance from the modulating disk, we may assume

$$r^2-r_0^2=(r+r_0)(r-r_0)\approx 2r(r-r_0).$$

Then

$$r=r_0-\frac{x\xi+y\eta+z\zeta}{r_0}+\frac{\xi^2+\eta^2+\zeta^2}{2r_0}. \qquad (3.45)$$

A plane light wave incident on the plane of the modulating disk has the complex amplitude

$$\mathscr{E}(\xi,\eta,\zeta,t)=\mathscr{E}_0(\eta,\zeta)\varkappa[-(\omega t-k\xi)], \qquad (3.46)$$

and its derivative with respect to the direction of the normal $\bar{n}$ in the plane of the aperture, i.e., for $\xi=0$, is defined as

$$\left[\frac{\partial\mathscr{E}(\xi,\eta,\zeta,t)}{\partial n}\right]_{\xi=0}=\left[\frac{\partial\mathscr{E}(\xi,\eta,\zeta,t)}{\partial\xi}\right]_{\xi=0}=ik\mathscr{E}_0(\eta,\zeta)\varkappa(-\omega t). \qquad (3.47)$$

The other partial derivative in Kirchoff's formula (3.44) is expressed by the relation

$$\frac{\partial}{\partial n}\left[\frac{\varkappa(-kr)}{r}\right]_{\xi=0}=$$
$$=\frac{\partial}{\partial\xi}\left\{\frac{\varkappa\left[-kr\left(r_0-\frac{x\xi+y\eta+z\zeta}{r_0}+\frac{\xi^2+\eta^2+\zeta^2}{2r_0}\right)\right]}{r}\right\}_{\xi=0}. \qquad (3.48)$$

For small diffraction angles θ and large r that are much greater than the dimensions of the modulating disk (which always is the case in practice), the quantity r in the denominator of expression (3.48) may be replaced by r_0. Then derivative (3.48) will be written as

$$\frac{\partial}{\partial\xi}\left[\frac{\varkappa(-kr)}{r}\right]_{\xi=0}=\frac{ikr}{r_0^2}\varkappa\left[-k\left(r_0-\frac{y\eta+z\zeta}{r_0}+\frac{\eta^2+\zeta^2}{2r_0}\right)\right], \qquad (3.49)$$

and

$$\frac{\eta^2+\zeta^2}{2r_0}\leqslant\frac{d}{r_0},$$

where d is the diameter, or the linear dimension of the aperture of the modulating disk.

If the condition

$$\frac{d^2}{r_0}\ll\lambda,$$

is observed, then the last term in expression (3.49) may be ignored:

$$\frac{\partial}{\partial\xi}\left[\frac{\chi(-kr)}{r}\right]_{\xi=0}=\frac{ikr}{r_0^2}\chi\left[-k\left(r_0-\frac{y\eta+z\zeta}{r_0}\right)\right]. \quad (3.50)$$

With allowance for expressions (3.47) and (3.50), the complex amplitude of the light field intensity in the plane of the diffraction pattern will be given by the relation

$$\mathscr{E}(y,z)=\frac{(kr_1(\omega t-kr_1)}{2\pi r}\iint_{\sigma_0}\mathscr{E}_0(\eta,\zeta)\chi\left[-\frac{k}{r_0}(y\eta+z\zeta)\right]d\sigma. \quad (3.51)$$

In experimental research it may be assumed that the light field incident on the modulating disk is steady. Steadiness does not at all mean that the field is time-independent; on the contrary, the field usually oscillates extremely rapidly. This means that our data on the field do not change with time. In this case by steadiness we mean equal probability of the statistical description of the light beam with respect to a shift in time.

When a monochromatic light source is used, so that $k=2\pi/\lambda_0=\text{const}$, the expression in front of the integral is independent of the independent variables y and z, and since we are only interested in the spatial distribution of the complex amplitude of the light field's intensity, we will rewrite formula (3.51) as

$$\mathscr{E}(y,z)=A\iint_{\sigma_0}\mathscr{E}_0(\eta,\zeta)\chi\left[-2\pi\left(\frac{y}{\lambda_0 r_0}\eta+\frac{z}{\lambda_0 r_0}\zeta\right)\right]d\eta\,d\zeta. \quad (3.52)$$

where

$$A=\frac{ix(-kr_0)}{\lambda_0 r_0}.$$

Let us convert to the new independent variables by substitution: $\frac{y}{\lambda_0 r_0}=\mu$, $\frac{z}{\lambda_0 r_0}=\nu$. We will divide expression (3.52) by A, and we find that the normalized complex amplitude of a light wave in the plane of the diffraction pattern is the analog of the spatial frequency transfer function of a very simple modulating disk:

$$\mathscr{E}(i\mu, i\nu)=W'(i\mu, i\nu)=$$
$$=\int_{-\infty}^{\infty}\int \mathscr{E}_0(\eta, \zeta)x[-2\pi(\mu\eta+\nu\zeta)]\,d\eta\,d\zeta. \qquad (3.53)$$

In formula (3.53) the limits of integration extend to infinity on the assumption that the function $\mathscr{E}_0(\eta, \xi)=\mathscr{E}_0 e^{-ik\xi}$ is equal to zero outside the area of an elementary transparent element.

The modulating disks used in optoelectronic devices have a more complicated arrangement of a large number of transparent and opaque sectors. However, when a coherent radiation source is used as the irradiator, each transparent element may be represented as a separate coherent source.

When elementary waves are added, a time-stable pattern of illuminance distribution that has the form of alternating maxima and minima is produced in the plane of the diffraction pattern. Thus, when a wavefront emanates from a coherent radiation source, the diffraction effects represent the interference of the elementary waves originating from each elementary sector of the surface of the original wave [sic].

To prove the validity of using multiray interference with wavefront division to obtain the spatial frequency transfer functions of modulating disks, we will show how the light field is distributed

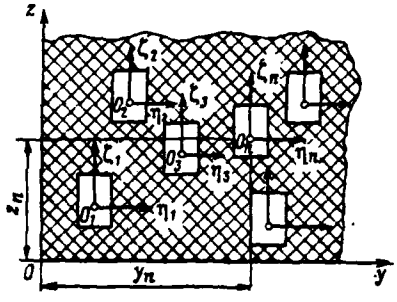

Fig. 3.9. Modulating disk with diffracting elements that are identically oriented in the plane of the disk.

in the interference pattern if the modulating disk has on its surface N transparent diffracting elements that are identically oriented in the plane of the disk (Fig. 3.9).

The coordinates of some diffracting point of the n-th transparent element are defined as

$$y=y_n+\eta, \quad z=z_n+\zeta. \tag{3.54}$$

The complex amplitude of the light wave in the diffraction pattern from the n-th transparent element is, according to (3.53),

$$\mathcal{E}_n(i\mu, i\nu)=\iint_{-\infty}^{\infty} x\{-2\pi[\mu(y_n+\eta)+\nu(z_n+\zeta)]\}d\eta\,dz. \tag{3.55}$$

Factors containing the quantities y_n and z_n may be removed from the integral sign, and, as a result of the interference effect, the complex amplitude of the light wave is equal to the sum of the complex amplitudes obtaining upon diffraction from each of the N elements of the modulating disk:

$$\mathcal{E}(i\mu, i\nu)=\sum_{n=1}^{N} x[-2\pi(\mu y_n+\nu z_n)]\times$$
$$\times\iint_{-\infty}^{\infty} x[-2\pi(\mu\eta+\nu\zeta)]\,d\eta\,d\zeta. \tag{3.56}$$

Thus, the distribution of the complex amplitude of a light wave is defined as the product of two factors:

$$\mathscr{E}(i\mu, i\nu)=\mathscr{E}_n(i\mu, i\nu)F(i\mu, i\nu), \qquad (3.57)$$

one of which, $\mathscr{E}_n(i\mu, i\nu)$, depends solely on the shape and size of the n-th individual transparent element, while the other, $F(i\mu, i\nu)$ characterizes the relative position of the transparent elements of the modulating disk with respect to each other, i.e., it reflects the frequency-shift and superposition principles. Hence, the use of diffraction effects and multibeam interference with wavefront division makes it possible to obtain experimentally the spatial frequency transfer functions of any modulating disks by measuring the illuminance in the interference pattern while the modulating disks are irradiated with a monochromatic parallel beam from a coherent radiation source.

We know that the complex amplitude of the light field intensity cannot be measured with recording instruments. Photoelectric devices that measure the energy parameters of the field usually are used as meters. In other words, they measure the square of the modulus of the light wave's amplitude:

$$E(\mu, \nu)=|\mathscr{E}(i\mu, i\nu)|^2. \qquad (3.58)$$

The sensor is located in the plane of the interference pattern and obeys a specific law in scanning over this plane. To improve resolution, during measurements the area of the sensor is made as small as possible, and the distance r_0 from the modulating disk to the interference pattern is made as large as possible. The scale of the spatial frequency is determined by the value of r_0 and the radiation wavelength according to the equation $m=1/(\lambda_0 r_0)$, which is constant for a monochromatic radiator.

Since the sensor measures the intensity of the light field in y and z coordinates (Fig. 3.8), we must multiply the coordinates of

plane Q_2 by a scaling factor in order to obtain a function that depends on the independent variables μ and ν:

$$\mu=my;\ \nu=mz$$

To eliminate errors in the measurement of the peak values of the function, we must have a radiation source with a time-constant light beam. It was demonstrated in the previous section that if the maximum value of the transmission function of the modulating disk is unity, then the spatial frequency transfer function has a maximum equal to the total area of the disk's transparent elements. In processing the experimental results it is best to deal with the normalized spatial frequency transfer function of the modulating disk, which can be defined as

$$|W(\mu, \nu)|_{\text{н}}=\left[\frac{E(\mu, \nu)}{E_{\max}}\right]^{1/2}, \qquad (3.59)$$

where $E(\mu, \nu)$--the measured value of the intensity function of the light field in the diffraction pattern for a given experiment;

E_{max}--the maximum value of the intensity of the light field in the given experiment.

A continuous-wave laser with a time-stable light beam, a high degree of coherence, and a high degree of monochromaticity is used as the light source. A block diagram of the experimental setup for determining the spatial frequency transfer function of modulating disks is shown in Fig. 3.10. In processing the measurements, the normalized value of the transfer function's modulus is defined as the mathematical expectation over discrete values of the illuminance at points of a plane. An estimate of the mathematical expectation is the arithmetic mean of the realizations of N successive measurements:

$$|W(\mu, \nu)|_H=\frac{1}{N}\sum_{n=1}^{N}\left[\frac{U_n(\mu, \nu)}{U_{n_{\max}}}\right]^{1/2}, \qquad (3.60)$$

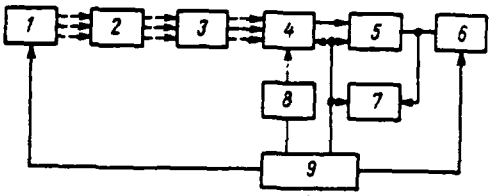

Fig. 3.10. Block diagram of the experimental setup for determining the spatial frequency transfer function of modulating disks: (1) radiation source; (2) optical collimator; (3) modulating disk; (4) sensor; (5) amplifier; (6) instrument; (7) oscillograph; (8) scanning mechanism; (9) power supply and control unit.

where $U_n(\mu, \nu)$--the value of the voltage of the instrument during the n-th measurement at a given point in the plane;

$U_{n_{max}}$--the maximum value of the voltage at the central maximum during the n-th measurement.

We will use several examples to demonstrate the experimental results and the degree of agreement between the experimental and theoretical data. If the modulating disk is a diaphragm with a circular aperture, then the diffraction pattern has a number of concentric circles after the disk is irradiated with a beam of parallel rays from a monochromatic coherent radiation source. The theoretical value of the spatial frequency transfer function of such a modulating disk is given by

$$W(\theta) = \sigma_0 \frac{I_1(2\pi\theta R)}{2\pi\theta R}, \qquad (3.61)$$

where σ_0--the aperture area;

r_0--the aperture radius;

θ--the modulus of the spatial frequency vector.

In Fig. 3.11 the solid lines indicate the theoretical moduli and the dashed lines the experimental normalized moduli of the spatial

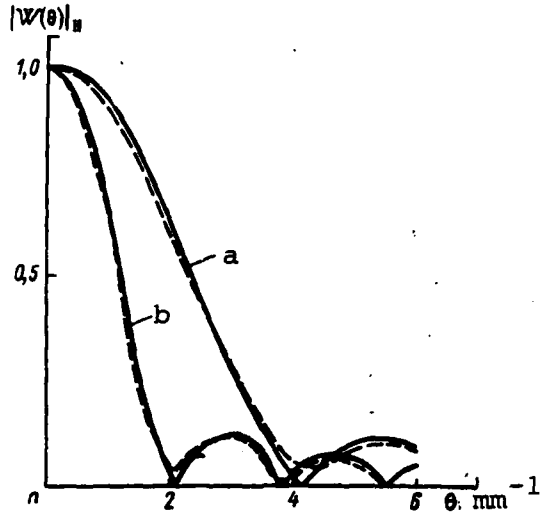

Fig. 3.11. One-dimensional cuts of the spatial frequency transfer functions of diaphragms with circular apertures: (a) d=0.3 mm; (b) d=0.6 mm.

frequency transfer functions of modulating disks with apertures having diameters of 0.3 and 0.6 mm. The experimental data are in good agreement with theoretical calculations and confirm the feasibility of experimental determination of the spatial frequency transfer function by the method described. Fig. 3.12 shows the distribution of illuminance in the interference pattern at the output of a modulating disk with 12 transparent and opaque sectors.

The interference pattern at the output of a modulating disk with a checkerboard pattern of transparent and opaque square elements (Fig. 3.13) shows the distribution of maxima in the space-frequency domain. Shown in Fig. 3.14 are the one-dimensional normalized spatial frequency responses, as calculated theoretically (curve a) and as obtained experimentally (curve b) at an angle of 45° to the coordinate axes.

For circular modulating disks, it is convenient to represent the spatial frequency transfer function as the product:

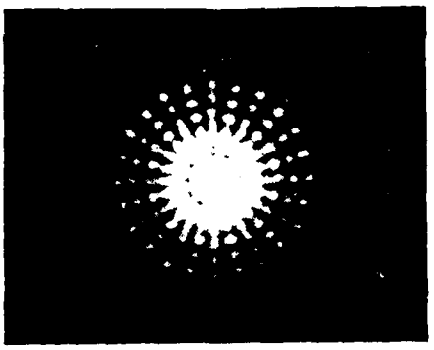

Fig. 3.12. Distribution of illuminance in the interference pattern at the output of a modulating disk with alternating transparent and opaque sectors.

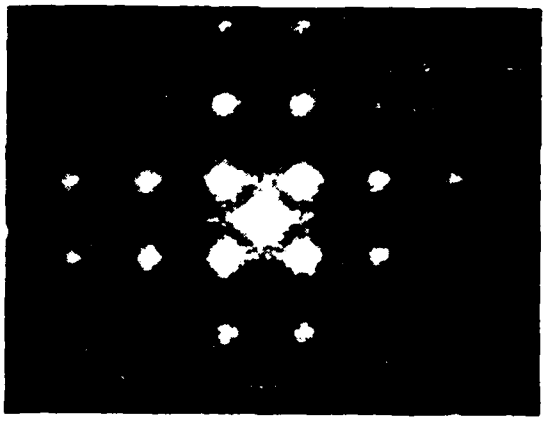

Fig. 3.13. Distribution of illuminance in the interference pattern at the output of a modulating disk with a checkerboard pattern of transparent and opaque elements.

$$W(i\theta, \psi) = W(i\theta) \cdot W(\psi), \qquad (3.62)$$

where $W(i\theta)$ and $W(\psi)$ respectively are the amplitude and phase spatial frequency responses.

Thus, for the modulating disk shown in Fig. 1.1j, which is a circle with an asymmetric arrangement (relative to the center) of

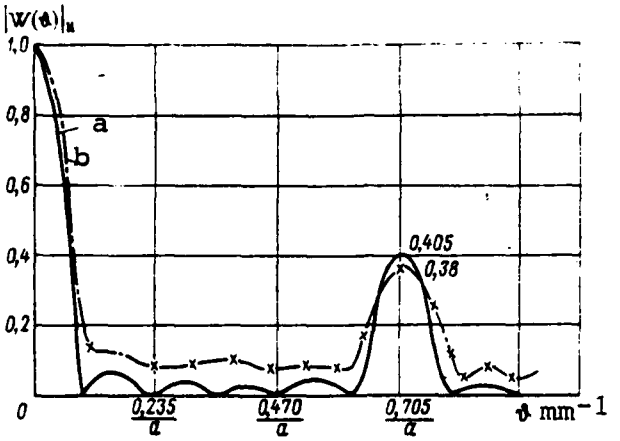

Fig. 3.14. One-dimensional normalized amplitude spatial frequency response of a modulating disk with a checkerboard pattern of transparent and opaque elements: (a) theoretically calculated; (b) experimental.

of transparent and opaque elements, the normalized modulus of the spatial frequency transfer function reduces to the form:

$$|W(\theta, \psi)|_H = |\cos 2\pi\theta\gamma| \exp\left(-\pi\theta\frac{1}{2}\right) + |W_1(\Delta\theta)|\, W_1(\psi). \tag{3.63}$$

In formula (3.63) the first term determines the shape and width of the maximum near the origin of frequency coordinates, while the second term describes the amplitude, shape, and width of the maxima of the spatial frequency transfer function of the disk at higher spatial frequencies. The functions in formula (3.63) can be approximated by some simple relations:

$$|W_1(\Delta\theta)| = A \exp[-\gamma(\theta-\theta_0)^2], \tag{3.64}$$

$$W_1(\psi) = \sin^2\frac{N}{2}\psi, \tag{3.65}$$

where the parameters γ and A depend on the dimensions, shape, and number of transparent elements; N characterizes the number of sectors on the checkerboard half of the modulating disk; and θ_0 is the modulus of the spatial frequency at which the maximum is located.

3.3. Conversion of Random Optical Signals by Multidimensional Filters

Radiating objects having various linear dimensions ranging from the minimum discernible to dimensions commensurate with the field of view are seen through optoelectronic devices. Amidst this diversity of objects, the device must obtain maximal information on the required object, which differs from the other objects in shape, size, or energy.

The task of filtering is known [12] to consist in determining the statistical characteristics of a filter's output signal from given statistical characteristics of one or several random processes that are the input variables. The methods of statistical analysis used in the investigation of electronic devices can be used to evaluate multidimensional spatial filters.

Let a random signal X(y, z) with an autocorrelation function $R_x(y, y', z, z')$ and a spectral density $S_x(\mu, \nu)$ be supplied to the input of a multidimensional filter with a weighting function $E_\delta(y, z)$. Then the autocorrelation function and spectral density of the output signal respectively are

$$R_{x_s}(\eta, \eta'; \zeta, \zeta') = \int_{-\infty}^{\infty}\int dy\,dz \int_{-\infty}^{\infty}\int E_\delta(\eta, y; \zeta, z) E_\delta(\eta', y'; \zeta', z') \times \\ \times R_x(y, y'; z, z')\,dy'\,dz', \qquad (3.66)$$

$$S_{x_s}(\mu, \nu) = |W(i\mu, i\nu)|^2 S_x(\mu, \nu). \qquad (3.67)$$

To determine the dispersion of the output signal of a multidimensional filter, it suffices to set $\eta' = \eta$ and $\zeta' = \zeta$ in formula (3.66). Then we obtain

$$D_{x_s}(\eta, \zeta) = R_{x_s}(\eta, \zeta) = \\ = \int_{-\infty}^{\infty}\int dy\,dz \int_{-\infty}^{\infty}\int E_\delta(\eta, y; \zeta, z) E_\delta(\eta, y'; \zeta, z') \times \\ \times R_x[(y, y'; z, z')]\,dy'\,dz'. \qquad (3.68)$$

Let us determine, for example, the dispersions of the output signals after spatial white noise passes through filters having

bell-shaped and rectangular weighting functions. As we know, the spectral density of spatial white noise is a constant, i.e., $S_x(\mu, \nu)=D_x=\text{const}$. After the signal passes through a multidimensional filter having a bell-shaped weighting function whose spatial frequency transfer function has the form

$$W(\mu, \nu)=\exp\left[-\frac{r_1^2}{4Q_1^2}(\mu^2+\nu^2)\right], \qquad (3.69)$$

the spectral density of the output signal is

$$S_{x_1}(\mu, \nu)=D_x\exp\left[-\frac{r_1^2}{2Q_1^2}(\mu^2+\nu^2)\right]. \qquad (3.70)$$

To find the dispersion of the output signal, we must integrate the spectral density:

$$D_{x_1}=\int_{-\infty}^{\infty}\int S_{x_1}(\mu, \nu)\,d\mu\,d\nu=$$

$$=D_x\int_{-\infty}^{\infty}\int\exp\left[-\frac{r_1^2}{2Q_1^2}(\mu^2+\nu^2)\right]d\mu\,d\nu=D_x\frac{Q_1}{2\pi r_1^2}. \qquad (3.71)$$

But if the white noise is converted by a filter having a rectangular weighting function, then the spectral density and dispersion of the output signal respectively are

$$S_{x_1}(\mu, \nu)=\frac{16D_x}{\mu^2\nu^2}\sin^2\mu\frac{y_1}{2}\sin^2\nu\frac{z_1}{2}, \qquad (3.72)$$

$$D_{x_1}=\frac{16D_x}{(2\pi)^2}\int_{-\infty}^{\infty}\int\frac{1}{\mu^2\nu^2}\sin^2\mu\frac{y_1}{2}\sin^2\nu\frac{z_1}{2}\,d\mu\,d\nu=D_xy_1z_1. \qquad (3.73)$$

i.e., the larger the area of the rectangle, the greater the dispersion of the output signal.

The quality of a spatial filter always can be evaluated if we know the signal-to-noise ratio at the filter's output, i.e., if we have data on the valid-signal and noise spectra. Let a valid signal

$E_c(\eta, \zeta)$ and a background or other noise signal $E_п(\eta, \zeta)$ be defined in the plane of the modulating disk in the form of spatial functions of irradiance. In the general case, these signals are random functions of coordinates. We will assume that these functions describe steady-state, ergodic, isotropic processes that are not intercorrelated. Then the overall irradiance distribution in the plane of the modulating disk, which determines the total input signal of the filter, is

$$E_0(\eta, \zeta)=E_c(\eta, \zeta)+E_п(\eta, \zeta) \qquad (3.74)$$

A spatial filter must isolate the valid signal $E_c(\eta, \zeta)$ from the overall signal $E_0(\eta, \zeta)$, and this can be done only when E_c and $E_п$ have different properties.

In analyzing the filtering properties of modulating disks, we must know the spectral power densities of the valid signal $E_c(\mu, \nu)$ and the noise signal $E_п(\mu, \nu)$.

The signal-to-noise (S/N) ratio often is used as a criterion of valid-signal detection. Hereafter by signal-to-noise we mean the ratio of the signal power from a legitimate source to the root-mean-square value of the noise signal power at the output of the modulating disk.

The signal power from a valid source at the output of a spatial filter can be represented as

$$[E_{c_{вых}}(\eta, \zeta)]^2=\left|\int\int_{-\infty}^{\infty} S_c(\mu, \nu)W(\mu, \nu)\times[2\pi(\mu, \eta+\nu\zeta)]\,d\mu\,d\nu\right|^2. \qquad (3.75)$$

If the Khinchine-Wiener spatial spectrum of the background-noise power in the plane of the modulating disk is defined by the function $S_п(\mu, \nu)$, then after the spatial filter this noise spectrum will be

$$S_{п_{вых}}(\mu, \nu)=S_п(\mu, \nu)|W(\mu, \nu)|^2. \qquad (3.76)$$

After the spatial filter the rms value of the background-noise power will be

$$P_{\text{п}}(\eta, \zeta) = \int_{-\infty}^{\infty}\int S_{\text{п}}(\mu, \nu)\,|W(\mu, \nu)|^2\, d\mu\, d\nu. \qquad (3.77)$$

In cartesian coordinates, the square of the ratio of the radiant power of a valid source to the rms noise power is given by the following expression:

$$\chi^2(\eta, \zeta) = \frac{[E_{c_{max}}(\eta, \zeta)]^2}{P_{\text{п}}(\eta, \zeta)} =$$

$$= \frac{\left|\int_{-\infty}^{\infty}\int S_{\text{c}}(\mu, \nu)\, W(i\mu, i\nu) \times [2\pi(\mu\eta + \nu\zeta)]\, d\mu\, d\nu\right|^2}{\int_{-\infty}^{\infty}\int S_{\text{п}}(\mu, \nu)\,|W(i\mu, i\nu)|^2\, d\mu\, d\nu}. \qquad (3.78)$$

In a polar coordinate system, the same formula will be

$$\chi^2 = \frac{\left|\int_0^R \theta\, d\theta \int_0^{2\pi} S_{\text{c}}(\theta) W(i\theta, \psi) \times [2\pi\theta r \cos(\varphi - \psi)]\, d\psi\right|^2}{\int_0^R S_{\text{п}}(\theta)\, \theta\, d\theta \int_0^{2\pi} |W(i\theta, \psi)|^2 d\psi}. \qquad (3.79)$$

The absence of a dependence of the functions S_{c} and $S_{\text{п}}$ on the independent variable ψ is explained by making the assumption of isotropic radiation from noise and from a valid source, and of an isotropic distribution of the irradiance from them in the plane of the modulating disk.

The S/N ratio is a characteristic that reflects the potential for separating a signal from background. A comparison of the filtering properties of modulating disks based on the S/N criterion makes it possible to obtain filtering performance that is acceptable in practice.

The identification of valid signals by optoelectronic devices is known to take place against a radiating background whose radiance distribution in space is a random function of coordinates, radiation

wavelength, and time. For many devices that have a small field of view and that operate for a short period of time, we may assume that a fully specific background formation that undergoes practically no change in shape in time falls within the field of vision.

The images of valid and spurious radiators in the plane of the modulating disk have different dimensions and shapes with different energy levels. The field of the background image brightness is seen as a two-dimensional random process B(y, z) which is a family of random values of brightness that are placed in correspondence with the nonrandom arguments y and z. When the background is considered, it is assumed to be steady. This is justified by the specific features of optical devices; by the small field of vision and low probability that the device will operate in regions of clear statistical nonuniformity--the horizontal line, the zone adjacent to the sun, etc. The assumption that the random process B(y, z) is isotropic presupposes that its statistical properties are constant in all directions. This is justified by the fact that when work is done far from the horizon and sun, there are no factors to cause a change in the probabilistic characteristics of the bright background field in any direction. The following expression for the energy spectrum of the natural background is given in Ref. 5:

$$S_{\text{п}}(\mu, \nu)=\frac{S_{\text{п}_0}}{(a\mu^2+b\nu^2+\alpha^2)^{\beta}}, \qquad (3.80)$$

where a, b--quantities that characterize the anisotropy of the background;

β--a quantity that determines the rate of decrease of the spectrum with increasing spatial frequency;

$S_{\text{п}_0}=S_{\text{п}}(0, 0)$.

Actual radiation sources that an optical device must identify from among the diverse radiators generally are point sources that occupy an insignificant fraction of the field of vision. Because of the electromagnetic nature of light and the finite dimensions of

the field of vision, the image from a point source has the form of a diffraction mottle in the general case. For an idealized optical system, the spatial frequency spectrum of the image of a point source is given by the formula [19]:

$$S_c(\mu, \nu)=\frac{2E_0'\sigma_0}{\lambda}\frac{J_1\left(2\pi r\sqrt{\mu^2+\nu^2}\right)}{2\pi r\sqrt{\mu^2+\nu^2}}, \qquad (3.81)$$

where r--the radius of the diffraction mottle;

$\sigma=\pi r^2$;

E_0'--the irradiance amplitude.

For a fixed wavelength λ_0

$$S_c(\mu, \nu)=2E_0\sigma_0\frac{J_1\left(2\pi r\sqrt{\mu^2+\nu^2}\right)}{2\pi r\sqrt{\mu^2+\nu^2}}, \qquad (3.82)$$

where $E_0=E_0'/\lambda_0$.

As the diameter of the image of a radiation source increases, the energy distribution in the spectrum draws closer and closer to the origin of frequency coordinates.

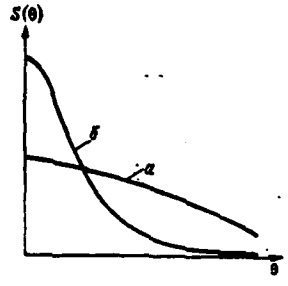

Fig. 3.15. One-dimensional spatial frequency spectra. (a) valid signal; (b) background.

Comparing the spatial spectra of the background and a valid signal (Fig. 3.15), we see that a significant fraction of the energy is distributed at low spatial frequencies in the spectra. Therefore,

we may conclude that it is difficult to isolate a valid signal at low spatial frequencies. It is best to determine the filtering properties of modulating disks at high frequencies.

All modulating disks are characterized by the fact that their spatial frequency transfer functions have subordinate maxima at higher-order frequencies. We will call these maxima the primary maxima and we will examine the filtering properties of some modulating disks in the region of the primary maxima. To do this, let us simplify expression (3.78) by applying the Cauchy-Schwarz inequality to the numerator:

$$\chi^2 \leqslant \frac{\left|\int\int_{-\infty}^{\infty} S_c(\mu, \nu)\, d\mu\, d\nu\right|^2 \left|\int\int_{-\infty}^{\infty} W(i\mu, i\nu)\, d\mu\, d\nu\right|^2}{\int\int_{-\infty}^{\infty} S_n(\mu,\nu) |W(\mu,\nu)|^2\, d\mu\, d\nu} \qquad (3.83)$$

and we determine all functions for values of the spatial frequencies μ_0 and ν_0 that correspond to the location of a primary maximum. Then the approximate S/N expression will be converted to the simple formula:

$$\chi \leqslant \frac{S_c(\mu_0, \nu_0)}{[S_n(\mu_0, \nu_0)]^{1/2}}. \qquad (3.84)$$

Formula (3.84) seemingly does not take into account the characteristics of the modulating disk, since its transfer function is missing. However, this does not indicate that the structure of the modulating disk does not affect the S/N ratio. Indeed, the primary maxima of the transfer functions of modulating disks are located at specific spatial frequencies whose values reflect the arrangement, size, and shape of the transparent and opaque elements of a given modulating disk. These factors also determine the number of primary maxima.

As an example, let us compare the filtering properties of two modulating disks: one with alternating transparent and opaque sectors

(disk I) and one with a checkerboard pattern of transparent and opaque sectors (disk II).

To simplify the solution of the problem, we will assume that the background is isotropic, i.e., that its spectrum is

$$S_{\text{п}}(\mu, \nu)=\frac{S_{\text{п}_0}}{(\mu^2+\nu^2+\alpha^2)^{\beta}}, \qquad (3.85)$$

and that the signal spectrum is described by expression (3.82).

We will assume that the width α of a transparent band of modulating disk I is equal to a side of a square of disk II, and that the valid-signal image has a radius $r=a/2$. Then the S/N ratio for modulating disk I is

$$\chi_1=\frac{\left|A\frac{I_1(2\pi\mu_{1_0}r)}{2\pi\mu_{1_0}r}\right|}{\sqrt{S_{\text{п}}(\mu_{1_0})}}(\mu_{1_0}^2+\alpha^2)^{\beta/2}, \qquad (3.86)$$

and for modulating disk II

$$\chi_2=\frac{\left|A\frac{I_1(2\pi r\sqrt{\mu_{2_0}^2+\nu_{2_0}^2})}{2\pi r\sqrt{\mu_{2_0}^2+\nu_{2_0}^2}}\right|}{\sqrt{S_{\text{п}}(\mu_{2_0}, \nu_{2_0})}}(\mu_{2_0}^2+\nu_{2_0}^2+\alpha^2)^{\beta/2}, \qquad (3.87)$$

where $A=2\pi r^2E_0$, $\mu_{1_0}=\mu_{2_0}=\nu_{2_0}=\mu_0=\frac{1}{2a}$.

If we assume that $S_{\text{П}}(\mu_{1_0})=S_{\text{П}}(\mu_{2_0}, \nu_{2_0})$, i.e., that the peak values of the background spectrum at these frequencies are equal, then the estimate of the effectiveness of the filtering properties of the modulating disks can be determined as the ratio

$$\varepsilon=\frac{\chi_2}{\chi_1}=\frac{I_1(2\sqrt{2}\pi\mu_0 r)}{I_1(2\pi\mu_0 r)}\left(\frac{2\mu_0^2+\alpha^2}{\mu_0^2+\alpha^2}\right)^{\beta/2}\frac{1}{\sqrt{2}}. \qquad (3.88)$$

When $\beta=3/2$, $\alpha<<\mu_0$, and $2r=a$, this ratio is equal to 1.163, i.e., modulating disk II ensures that a valid signal will exceed the background by approximately 16% compared with modulating disk I.

For an anisotropic distribution of irradiance in the image of a background process in the plane of the modulating disk, the spatial frequency spectrum of the background is written as

$$S_{\text{ш}}(\mu, \nu)=\frac{S_{\text{ш}_0}}{(a\mu^2+b\nu^2+\alpha^2)^\beta}. \qquad (3.89)$$

Let us examine the effect of background anisotropy on the estimate of the effectiveness of modulating disks I and II. We will assume that in formula (3.89) a=1 and b→0, i.e., a background process represents the edge of a solar-illuminated cloud or the skyline that is perpendicular to bands of modulating disk I. In this case the formula for estimating the effectiveness is

$$\varepsilon=\frac{\chi_2}{\chi_1}=\frac{I_1(2\sqrt{2}\pi\mu_0 r)}{\sqrt{2}I_1(2\pi\mu_0 r)}=\text{const}, \qquad (3.90)$$

i.e., for a specific value of the radii of the image of a valid object is a constant [sic].

If the edge of a cloud or the skyline is parallel to transparent bands of modulating disk I, i.e., b=1 and a→0, then the estimate of effectiveness will be given by the formula

$$\varepsilon=\frac{\chi_2}{\chi_1}=\frac{I_1(2\sqrt{2}\pi\mu_0 r)}{\sqrt{2}I_1(2\pi\mu_0 r)}\left(\frac{\mu_0^2+\alpha^2}{\alpha^2}\right)^{\beta\cdot 2}. \qquad (3.91)$$

If $\alpha<<\mu$, then $\varepsilon\to\infty$, since the value of χ_1 tends toward zero. The results obtained are fully consistent with the physics of the process of modulation of the light from radiating objects. Modulation of the background is not observed in the first case, where a=1 and b→0, and the values of χ_1 and χ_2 remain constant, depending solely on the amplitudes of the luminous fluxes of a valid radiator and the background. The second case, with a→0 and b=1, leads to a situation in which modulating disk I obtains an identical percentage modulation for the light from a valid radiator and the background, since the dimensions of the valid-object and background images are commensurate.

To investigate the transmission of information from radiating objects through circular modulating disks, the Khinchine-Wiener spectrum of background radiation is expressed by the relation

$$S_n(\theta, \psi)=\frac{S_{n_0}}{[\theta^2(a\cos^2\psi+b\sin^2\psi+\alpha^2)]^\beta}. \qquad (3.92)$$

Let us consider the effect of anisotropy of a background process on the filtering properties of the modulating disk shown in Fig. 1.11, using the primary maxima of its spatial frequency transfer function and the phase-frequency response:

$$W(\psi)=\sin^2\frac{N}{2}\psi. \qquad (3.93)$$

If the background process is isotropic, then the S/N ratio based on formula (3.84) will assume the form

$$\chi=\frac{\left|A\frac{f_1(2\pi\theta_0 r)}{2\pi\theta_0 r}\right|}{S_{n_0}^{1/2}}[\theta_0^2(1+\alpha^2)]^{\beta/2}. \qquad (3.94)$$

For extreme anisotropy, i.e., when the edge of an illuminated cloud or the skyline is located in the field of vision of the optical device (α=1, b→0), the S/N ratio is

$$\chi^*=\left[\frac{S_c^2(\theta_0)\int_0^{2\pi}|1-\cos N\psi|^2\,d\psi}{S_{n_0}\int_0^{2\pi}\frac{|1-\cos N\psi|^2\,d\psi}{[\theta^2(\cos^2\psi+\alpha^2)]^\beta}}\right]^{1/2}, \qquad (3.95)$$

where the superscript * means that the investigation is done in the presence of an anisotropic background.

After the integrals of formula (3.95) are calculated, the S/N ratio for the extreme case of anisotropy turns out to be lower than the analogous ratio for an anisotropic background process by a factor of approximately 3. This indicates that background anisotropy greatly impairs a modulating disk's ability to discriminate a valid signal.

3.4. Some Problems of the Optimization of Spatial Filters

If a random valid signal m(y, z) and noise n(y, z) are supplied to the input of a multidimensional filter, then it is desirable that the filter reproduce the valid signal with a minimal rms error at its output.

We will use the following conventions:

$(y, z)=m(y, z)+n(y, z)$--the total input signal;

$g(y, z)$--the required output signal, which is equal to the valid signal m(y, z) in the case in question;

S_φ, S_m, S_n, S_g--the spectral densities of signals φ, m, n, and g, respectively;

S_{mn}, S_{nm}--the Fourier images of the cross-correlation functions of the valid signal and noise.

The spectral densities of spatial valid signals and noise that are encountered in practice usually are rational functions of the spatial frequencies μ and ν. For example, the spectral density of a valid signal can be represented as

$$S_m(\mu, \nu)=\frac{a^2}{|b(i\mu, i\nu)|^2}, \qquad (3.96)$$

and the noise spectrum can be represented by the expression

$$S_n(\mu, \nu)=\frac{S_{n_0}}{|c(i\mu, i\nu)|^\beta}. \qquad (3.97)$$

In the absence of a cross correlation between the valid signal and the noise, the cross-correlation functions are equal to zero; therefore, their Fourier transforms also are equal to zero:

$$S_{nm}=S_{mn}=0$$

The solution of the problem of an optimal filter that was found by Wiener and Kolmogorov also can be extended to spatial filters if we introduce the assumption of steadiness and isotropy of the radiation from background noise and observed objects that the filter isolates from the overall light flux that falls within the field of vision of the device's optical system.

By analogy with an electronic filter, the expression for the optimal transfer function of a spatial filter has the form

$$W_{опт}(p, q)=\frac{1}{\Phi(p, q)}\left[\frac{W_1(p, q) S_m\left(\frac{p}{i}; \frac{q}{i}\right)}{\Phi(-p, -q)}\right], \quad (3.98)$$

where $W_1(p, q)$--the desired transfer function;

$p=i\mu$, $q=i\nu$--operators.

$$\Phi(pq)\cdot\Phi(-p, -q)=S_m(\mu, \nu)+S_n(\mu, \nu). \quad (3.99)$$

We will assume that the filter must reproduce the input signal at the output, i.e., that the desired transfer function of the filter is $W_1(i\mu, i\nu)=1$.

To determine the optimal transfer function of a spatial filter, we will convert the bracketed expression in formula (3.98):

$$\frac{W_1(p, q) S_m\left(\frac{p}{i}; \frac{q}{i}\right)}{\Phi(-p, -q)}=\frac{a^2}{b(p, q) A(-p, -q)}=$$

$$=[\ ]_+ +[\ ]_-=\frac{ak_nB_n(p, q)}{b(p, q)}+\frac{al_nC_n(p, q)}{A(-p, -q)}, \quad (3.100)$$

where k_n and l_n--constants that can be determined by the method of coefficient comparison;

$B_n(p, q)$ and $C_n(p, q)$--functions of the operators p and q.

In the theory of electrical filters the frequency transfer function is determined uniquely by the locations of two singularities: poles and zeros. For a physically feasible system, i.e., for one

whose weighting function is g(t)=0 when t<0, the poles of the transfer function are located in the left half-plane. Therefore, to determine the optimal transfer function from (3.98) we use only that portion of expression (3.100) which is marked with the symbol $[\ ]_+$.

For spatial filters the weighting function $E_3(y, z)$ exists when $y, z \leqslant 0$, therefore, the criterion for physical feasibility of the frequency response of a spatial filter is that the arrangement of the poles must be symmetric with respect to the coordinate axes. Hence, expression (3.100) is used in its entirety to determine the optimal transfer function from formula (3.98). Then the expression for the transfer function of an optimal multidimensional filter will have the form

$$W_{опт}(i\mu, i\nu)=\frac{S_m(\mu, \nu)}{S_m(\mu, \nu)+S_n(\mu, \nu)}. \qquad (3.101)$$

We will illustrate the use of formula (3.101) by solving several examples.

Let a valid signal be supplied to the input of an optimal multidimensional filter. The spectral density of the signal is

$$S_m(\mu, \nu)=D_m \exp\left[-\frac{r_1^2}{4q_1^2}(\mu^2+\nu^2)\right],$$

Let the noise be spatial white noise with a spectral density

$$S_n(\mu, \nu)=D_n$$

The spatial frequency transfer function of an optimal filter is

$$W_{опт}(\mu, \nu)=\frac{1}{1+\frac{D_n}{D_m}\exp\frac{r_1^2}{4q_1^2}(\mu^2+\nu^2)}. \qquad (3.102)$$

When

$$\frac{D_m}{D_n} \gg 1 \quad W_{опт}(\mu, \nu)=1;$$

if

$$\frac{D_m}{D_n} \ll 1 \quad W_{опт}(\mu, \nu) = \frac{D_m}{D_n} \exp\left[-\frac{r_1^2}{4\varrho_1^2} (\mu^2 + \nu^2) \right].$$

For real backgrounds and valid signals, the most frequent case is $D_m << D_п$, in which the optimal spatial frequency transfer function of a spatial filter has the following form if the background noise is spatial white noise:

$$W_{опт}(\mu, \nu) = \frac{D_m}{D_n} \exp\left[-\frac{r_1^2}{4\varrho_1^2} (\mu^2 + \nu^2) \right]. \quad (3.103)$$

Since this function is symmetric with respect to the origin of frequency coordinates, we will write it in one-dimensional space:

$$W_{опт}(\vartheta) = \frac{D_m}{D_n} \exp(-\alpha^2 \vartheta^2), \quad (3.104)$$

where

$$\alpha^2 = \frac{r_1^2}{4\varrho_1^2}.$$

The one-dimensional weighting function of an optimal spatial filter will be determined by the inverse Fourier transform of its spatial frequency transfer function:

$$E_з(\eta) = \frac{D_m}{D_n} \int_{-\infty}^{\infty} \exp(-\alpha^2 \vartheta^2) \exp(2\pi i \eta \vartheta) d\vartheta. \quad (3.105)$$

The integral in formula (3.105) is the tabular one [2]. It is equal to:

$$E_з(\eta) = \frac{\sqrt{\pi}}{\alpha} \frac{D_m}{D_n} \exp\left(-\frac{\pi^2 \eta^2}{\alpha^2} \right)$$

or, if the weighting function and the transmission function are equivalent,

$$\tau_{опт}(\eta)=\frac{D_m}{D_n}\frac{2\rho_1}{r_1}\sqrt{\pi}\exp\left(-\frac{4\pi^2\eta^2\rho_1^2}{r_1^2}\right). \quad (3.106)$$

The function $\tau_{опт}(\eta)$ takes on its maximum value when $\eta=0$. It was noted above that the maximum value of the transmission function of a modulating disk does not exceed unity. In the example considered,

$$\tau_{опт_{max}}=\frac{D_m'}{D_n}\frac{2\rho_1}{r_1}\sqrt{\pi}=1,$$

whence

$$\frac{D_m}{D_n}=\frac{r_1}{2\rho_1\sqrt{\pi}}.$$

Given $\rho_1=0.4679$ and r=0.1 mm, we obtain

$$\frac{D_m}{D_n}=0{,}06\ll 1,$$

This confirms the legitimacy of the assumption made above.

If the spectral characteristics of the valid signal and background are expressed by the relations

$$S_m(\mu,\ \nu)=D_m\frac{J_1(2\pi r\sqrt{\mu^2+\nu^2})}{2\pi r\sqrt{\mu^2+\nu^2}} \quad (3.107)$$

and

$$S_n(\mu,\ \nu)=\frac{D_n'}{(\mu^2+\nu^2+\alpha^2)^\beta}, \quad (3.108)$$

then the spatial frequency transfer function of an optimal spatial filter is

$$W_{опт}(i\mu,\ i\nu)=\frac{1}{1+\frac{D_n}{D_m}\frac{2\pi r\sqrt{\mu^2+\nu^2}}{J_1(2\pi r\sqrt{\mu^2+\nu^2})(\mu^2+\nu^2+\alpha^2)^\beta}} \quad (3.109)$$

and it is a symmetric function with respect to the origin of coordinates Oμ and Oν.

Let us write this function in a one-dimensional version and on the assumption that $D_m << D_n$:

$$W_{опт}(l\vartheta)=\frac{D_m}{D_n}\frac{(\vartheta^2+\alpha^2)^{\beta}I_1(2\pi r\vartheta)}{2\pi r\vartheta}. \qquad (3.110)$$

The one-dimensional transmission function of an optimal modulating disk will be given by the expression

$$\tau_{опт}(\eta)=\frac{D_m}{2\pi r D_n}\int_{-\infty}^{\infty}\frac{I_1(2\pi r\vartheta)}{\vartheta}(\vartheta^2+\alpha^2)^{\beta}\exp(2\pi i\eta\vartheta)\,d\vartheta. \qquad (3.111)$$

The transmission function of a modulating disk is real; therefore:

$$\tau_{опт}(\eta)=\frac{D_m}{D_n}\frac{1}{2\pi r}\int_{-\infty}^{\infty}I_1(2\pi r\vartheta)\frac{(\vartheta^2+\alpha^2)^{\beta}}{\vartheta}\cos 2\pi\eta\vartheta\,d\vartheta. \qquad (3.112)$$

We will designate the integral in formula (3.112) as J_0 and express it as the sum of two integrals J_1 and J_2 on the assumption that $\beta=1$:

$$J_0=J_1+J_2=\int_{-\infty}^{\infty}I_1(2\pi r\vartheta)\,\vartheta\cos 2\pi\eta\vartheta\,d\vartheta+$$

$$+\alpha^2\int_{-\infty}^{\infty}I_1(2\pi r\vartheta)\,\frac{1}{\vartheta}\cos 2\pi\eta\vartheta\,d\vartheta. \qquad (3.113)$$

Both integrals are tabular and can be calculated as

$$J_1=\frac{r\Gamma\left(\frac{3}{2}\right)}{\pi^{5/2}(r^2-\eta^2)^{3/2}}=\frac{0.05r}{(r^2-\eta^2)^{3/2}}. \qquad (3.114)$$

$$J_2=2\alpha^2\cos\arcsin\frac{\eta}{r}=\frac{2\alpha^2}{r}(r^2-\eta^2)^{1/2}, \qquad (3.115)$$

where $\Gamma(\frac{3}{2})=0.89$ is the gamma function of the argument $\frac{3}{2}$.

Hence

$$J_0=\frac{2\alpha^2}{r}\left[1+\frac{0.05r^2}{(r^2-\eta^2)^2}\right](r^2-\eta^2)^{1/2}. \qquad (3.116)$$

Then the transmission function of an optimal modulating disk for input signals having spectral densities (3.107) and (3.108) will be expressed by the formula:

$$\tau_{опт}(\eta)=\frac{D_m}{D_n}\frac{\alpha^2}{\pi r^2}(r^2-\eta^2)^{1/2}\left[1+\frac{0{,}05r^2}{(r^2-\eta^2)^2}\right]. \quad (3.117)$$

When $\eta=0$, the function is $\tau_{опт}(0)=\tau_{max}=1$, i.e.,

$$\tau_{max}=\frac{D_m}{D_n}\frac{\alpha^2}{\pi r}\left(1+\frac{0{,}05}{r^2}\right)=1,$$

whence

$$\frac{D_m}{D_n}=\frac{\pi r^3}{\alpha^2(r^2+0{,}05)}. \quad (3.118)$$

It follows from expression (3.118) that in order to preserve the conditions $\tau_{max}=1$ and $D_m<<D_n$, the radius r of the image of a valid radiation source must be increased or the quantity α must be larger than unity. For example, for r=0.1 mm and $D_m=0.05D_n$, $\alpha=3.16$.

To determine the dimensions of the transparent apertures of a modulating disk, we set expression (3.117) equal to zero:

$$\frac{D_m}{D_n}\frac{\alpha^2}{\pi r^2}(r^2-\eta^2)^{1/2}\left[1+\frac{0{,}05r^2}{(r^2-\eta^2)^2}\right]=0,$$

Hence we obtain

$$\eta=\pm r$$

i.e., once again we find that the dimensions of the apertures of the modulating disk must be equal to those of the image of a valid radiator.

LITERATURE

1. Андреев В. Д. Прохождение полезного сигнала и сигнала фона через радиально-щелевые обтюраторы систем индикации светящихся объектов — «Известия АН СССР, ОТН, Техническая кибернетика», 1963, № 3.

2. Градштейн И. С., Рыжик И. М. Таблицы интегралов, сумм, рядов и произведений. М., Физматгиз, 1962.

3. Гудмен Дж. Введение в Фурье-оптику (пер. с англ.) М «Мир», 1970.

4. Деньщиков К. К. *Метод имитации* ИК фонов облачного неба для исследования помехозащищенности оптико-электронных САР. — «Известия вузов СССР», Приборостроение», 1969, т. XII, № 10.

5. Джемиссон Дж. Э. и др. Физика и техника инфракрасного излучения. М., «Советское радио», 1965.

6. *Дубиновский* А. М. К расчету оптимальных характеристик пространственных фильтров. — «Оптико-механическая промышленность», 1964, № 2.

7. Ефимов М. В. Следящие системы с оптическими связями. М., «Энергия», 1969.

8. Заверев В. А., Орлов Е. Ф. Оптические анализаторы. М., «Советское радио», 1971.

9. Катыс Г. П. Автоматическое сканирование. М., «Машиностроение», 1969.

10. Коган Б. Я. Электронные моделирующие устройства и их применение для исследования систем автоматического регулирования. М., Физматгиз, 1963.

11. Королев Ф. А. Теоретическая оптика. М., «Высшая школа», 1966.

12. Костюк В. И. Самонастраивающиеся следящие системы. Киев, «Техника», 1966.

13. Криксунов Л. З. Системы информации с оптическими квантовыми генераторами. Киев «Техника», 1970.

14. Криксунов Л. З., Усольцев И. Ф. Инфракрасные системы. М., «Советское радио», 1968.

15. Ламберт, Гейдрих. Техника моделирования радиолокационных систем. — «Зарубежная радиоэлектроника», 1960, № 5.

16. Лахти Б. П. Системы передачи информации (перевод с англ.). М., «Связь», 1971.

17. Левин Л. А. Методы решения [illegible] пользованием аналоговых вычислительных машин. М., Мир, 1966.

18. Левшин В. Н. [illegible] ских системах управления. М., «Советское радио», 1971.

19. Марешаль А., Франсон М. Структура оптического изображения. М., «Мир», 1964.

20. Папулис А. Теория систем преобразований в оптике (*перевод с англ.*). М., «Мир», 1971.

21. Романовский П. И. Ряды Фурье. М., Гостехиздат, 1957.

22. Слюсарев Г. Г. Методы расчета оптических систем. М., «Машиностроение», 1969.

23. Справочник по вычислительной технике. М., «Энергия», 1964.

24. Харкевич А. А. Спектры и анализ. М., Гостехиздат, 1957.

25. Якушенков Я. Г. Основы теории и расчета оптико-электронных приборов. М., «Советское радио», 1965.

26. Aroyan G. F. The Technique of Spatial Filtering. Proc. of the IRE, 1959, vol. 47, No. 9.

27. Jóźwicki R. Optyka Instrumentalna. Warszawa, 1970.

28. Montgomery W. D., Broon P. M. Spatial Filtering. JOSA, 1962, vol. 52, No. 11.

29. Seyrafi K., Davison C. A. Spatial Filtering Synthesis. Y. R. Physics, 1964, vol. 4, No. 4.

30. Trabka I. B., Retling F. I. Image Processing for Pattern Recognition. JOSA, 1964, vol. 54, No. 10.

31. Yates H. W., Fisher R. F. and Leftwich. Survey of Infrared Trackers. Applied Optics, 1966, vol. 5, No. 4.